2010

SV40 Infection in Human Lymphocyte Cell Lines

Aoife Kelly
Technological University Dublin

SV40 Infection in Human Lymphocyte Cell Lines

By

Aoife Kelly

M.Phil. Biomedical Science

School of Biological Sciences,

Dublin Institute of Technology,

Kevin Street, Dublin 8

In conjunction with FAS Science Challenge Internship programme at

Baylor College of Medicine, Houston, Texas

Abstract

The oncogenic DNA virus Simian virus 40 (SV40) was introduced into the human population as an inadvertent contaminant of polio vaccines that were prepared in cultures of primary monkey kidney cells. It is estimated that, as a result, millions of people worldwide were exposed to SV40 between the years 1955-1963. Research indicates that the virus is still present in the human population today, based on the finding of neutralising antibodies and viral DNA sequences in children and adults. Of concern is that SV40 has also been detected in human tumours including primary brain cancer, malignant mesothelioma, bone tumours and systemic lymphomas. Recent studies have found a significant association of SV40 with certain types of Non-Hodgkin's Lymphoma (NHL). However, the interaction between SV40 and lymphocytes has not yet been fully characterised. In this study, the characteristics of SV40 infections were evaluated in human B and T lymphocyte cell lines. Three strains of SV40 were compared: wild type 776-1E with a single enhancer, 776-2E with a duplicated enhancer and a micro RNA mutant virus, 776-2E-SM. Following infection, cell proliferation and viability, cell surface marker expression, viral large tumour antigen (T-ag) expression, and quantification of viral genomes were measured. The results showed increased B cell proliferation and cell activation as shown by the upregulation of CD69. Downregulation of CD80, a co-stimulatory molecule, was also observed. T-ag expression was detected in a small percentage of B cells and RQ-PCR analysis showed maintenance of the viral genome in B cells during passage of the cultures. In all, these initial observations indicate that some human B lymphocyte cell lines are susceptible to SV40 infection. Viral maintenance and oncoprotein expression in lymphocytes may bear relevance to SV40 persistence in the host and the detection of the virus in human lymphomas.

Declaration

I certify that this thesis which I now submit for examination for the award of M.Phil., is entirely my own work and has not been taken from the work of others, save and to the extent that such work has been cited and acknowledged within the text of my work.

This thesis was prepared according to the regulations for postgraduate study by research of the Dublin Institute of Technology and has not been submitted in whole or in part for another award in any Institute.

The work reported on in this thesis conforms to the principles and requirements of the Institute's guidelines for ethics in research.

The Institute has permission to keep, lend or copy this thesis in whole or in part, on condition that any such use of the material of the thesis be duly acknowledged.

Signature Aoife Kelly Date 29.05.10

Candidate

Acknowledgements

I would like to thank the following people:

To everyone involved in the FAS Science Challenge Programme - Dr. Pauline Ward, John Cahill and Grainne Timlin and to the people who supported this programme - Dr. Denis Headon and Dr. Austin Cooney of Biolink USA Ireland and Dr. Bert O'Malley, Baylor College of Medicine - for providing me with the fantastic opportunity to complete my project in America.

To Dr. Janet Butel for allowing me to participate in her research and for her inspirational mentorship and kindness. Thank you for opening my eyes to the fascinating world of virology! To Dr. Adrienne McNees for supervising this project - thank you for your patience, teaching and constant encouragement that meant so much. To all of the wonderful people in the Butel laboratory – your kindness and constant willingness to help created a fantastic work environment and made my time in your laboratory thoroughly enjoyable.

To everyone in DIT for your guidance and encouragement in the completion of this thesis; Dr. Fergus Ryan, Dr. Joe Vaughan, Dr. James Curtin and in particular Dr. Celine Herra, for your tireless efforts and dedication in helping me to put this project into words. Your teaching and support throughout the past year has been very much valued and appreciated!

To my family and friends for their support and patience and finally, to all my fellow FAS students in Houston with whom I spent the best six months of my life!

Table of Contents

List of Figures

List of Tables

Abbreviations

APC	Allophycocyanin
APCs	Antigen presenting cells
BKV	BK virus
bp	Base pairs
BSA	Bovine serum albumin
CD	Cluster of differentiation
Cdk	Cyclin dependent kinases
C_T	Threshold cycle
CTL	Cytotoxic lymphocyte
DNA	Deoxyribonucleic acid
EBV	Epstein-Barr virus
FACS	Fluorescence Activated Cell Sorting
FBS	Foetal Bovine Serum
FITC	Fluorescein isothiocyanate
FRET	Fluorescence resonance energy transfer
FSC	Forward scatter
GCB	Germinal centre B cell
HBV	Hepatitis B virus
HIV	Human immunodeficiency virus
HTLV-1	Human T lymphotropic virus type 1
HCMV	Human Cytomegalovirus
IC	Isotype Control
JCV	JC virus
KIV	KI virus

KSHV	Kaposi's sarcoma herpesvirus
LCL	Lymphoblastic cell line
LPV	Lymphotropic polyomavirus (African green monkey polyomavirus)
MCV	Merkel cell virus
MEM	Minimum essential medium
MGB	Minor groove binder
MHC I	Major Histocompatibility Complex class I
min	minute(s)
miRNA	micro RNA
mRNA	messenger RNA
MuPyV	Murine polyomavirus
NFQ	Non-fluorescent quencher
NHL	Non-Hodgkin's Lymphoma
NTC	Non-template control
nm	nanometres
nt	Nucleotide
ori	Origin of replication
PBS	Phosphate buffered saline
PCR	Polymerase chain reaction
PE	Phycoerythrin
Pen-strep	Penicillin-streptomycin
PFU	Plaque forming units
PML	Progressive multifocal leukoencephalopathy
PP2A	Protein phosphatase 2A
PyV	Polyomavirus

Rb	Retinoblastoma
RNA	Ribonucleic acid
RQ-PCR	Real time quantitative PCR
RR	Regulatory Region
s	second(s)
S phase	Synthesis phase of cell cycle
SF medium	Serum-free medium
SIV	Simian immunodeficiency virus
SSC	Side scatter
SV40	Simian virus 40
T-ag	Large tumour antigen
t-ag	Small tumour antigen
TBS	Tris buffered saline
TCR	T cell receptor
UK	United Kingdom
US	United States
UV	Ultraviolet
WHO	World Health Organisation
WT	Wild-type
WUV	WU virus

1.0 Introduction

1.1 Simian virus 40: from monkey to man

The polyomavirus Simian virus 40 (SV40) is a member of the *Polyomaviridae*, a family of small DNA viruses, which includes the human polyomaviruses BK virus (BKV) and JC virus (JCV). The family name is derived from the first recognised member of the *Polyomaviridae*, murine polyomavirus (MuPyV). This MuPyV virus was originally discovered in 1953 by Ludwik Gross as a cause of salivary gland tumours in mice and it was initially designated 'polyomavirus' from the Greek 'poly' meaning many and 'oma' meaning tumours, due to its ability to induce a variety of solid tumours in mice (Gross, 1953, Stewart *et al*, 1958).

Soon after the discovery of MuPyV, the monkey polyomavirus SV40 was recognised when Sweet and Hilleman observed cytopathic effects and vacuole formation in monkey kidney cell cultures (Sweet and Hilleman, 1960). SV40 discovery was linked to the development of polio vaccines in the 1950s and 1960s as poliovirus was grown in primary kidney cells of rhesus and cynomolgus macaques, which were often naturally infected with SV40 (Stratton *et al*, 2002). The virus was then inadvertently introduced into the human population through administration of these contaminated poliovirus vaccines. In the years following, SV40 became known as a potent DNA tumour virus and along with MuPyV, it was intensely studied due to its tumourigenic capabilities in animal models and *in vitro* experiments. In the past two decades, mounting evidence of the presence of SV40 in a number of human tumours has seen this 'monkey virus' emerge as a potential human pathogen, a topic that is continually under debate (Vilchez and Butel, 2004).

1.2 SV40 and polyomaviruses: infection in the natural host

To date, there are 22 known members of the *Polyomaviridae*, which infect a range of species including monkeys, rodents and birds (Table 1.1, Dalianis *et al*, 2009). Phylogenetic analysis of the polyomaviruses has revealed three genetically distinct groups: (i) avian polyomaviruses, (ii) mammalian polyomaviruses related to MuPyV and (iii) mammalian polyomaviruses related to SV40 (Feng *et al*, 2008). The natural host of SV40 is the Rhesus macaque (*macaca mulatta*), but several related species of monkey are also capable of being infected (Butel and Lednicky, 1999). SV40 transmission in the monkey is thought to be by viral shedding in the urine, with host infection occurring by the oral, respiratory and subcutaneous routes. In healthy monkeys, SV40 appears to cause a low level persistent infection in the kidney, indicating that SV40 is a nephrotropic virus (Butel and Lednicky, 1999). In immunocompromised monkeys with Simian Immunodeficiency Virus (SIV), SV40 is associated with widespread infection, with the virus being detected in the brain, lung, kidney, lymph node, spleen and peripheral blood, suggesting SV40 may also have neurotropic and lymphotropic properties (Newman *et al*, 1998; Lednicky *et al*, 1998).

Polyomaviruses are also present in the human host. BK virus (BKV) and JC virus (JCV) are exclusive human pathogens and were both discovered in 1971 (Gardner *et al*, 1971; Padgett *et al*, 1971). BKV and JCV infection is widespread in humans and usually occurs in childhood. Seropositivity for BKV reaches 90% in children aged five to nine, with JCV seropositivity at 50 to 60% by the age of ten (Jiang *et al*, 2009). BKV infection usually occurs at an earlier age than JCV (Imperiale, 2001).

Table 1.1: Known members of the *Polyomaviridae* family

Virus	Natural host	Year of discovery
Murine polyomavirus	Mouse	1953
Murine pneumotropic virus	Mouse	1953
SV40	Monkey (rhesus macaque)	1960
SA12	Monkey (chacma baboon)	1963
Rabbit polyomavirus	Rabbit	1964
Hamster polyomavirus	Hamster	1968
BK virus	Human	1971
JC virus	Human	1971
Bovine polyomavirus	Cattle	1974
Lymphotropic papovavirus	Monkey (African green monkey)	1979
Avian polyomavirus	Bird	1981
Rat polyomavirus	Rat	1984
Baboon polyomavirus type 2	Baboon	1989
Cynomolgus polyomavirus	Monkey (cynomolgus)	1999
Goose hemorrhagic polyomavirus	Goose	2000
Chimpanzee polyomavirus	Chimpanzee	2005
Crow polyomavirus	Bird (crow)	2006
Finch polyomavirus	Bird (finch)	2006
KI polyomavirus	Human	2007
WU polyomavirus	Human	2007
Squirrel monkey polyomavirus	Monkey (squirrel monkey)	2008
MC polyomavirus	Human	2008

Table adapted from Dalianis *et al*, 2009

Both of these viruses have been found in tonsillar tissue (Goudsmit *et al*, 1982; Monaco *et al*, 1996), from where the viruses are thought to disseminate and establish an asymptomatic primary infection in childhood, normally leading to lifelong persistence (Imperiale, 2001). The major sites of persistence for human polyomaviruses are the kidney, the central nervous system and the haematopoietic system (Krumbholz *et al*, 2009). BKV was first isolated from the urine of a renal transplant patient with ureteric stenosis (Padgett *et al*, 1971). Although the virus is ubiquitous, it does not cause disease in the healthy host, but can produce pathological effects in immunocompromised individuals such as renal transplant recipients, in whom it can affect as many as five per cent (Randhawa and Demetris, 2000; Hirsch *et al*, 2002). JCV was first isolated from the brain tissue of a patient with progressive multifocal leukoencephalopathy (PML) (Gardner *et al*, 1971), a demyelinating disease of the central nervous system caused by a lytic infection of oligodendrocytes (Imperiale, 2001). Similar to BKV, JCV is also associated with disease in the immunocompromised host, with PML usually only developing in individuals with a severely compromised immune system. PML was rare before the emergence of Human Immunodeficiency Virus (HIV) but this disease now affects about five per cent of HIV-infected patients and is considered to be an Acquired Immunodeficiency Syndrome-defining disease (Berger, 2003).

In the past three years, three new human polyomaviruses have been discovered; KI virus (KIV), WU virus (WUV) and Merkel cell virus (MCV). The novel polyomaviruses KIV and WUV have been found in respiratory fluids in individuals with respiratory infection (Allander *et al,* 2007; Gaynor *et al,* 2007) whilst MCV has been found associated with Merkel Cell Carcinoma, a rare but aggressive human cancer of neuroendocrine origin (Feng *et al*, 2008). Phylogenetically, MCV is the only human polyomavirus that does not

belong to the SV40 subgroup (Figure 1.1). This most recently discovered member of the *Polyomaviridae* has been shown to have the highest homology to the mouse polyomavirus subgroup and is most closely related to the lymphotropic polyomavirus (LPV, African green monkey polyomavirus), presumed to be of simian origin. While the polyomaviruses are thought to be highly species-specific and are believed to evolve in close association with their host, the close evolutionary relationship of MCV to LPV and SV40 to BKV and JCV calls this concept into question and may indicate the possibility that host switching can occur (Viscidi and Shah, 2008).

The emerging role of the polyomaviruses as opportunistic pathogens in the ever-increasing immunocompromised patient population and the recent discovery of new polyomaviruses has re-ignited interest in this family, with the possibility of more new viruses yet to be discovered.

1.3 SV40: association with the human host

The natural host of SV40 is the Rhesus macaque. Its association with the human host dates back to the 1950s and 1960s when SV40 contamination of polio vaccines occurred due to the ability of the virus to survive the formalin treatment used to inactivate the poliovirus. It was not until five years after the polio vaccine was licensed that it was recognised that inactivated (Salk) and early live attenuated (Sabin) forms of polio vaccines had been contaminated with SV40 (Shah, 2007). As a result of this contamination, it was estimated that 98 million adults and children, most of whom were under 20 years old, were exposed to SV40 in the US between the years of 1955-1963 following administration of one or more doses of the inactivated Salk polio vaccine (Stratton *et al* 2002). When stored stocks of polio vaccine were later tested for SV40, it

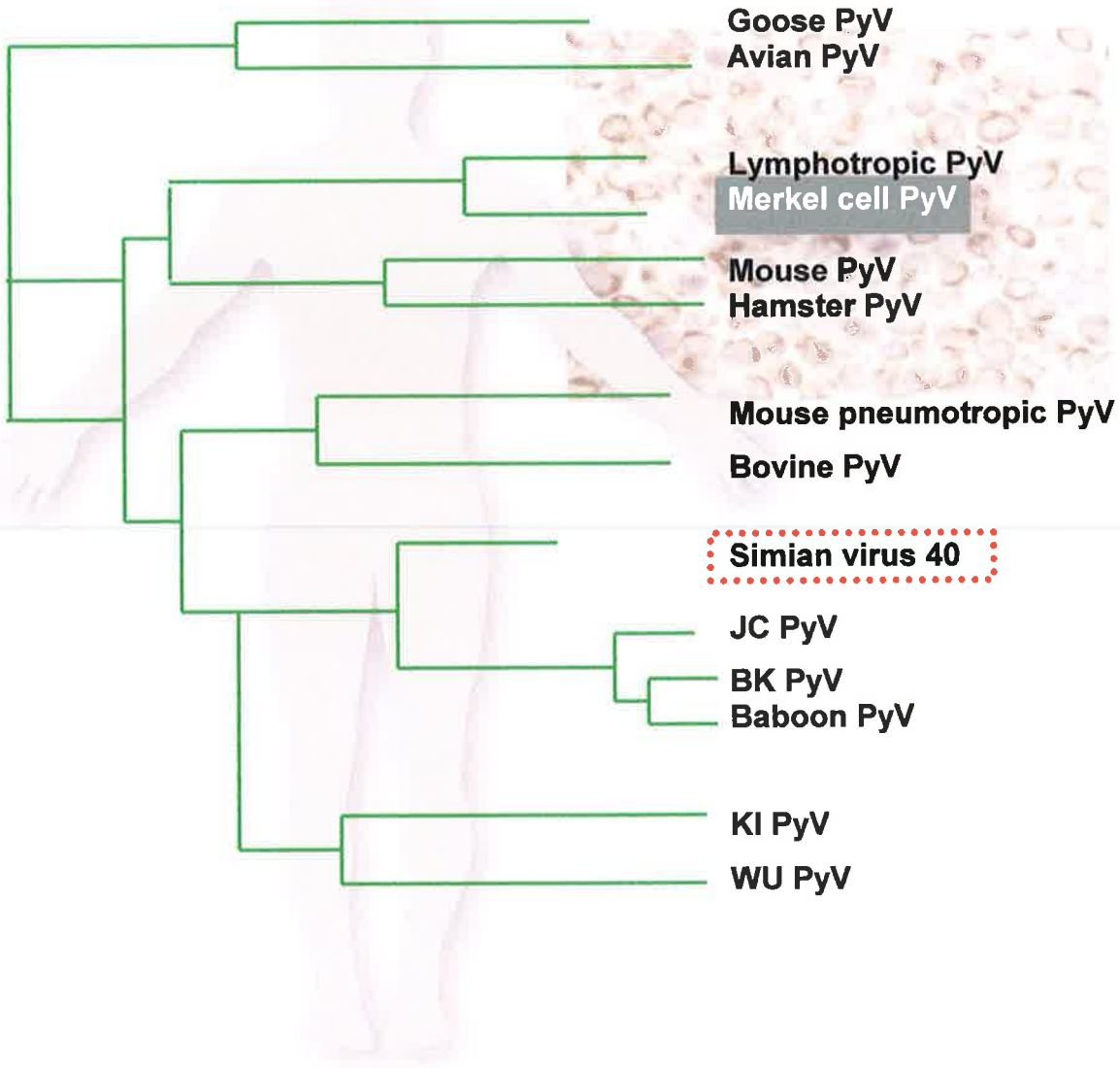

Figure 1.1: Evolutionary relationships of the *Polyomaviridae*
A schematic representation of the evolutionary relationships among the animal and mammalian polyomaviruses, including Simian virus 40 (SV40) highlighted in red, and BK PyV, JC PyV, and the newly discovered KI PyV, WU PyV and Merkel cell PyV, which infect humans.

PyV; polyomavirus

Figure adapted from Viscidi and Shah, 2008

was estimated that the virus was present in 10-30% of the vaccines (Stratton *et al*, 2002). Since these vaccines were distributed and used in other countries, millions of people worldwide were also potentially exposed (Vilchez and Butel, 2003*a*). Furthermore, it is thought that a major Eastern European manufacturer distributed SV40-contaminated vaccines until as recently as 1978 (Cutrone *et al*, 2005).

Once discovered, SV40-vaccine contamination raised concerns and prompted research into the potential risk to human health. Not long after the identification of SV40 as a polio vaccine contaminant, SV40 was found to induce tumours in experimental animal models in studies using hamsters. It was observed that subcutaneous injection of rhesus monkey kidney cell extracts into newborn hamsters led to the formation of sarcomas at the site of inoculation (Eddy *et al*, 1961). Later, intracranial injection of SV40 into hamsters was shown to induce ependymomas, a type of brain cancer (Kirschstein and Gerber, 1962). The Syrian golden hamster has been developed as an animal model for SV40-induced tumours with primary brain cancers, malignant mesotheliomas (Cicala *et al*, 1993), bone tumours (Diamandopoulos, 1973) and systemic lymphomas (Diamandopoulos, 1972), developing in a manner depending on route of SV40 inoculation.

The human immune response to SV40 and susceptibility to tumour formation has not been well characterised. It was first noted that some individuals developed antibodies against SV40 following exposure to contaminated vaccines (Sweet and Hilleman, 1960). In one study, adult volunteers given SV40-contaminated intranasal respiratory syncytial virus stocks, developed sub-clinical SV40 infection (Morris *et al*, 1961). Furthermore, children who received the oral polio vaccines excreted SV40 in their stools for at least

five weeks following vaccination (Melnick and Stinbaugh, 1962). These findings confirmed that SV40 may replicate in humans and raised the possibility that SV40 could be transmitted through the faecal-oral route (Carbone *et al*, 1997).

Significantly, following on from laboratory experiments using hamsters, SV40 was shown to transform many human cell types in culture (Schein and Enders, 1962). In 1964, an interesting albeit unethical study by Jensen *et al* demonstrated that SV40-transformed human cells were able to produce subcutaneous tumours when injected into human volunteers (Jensen *et al*, 1964). These SV40 transformed human cells grew as subcutaneous nodules for two weeks and then regressed, possibly because of an immune response.

Despite these initial data indicating the possible role of SV40 in human infections and transformation, follow-up epidemiological studies on the exposed population proved difficult. The requirement to monitor the vaccination over a long period of time was further complicated by incomplete details on the recipients and dosage received. Many of these follow-up studies were subsequently discontinued due to the lack of immediate side effects in vaccinated individuals observed in the years that followed administration of the polio vaccine.

Nevertheless, these early studies of SV40-mediated tumour induction in animal models indicated that SV40 was a potent cancer-causing virus and fuelled concerns about the exposure of the human population to the SV40 in contaminated polio vaccines. SV40 has since been detected in various human tissues, both normal and malignant (Vilchez and Butel, 2004). In more recent studies, evidence of SV40 exposure has been found in

people born in the years following the use of contaminated vaccines, including children, suggesting that SV40 is being transmitted in the population to this day (Butel *et al*, 1999).

The route of SV40 transmission in humans is still largely unknown. Although serological studies have yet to provide comprehensive SV40 seroprevalence data, seropositivity rates appear to be low with US studies estimating rates of between 2 and 20% of the population (Vilchez and Butel, 2004, Figure 1.2). In addition to low SV40 seropositivity, the SV40 antibody titre in humans is also low compared to the high antibody titre observed in the natural monkey host (Minor *et al*, 2003). It is thought that the low antibody titre observed in humans could be due to limited viral replication in the human host or failure of the human immune system to recognise and respond robustly to SV40 infection (Vilchez and Butel, 2003*b*).

Currently, the association between SV40 and human cancer remains controversial. The discovery of the new human polyomavirus, MCV, integrated into merkel cell tumours, and the continuing studies on the cancer association of BKV and JCV, adds weight to the association of this family of viruses with human cancer.

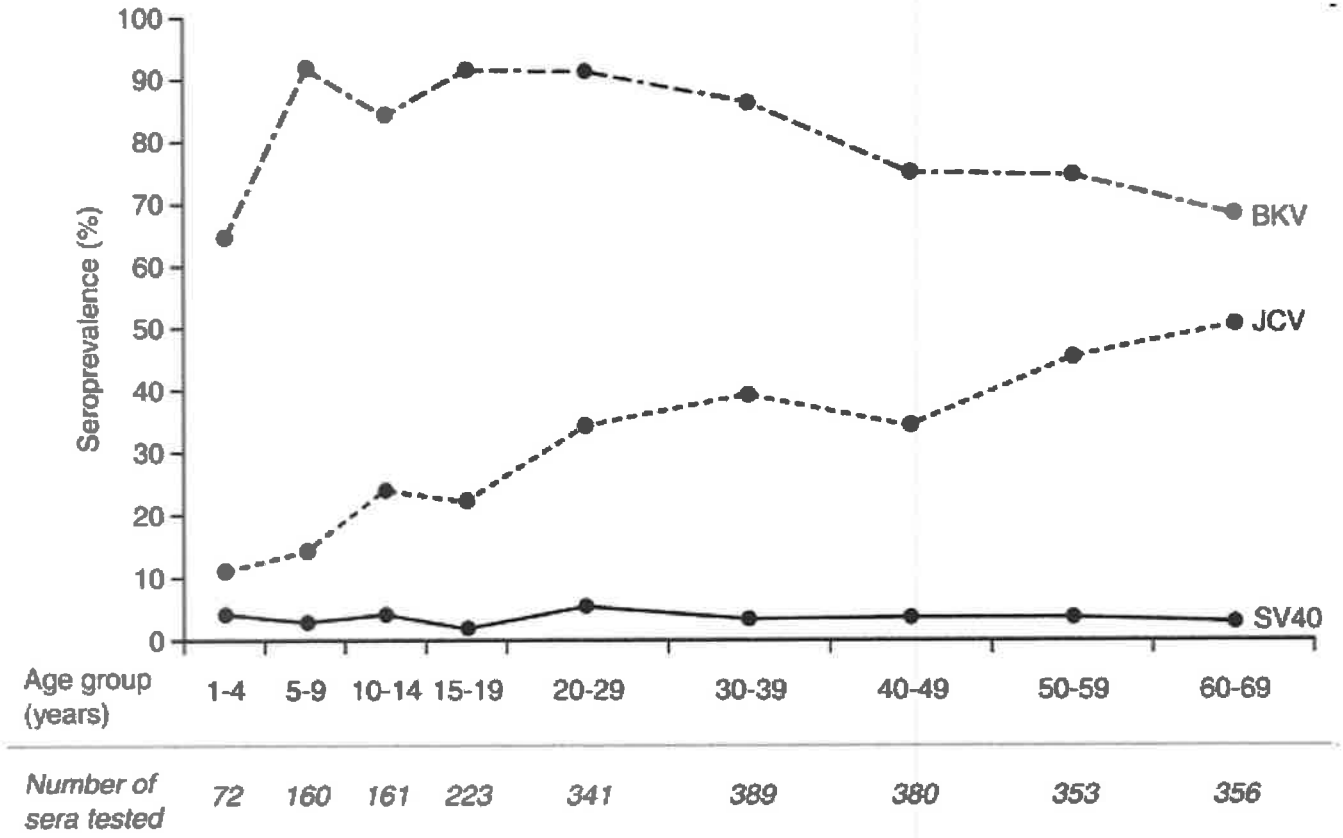

Figure 1.2: Seroprevalence of polyomaviruses SV40, BKV and JCV

Figure taken from Knowles *et al*, 2003

1.4 SV40 structure and genome

Polyomaviruses have a small virion size, with a diameter of 40-45nm. They are non-enveloped viruses with an icosahedral capsid composed of 72 pentameric capsomers. On a genomic level SV40 is closely related to BKV and JCV, sharing approximately 70% homology (Vilchez and Butel, 2004). Although these three viruses are closely related they can be distinguished at the DNA and protein levels and also serologically by neutralisation and haemagglutination inhibition assays (Butel and Lednicky, 1999). The genomic organisation of SV40, BKV and JCV is conserved with the genomes divided into three functional domains: the early region, the late region, and the regulatory region. The early genes are transcribed from one strand of the genome and the late genes are transcribed in the opposite direction from the complementary strand (Imperiale, 2001).

The SV40 genome consists of a single copy of circular superhelical double stranded DNA of 5,243bp in length in the reference strain SV40-776, with slight nucleotide variations in other strains (Butel and Lednicky, 1999). Most of the SV40 genome is conserved among isolates. There is only one known serotype of SV40 but different strains exist based on variation in the C terminus of the large tumour antigen, T-ag (Stewart *et al*, 1998). Variants are derived from differences in the regulatory region (Lednicky and Butel, 1997). The SV40 early region codes for large T-ag, small t-ag and 17kT antigen, referred to as tumour (T) antigens. The late region encodes the structural proteins VP1, VP2 and VP3 and a small regulatory protein called agnoprotein, sometimes referred to as VPx (Figure 1.3).

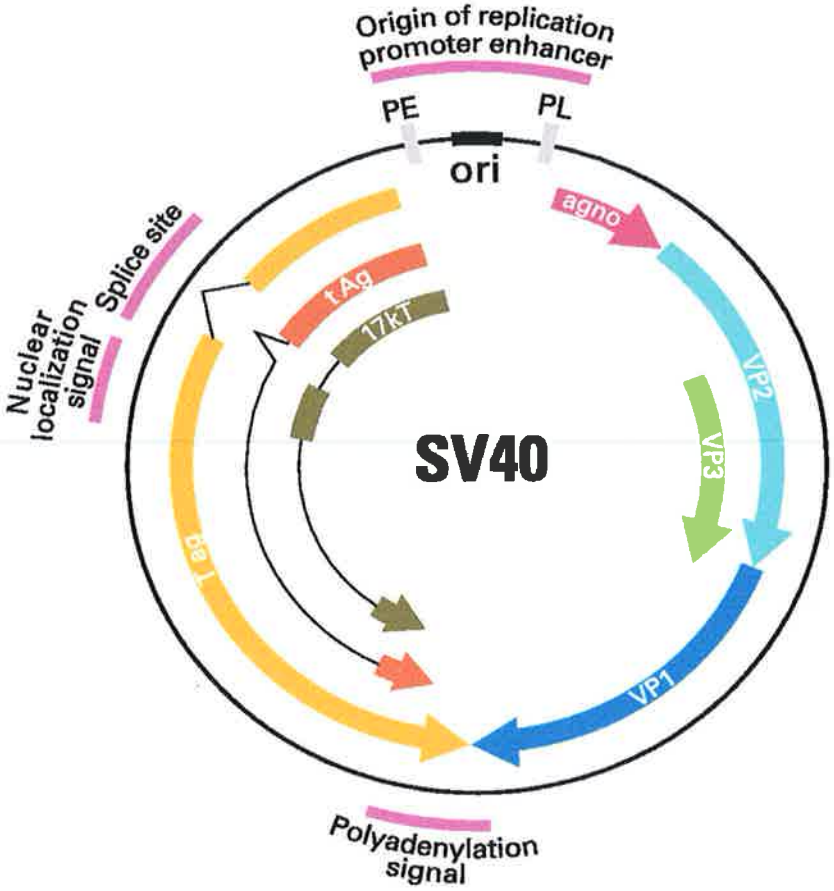

Figure 1.3: Simian virus 40 (SV40) genome organisation

Simian virus 40 (SV40) genome organization showing the large T antigen (T-ag), small t antigen (t-ag) and tiny T antigen (17kT) in the early region. In the late region of the viral genome, the capsid proteins VP1, VP2 and VP3 are shown along with the regulatory protein, agnoprotein (agno). The early (PE) and late (PL) promoters and the origin of replication (ori) in the regulatory region are also represented.

Figure taken from Poulin and DeCaprio, 2006

1.4.1 SV40 early genome region:

Large T-antigen (T-ag)

The large tumour antigen (T-ag) of SV40 is a 708 amino acid protein that has many functions. It is the major transforming protein of the virus. T-ag is required for initiation of viral DNA synthesis and stimulates host cells to enter S phase. The oncogenic capacity of SV40 stems largely from the ability of this oncoprotein to bind to and inactivate the cellular tumour suppressor proteins p53 and pRb involved in cell cycle control (Vilchez and Butel, 2003*a*). T-ag protein is found predominantly in the nuclei of SV40-infected and/or transformed cells (Carbone *et al*, 1997).

Small t-ag

Small t-ag, a 174 amino acid protein is an early gene product that modulates cell transformation through its negative regulation of the protein phosphatase 2A (PP2A) family of serine-threonine phosphatases (Ahuja *et al*, 2005). PP2A has been implicated in the regulation of numerous signalling pathways (Krumbholz *et al*, 2009).

17kT

17kT is referred to as tiny T antigen or T'. The role of this protein in SV40 infection and transformation has yet to be characterised (Saenz-Robles *et al*, 2001).

1.4.2 SV40 late genome region:

VP1, VP2, VP3

VP1 is the major capsid protein forming the pentameric capsomers that make up the surface of the virus particle (Butel and Lednicky, 1999). VP2 and VP3 are the minor

capsid proteins. These three structural proteins are the only virus-encoded proteins found in mature virions (Saenz-Robles *et al*, 2001).

VP4

VP4 is a recently described protein and its expression is thought to coincide with viral lysis. VP4 expression is thought to represent a mechanism by which SV40 regulates its life cycle to enable optimal spreading of the virus (Daniels *et al*, 2007).

Agnoprotein

Agnoprotein is a regulatory protein thought to function in virion assembly and exit from infected cells (Saenz-Robles *et al*, 2001), facilitating viral spreading (Krumbholz *et al*, 2009). Like VP4, it is produced late in infection and is not incorporated into virions (White and Khalili, 2004).

1.4.3 Regulatory region

The regulatory region of SV40 is a non-coding region of the viral genome, consisting of an origin of DNA replication and promoter/enhancer elements. It functions to orchestrate viral transcription and replication. The region contains a series of specific nucleotide motifs that serve as binding or interaction sites for proteins involved in transcription or DNA replication (Lednicky and Butel, 2001). There are two types of regulatory region structure in SV40 viruses based on the number of enhancer elements present, as illustrated in Figure 1.4. Strains having two 72-base pair enhancer elements are referred to as having a 'non-archetypal' or complex regulatory region structure. Regulatory regions lacking a duplicated enhancer element are considered 'archetypal' or simple structures (Lednicky *et al*, 1995*a,b*).

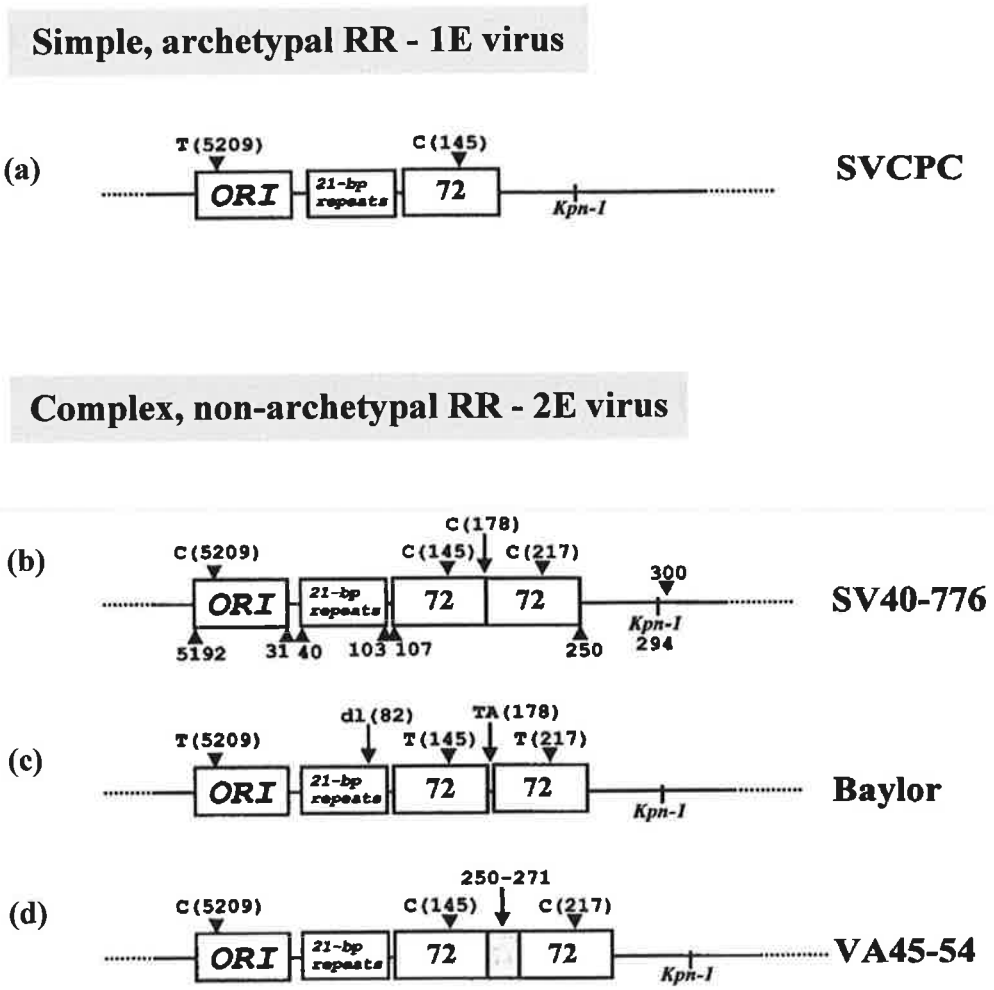

Figure 1.4: Regulatory regions of SV40 strains

Examples of the differing regulatory region (RR) of SV40 strains. The distinct functional sections with the regulatory region include enhancer elements, promoter elements and an origin of replication *ori*. There are two types of the regulatory region in SV40 viruses based on the number of enhancer elements present. Strains having one 72-base pair (bp) enhancer element are referred to as having 'archetypal' or simple regulatory region structure, (a) SVCPC. Regulatory regions containing a duplicated enhancer element are considered 'non-archetypal' or complex structures, (b) 776, (c) Baylor and (d) VA45-54. Varying numbers of 21bp repeats also exist within the G/C-rich region. Arrows indicate the polymorphisms and their nucleotide position in brackets, which exist in the strains shown.

Figure adapted from Lednicky and Butel, 2001

In the case of the reference strain of SV40-776, variants containing one enhancer element are designated 776-1E (-1E virus) while viruses with a duplicated enhancer are called 776-2E (-2E virus). These -2E viruses have been shown to replicate faster in tissue culture (Lednicky *et al*, 1995*a*). In contrast with natural isolates of SV40 or virus isolated from human tumours, which generally do not contain enhancer duplications, laboratory-adapted monkey strains of SV40 usually contain two 72-base pair enhancer elements (Vilchez *et al*, 2004). However, it is thought that a mixture of both archetypal and non-archetypal regulatory regions may be present in monkey isolates and that laboratory tissue culture allows the selection of the faster growing variants (Lednicky and Butel, 2001).

Studies have shown that the regulatory region of SV40 may exert a significant influence on tumour incidence. In studies on SV40 tumour induction in Syrian golden hamsters (*Mesocricetus auratus*), the -1E virus was found to induce tumours in a larger proportion of animals than the -2E virus (Sroller *et al*, 2008). While the faster speed of viral replication has typically been seen as an advantage for a virus in overcoming the ability of the immune system to control its growth, it has been proposed that slower replicating viruses may evoke a weaker immune response and therefore enhance their likelihood of persistence by circumventing immune surveillance (Bocharov *et al*, 2004). Based on this theory, it is thought that the faster replicating SV40 -2E virus is recognised and cleared more efficiently by the host immune response than the slower replicating -1E virus which would be more likely to evade the immune system and persist (Vilchez *et al*, 2004). It has also been recently recognised that the viral regulatory region of SV40 may exert effects on vertical transmission in hamsters (Patel *et al*, 2009). In a study investigating SV40 transmission in the hamster model it was found that hamsters inoculated with SV40 strains containing complex regulatory regions (-2E) transmitted virus more frequently

than those infected with simple enhancer (-1E) viruses. Further studies are required to determine the relationship between the regulatory region and pathogenesis of SV40 infection, including the possibility that some SV40 strains or variants are more pathogenic than others.

1.4.4 Micro RNA

SV40 also encodes a viral microRNA, one of the first miRNAs that has been shown to have a function in the virus life cycle. Cellular and viral miRNAs are small regulatory RNAs that play a critical role in gene regulation and are an important focus of molecular biology research, having only been discovered in the 1990s (Filipowicz *et al*, 2008). miRNAs function by binding to complementary sequences in the 3' untranslated regions of messenger RNA (mRNAs), and then mediating mRNA degradation or repressing translation, ultimately leading to reduced protein expression. It has been known for some time that some viral genomes include non-coding RNA such as miRNAs, but their function is only starting to come to light. Recent studies suggest that viral miRNAs may function to evade the host innate immune response, regulate gene expression and possibly contribute to viral-mediated tumourigenesis (reviewed in Cullen, 2006; Sarnow, 2006). miRNAs are useful to the virus in that they are non-immunogenic, take up a small amount of genomic space and are powerful regulators of gene expression (Sullivan, 2008).

SV40 encodes a pre-miRNA, designated miR-S1, which is processed into two miRNAs that bind to the early RNAs, thereby directing their cleavage at a late stage of the viral cell cycle (Sullivan *et al*, 2005). The end result of the miRNA action in SV40 is a reduction in the expression of viral T antigens. It is known that some protein products of early SV40 genome, such as T-ag, are very immunogenic and generate a strong cytotoxic

lymphocyte (CTL) immune response. The function of the SV40 miRNA in downregulating expression of these immunogenic proteins suggests that the miRNA is involved in immune evasion strategies. Studies conducted using a mutant SV40 virus named 776-2E-SM, that lacks the viral miRNA, have shown that target cells infected with the mutant are more sensitive to CTL-mediated death than cells infected with a wild type SV40 (Sullivan *et al*, 2005). In addition, release of the cytokine interferon-γ was also diminished when CTLs encountered cells infected with the wild type SV40. Together these results suggest that SV40 miRNA may play a role in evading the adaptive immune response (Sullivan *et al*, 2005). Viral miRNAs in the herpesviruses Epstein Barr virus (EBV), human cytomegalovirus (HCMV) and Kaposi's sarcoma herpesvirus (KSHV), have been shown to function in modulating the virus life cycle and human immune response, thereby underlining the importance of miRNAs in viral infections (Swaminathan, 2008).

1.5 The life cycle of SV40 in host cells

In the natural monkey host, SV40 infection is known to result in a lytic infection. This viral production is controlled by the immune response and the virus thus persists in the kidney where it can be reactivated in immunosuppression (White and Khalili, 2004). The life cycle of SV40 in human cells is less well understood. Cellular infection with SV40 is initiated by binding of the virion to a receptor on the cell membrane. On human cells, the Major Histocompatibility Complex class I (MHC class I) molecule is thought to be the specific cell surface receptor for SV40 (Breau *et al*, 1992; Norkin, 1999). The expression of MHC class I by nearly all nucleated cells thus explains the broad tropism of SV40 and its ability to infect and induce transformation in many types of cells and tissues (Vilchez and Butel, 2003*a*). Not all cells expressing MHC class I are, however, susceptible to SV40 infection and differential ability in infecting polarized epithelial cells via the apical or basolateral surfaces have been reported, despite similar MHC expression on both membranes (Imperiale, 2001). This indicates that other factors may contribute to SV40 tropism, such as the requirement for a co-receptor for viral entry after binding or additional transcription factors that may need to be present for viral replication to occur (Atwood, 2001).

After binding, cellular entry of SV40 occurs when the polyomavirus capsid undergoes caveola-mediated endocytosis and is transported to the nucleus (Anderson *et al*, 1996). The viral DNA is uncoated and transcription of the early region of the genome begins. The primary transcript from the early region is alternatively spliced to produce two mRNAs that encode large T-ag and small t-ag. SV40 large T-ag, a nuclear phosphoprotein, is an essential factor for viral DNA replication. It binds to the viral origin of replication where it promotes unwinding of the DNA double helix and

recruitment of cellular proteins that are required for DNA synthesis, including DNA polymerase-α and replication protein A (Martini *et al*, 2007). SV40 relies on its host cell to provide enzymes and co-factors for viral DNA replication, all of which the virus lacks (Imperiale, 2001). These proteins are expressed in the S phase of the cell cycle, the phase at which cellular DNA synthesis and subsequent cell cycle progression occurs, thereby producing the optimal environment for viral replication (Martini *et al*, 2007). Since SV40 naturally infects differentiated kidney cells in monkeys, the virus has evolved a strategy to stimulate the cell cycle through ability the of T-ag to bind to several cellular proteins that are involved in control of cell cycle progression and apoptosis (Krumbholz *et al*, 2009). Thus, in human cells, through binding to the cellular tumour suppressor proteins of the pRb family, T-ag expression leads to the induction of S phase. pRb normally binds the transcription factor E2F to form a transcriptional repressor complex. However, on binding to SV40 T-ag, a dissociation of E2F-pRb complexes occurs, releasing E2F to activate expression of growth stimulatory genes (Figure 1.5 a).

This pre-emptive signal for S phase induction and cell division and the resulting unbalanced DNA synthesis induces the cell to initiate a p53 response. p53 normally senses DNA damage and either pauses the cell cycle to repair the DNA or directs the cell to enter the apoptotic pathway, known as programmed cell death. However, T-ag overcomes this 'roadblock' by binding to p53 and inhibiting its function (Figure 1.5 b). The cell is thus induced to proliferate and the p53-mediated checkpoint is abolished. This T-ag-mediated subversion of cell cycle control allows cells with genetic damage to survive and enter S phase, leading to an accumulation of T-ag-expressing cells with genomic mutations that may promote tumour growth as an accidental side effect of the viral replication strategy.

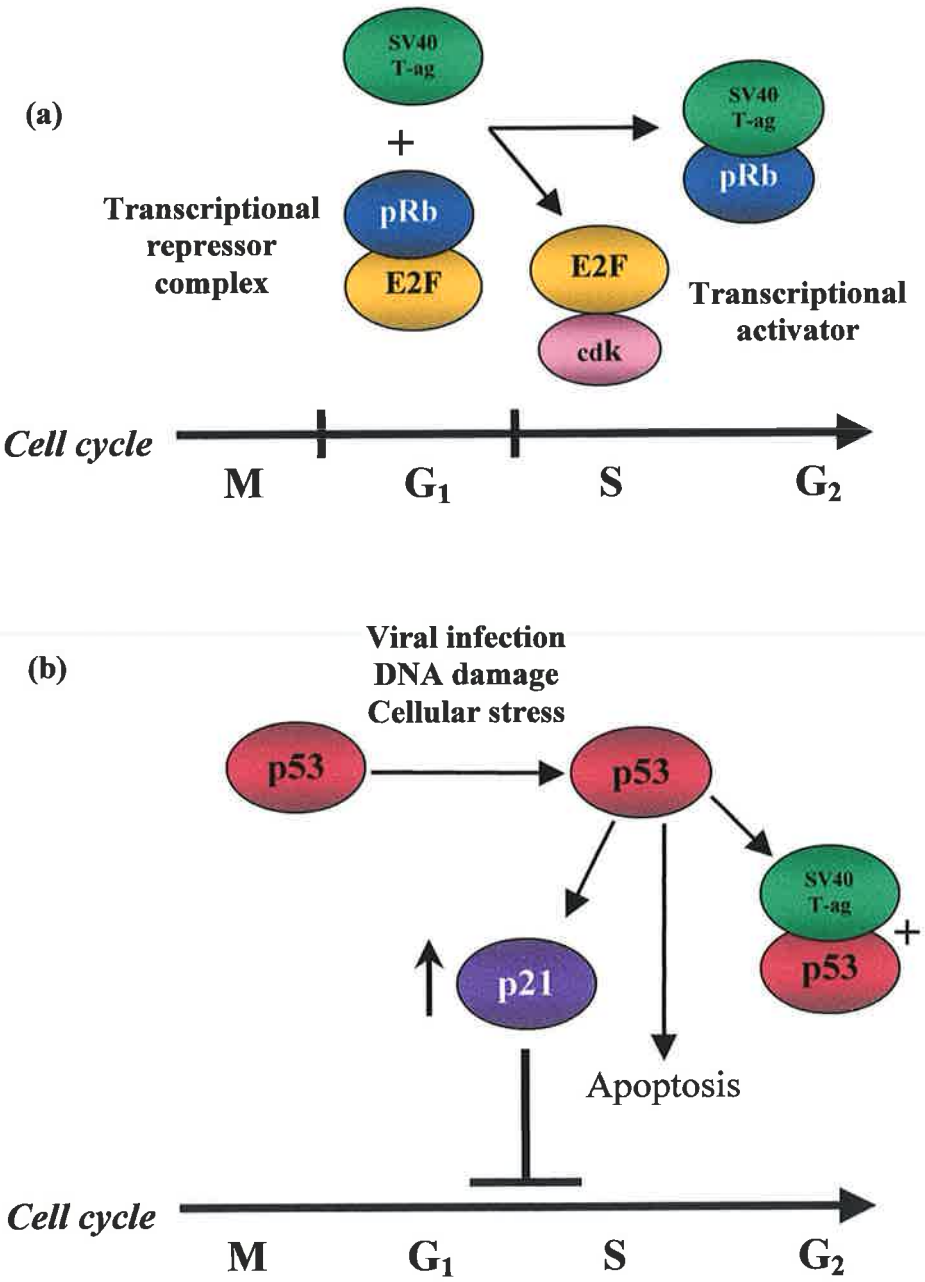

Figure 1.5: Interaction of SV40 T-ag with pRb and p53
Schematic representation of the interaction of SV40 T-ag with tumour suppressor proteins pRb and p53. (a) pRb normally binds transcription factor E2F, forming a transcriptional repressor complex in early G_1 phase of the cell cycle. Normally, when pRb is phosphorylated by cyclin-dependent kinases (cdk), E2F is released and activates growth-stimulatory genes. T-ag binding to pRb causes unscheduled dissociation of pRb-E2F complexes, releasing active E2F. (b) The function of p53 is to sense DNA damage and either cause the cell to pause in late G_1 phase for DNA repair or direct the cell to commit suicide through the apoptotic pathway if repair is not possible. p53 can transcriptionally induce p21, a cyclin-dependent kinase inhibitor, which blocks the activity of G_1 cyclin-cdk complexes arresting cell cycle progression in late G_1 phase. Binding of the SV40 T-ag results in p53 being sequestered, abolishing its function and allowing cells with genetic damage to survive and enter S phase. As a result, T-ag-expressing cells with genomic mutations accumulate that may promote tumourigenic growth.

Figure adapted from Lednicky and Butel, 2003,

In a lytic infection in the natural host, the purpose of the T-antigen interaction with host cell proteins is to drive the cell into an optimal environment for the support of viral DNA replication and to maintain cellular viability as long as possible to facilitate virus production (Imperiale, 2001). The role of the small t-ag in the polyomavirus life cycle is less clear than that of large T-ag. Small t-ag is not essential for lytic infection in culture but it is known to co-operate with T-ag in the transformation of cells by SV40 and increases virus yield in permissive cells (Martini *et al*, 2007).

As SV40 virus replication proceeds, expression of the late genes begins. The gene products of the late region are the capsid proteins VP1, VP2, VP3, which assemble with the replicated viral DNA to form virions. In infection of the natural monkey host these virions are released upon cell lysis, resulting in death of the host cell (Martini *et al*, 2007). The life cycle of SV40 from infection to the production of new virions is thought to take 96 hours in permissive cells, resulting in about 300 infectious progeny virions per cell (Saenz-Robles *et al*, 2001, Figure 1.6).

Although polyomaviruses grow most efficiently in the cells of their natural host species they do not display absolute host specificity (Krumbholz *et al*, 2009). There is more than one possible outcome to cellular infection by a polyomavirus. In the natural host, cells are permissive to viral infection and are able to support viral replication with resultant lytic infection and viral amplification (White and Khalili, 2004). In general, these infections are non-oncogenic for their natural hosts (zur Hausen, 2008). However, SV40 and other tumour viruses may become more oncogenic when they cross species (Carbone *et al*, 2003).

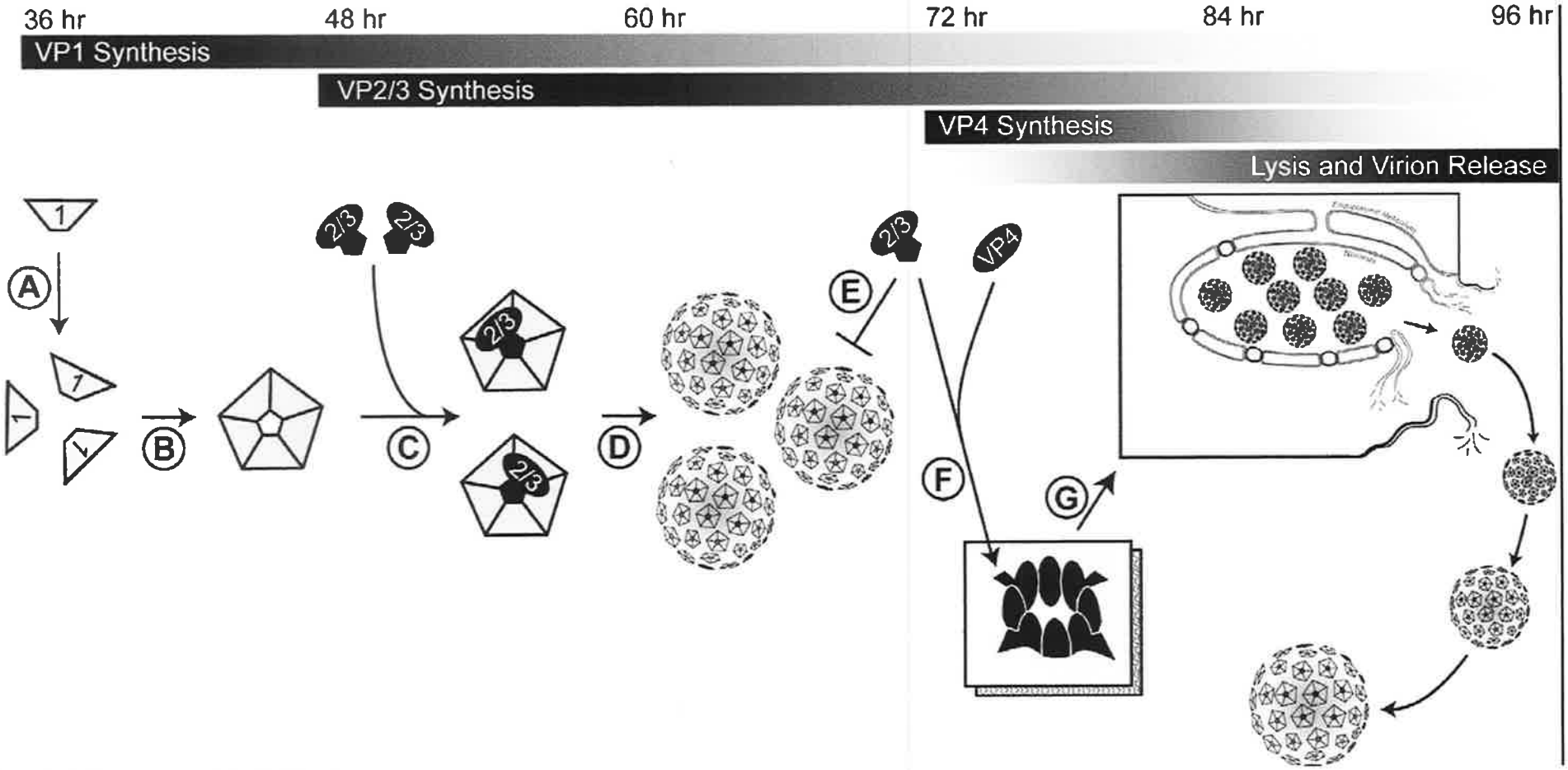

Figure 1.6: Proposed model of SV40 life cycle

Figure taken from Daniels et al, 2007

In a foreign host such as the mouse, cells are non-permissive to SV40 due to an inability to use the host DNA polymerase for viral synthesis. Infection in a non-permissive host thus results in cell transformation (Imperiale, 2001, Figure 1.7). In contrast, some human cell types can support transformation and low-level SV40 replication and may be described as 'semi-permissive' for SV40 infection (White and Khalili, 2004). Furthermore, it has been reported that cell type differences may dictate the outcome of SV40 infection in humans. Studies have shown that while SV40 infection of human fibroblasts leads to a productive outcome with viral replication, the virus establishes a persistent, non-lytic infection in mesothelial cells (Bocchetta *et al*, 2000).

In SV40 non-permissive and semi-permissive cells, transformation is thought to occur when there is a block in productive infection, but continuing expression of T-ag. This viral replication block leads to cell proliferation in the absence of cell death, ultimately resulting in tumour formation in the non-natural host (Imperiale, 2001). The rate-limiting step to sustained transformation is thought to be the random integration of viral DNA into the cellular genome by non-homologous recombination. If this integration occurs such that the early coding sequences are intact allowing T-ag to be expressed, the host cell and its subsequent descendants are transformed (Ahuja *et al*, 2005).

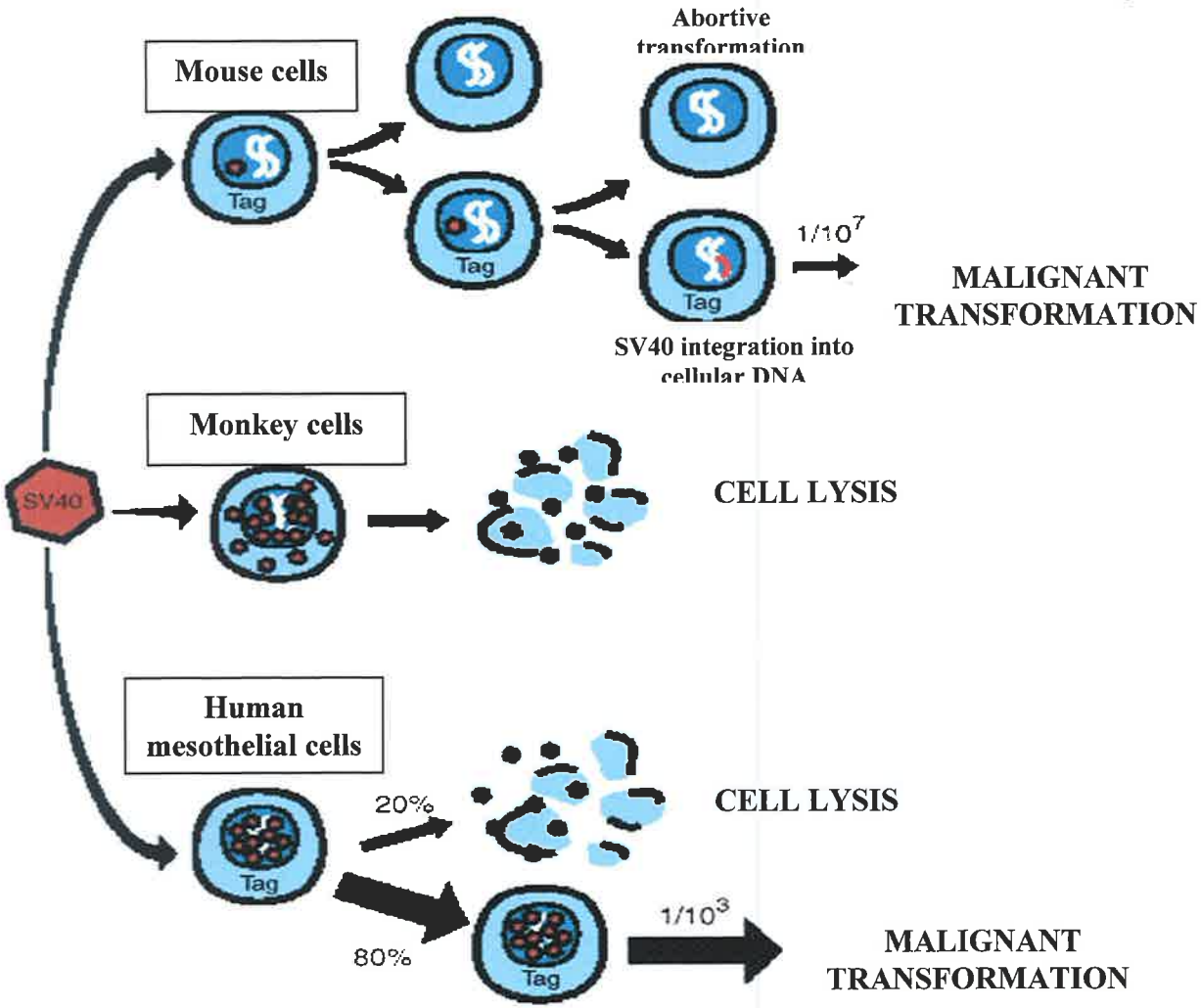

Figure 1.7: Possible outcomes of SV40 infection
(Top) In SV40 infection of non-permissive mouse cells, no viral particles are produced and malignant transformation can occur. (Middle) Infection of permissive monkey cells results in many viral particles being produced and the cells are lysed. (Bottom) Infection of human mesothelial cells leads to limited viral production, limited cell lysis and frequent malignant transformation.

Figure adapted from Carbone *et al*, 2003

1.6 SV40 association with human cancer

SV40 has been proven to be a potent transforming virus, having been shown to induce tumours in laboratory animal models and various types of cells *in vitro*. More recent evidence from serological and molecular studies revealing its presence in the humans raise the possibility that the virus could have transforming capabilities in human cells *in vivo* as well as *in vitro*.

SV40 and Brain Tumours

In early studies conducted in the 1960s and 1970s, SV40 was initially found in rare cases in human brain tumours, supporting previous findings showing SV40-induction of brain tumours in hamsters. However, the viral detection methods used at the time were based on Southern hybridisation techniques, immunostaining for large T-ag and electron microscopy and were of relatively low sensitivity (Garcea and Imperiale, 2003). The introduction of amplification-based detection methods such as polymerase chain reaction (PCR) in 1992 brought about a breakthrough in SV40 research, providing a sensitive method of DNA detection in human samples. Consequently, in that same year, there was a reported finding of SV40-like DNA sequences by PCR and large T-ag expression in two types of rare childhood brain tumours, with SV40 DNA sequences detected in 50% of choroids plexus neoplasms and most of the ependymomas examined (Bergsagel *et al*, 1992). On further analysis, DNA sequencing revealed the presence of authentic SV40 DNA sequences (Lednicky *et al*, 1995*b*). Furthermore, following lipofection of the tumour DNA into monkey kidney cells, infectious SV40 virus was recovered and it was observed that the regulatory region contained an unduplicated enhancer element (-1E virus), a characteristic of direct primate isolates (Lednicky *et al*, 1995*b*).

Since these landmark studies investigating the oncogenic role of SV40, there are continuing reports of SV40 detection in brain tumours (reviewed in Vilchez *et al* 2003). Not only has the virus been detected but SV40 T-ag has also been found complexed with tumour suppressors p53 and pRb in brain tumours, providing further evidence of a direct functional role for the virus in tumourigenesis (Zhen *et al*, 1999). In addition to patient studies, an interesting report was published detailing the development of a meningioma in a laboratory scientist who had worked with an SV40-transformed cell line (Arrington *et al*, 2004). This brain tumour was found to contain SV40 DNA sequences indistinguishable from the laboratory virus, suggesting that laboratory-acquired SV40 infection may have been responsible for tumour development. A meta-analysis of the association of SV40 with brain tumours revealed that samples from patients with brain tumours were almost four times more likely to have evidence of SV40 infection than those from controls (Vilchez *et al*, 2003).

SV40 has been detected in multiple histological types of brain tumour, in both children and adults. Indeed, since brain tumours represent 21% of all cancers in children, it has been hypothesised that this high incidence of paediatric brain tumours may suggest acquisition of an infectious agent such as SV40 from the mother (Vilchez *et al*, 2003). Brain tumour incidence in the US has increased by 20% since 1973 but it is unknown if the introduction of SV40 into the human population may in some way be linked to this increase (Carbone *et al*, 1997).

SV40 and malignant mesothelioma

In addition to the link with brain tumours, SV40 has also been associated with malignant mesothelioma. Early studies demonstrated that mesothelioma was induced in 100% of hamsters when SV40 was injected into the pleural cavities (Cicala *et al*, 1993). Subsequently, using the same PCR-based strategy employed to detect SV40 in brain tumours, SV40 DNA sequences were detected in 60% of human mesotheliomas compared with 5% in malignant and non-malignant control samples (Carbone *et al*, 1994). Microdissection studies appeared to confirm the specificity of these positive findings in human tumours by showing that SV40 was present only in the malignant cells and not in the surrounding non-cancerous cells (Shivapurkar *et al*, 1999).

Malignant mesothelioma is an aggressive tumour of the lung pleura, pericardium or peritoneum, with mean patient survival of only one year from time of diagnosis (Rizzo *et al*, 2001). Mesothelioma has been firmly linked to asbestos exposure. However, since 10-20% of occurrence is in people with no known exposure and only 5-10% of those exposed to high levels of asbestos develop this type of cancer, it is thought other factors may be involved in mesothelioma development (Bocchetta *et al*, 2000). Asbestos and SV40 have been shown to be co-carcinogens, with SV40 infection lowering the amount of asbestos required for malignant mesothelioma to develop in hamsters. This raises the possibility that SV40 may act as a co-factor in other cancer types (Kroczynska *et al*, 2006).

Whilst malignant mesothelioma was almost unknown before 1960, in a similar trend to brain tumours, incidence of this cancer has increased significantly in the past few decades to almost 2,000 cases per year in the US (Carbone *et al*, 1997). Furthermore, it has been

observed that there is a low incidence of mesothelioma in countries that did not receive SV40-contaminated vaccines, such as Finland, providing a possible link between increased mesothelioma incidence and the distribution of contaminated vaccines (Hirvonen *et al*, 1999). The association between SV40 and malignant mesothelioma appears to be the strongest for any SV40-associated cancer (Garcea and Imperiale, 2003).

SV40 and bone tumours

Like brain tumours and mesothelioma, the association of SV40 with bone tumours was preceded by studies in rodents, showing that sarcomas of different histiotypes could be induced in these animal models (Diamandopoulos, 1973). SV40 was first detected in bone tumours in a study designed to screen 200 different human (Carbone *et al*, 1996). Out of 200 samples, 18 were positive for SV40 and of these positives, 11 were osteosarcomas, thus uncovering a possible link to tumours of the bone. A follow up study detected SV40 in about 30% of osteosarcomas and 40% of other bone-related tumours compared with none in cancer controls, strengthening the initial observation (Carbone *et al*, 1996). Additional research supported this association with the further finding of SV40 in bone tumours (Lednicky *et al*, 1997; Mendoza *et al*, 1998; Martini *et al*, 2002). In one of these studies, integration of SV40 into the host genome was observed in half of the osteosarcoma tumours analysed in addition to the detection of mutations in the p53 and pRb tumour suppressor genes (Mendoza *et al*, 1998).

1.7 SV40 association with Non-Hodgkin's Lymphoma (NHL)

While the tumour types induced by SV40 in hamsters are of the same spectrum as human tumours containing SV40 DNA, it is only in the past decade that the role of the virus has been investigated in human lymphomas. This is despite the fact that the lymphomagenic potential of SV40 had long been established in laboratory animals, where it was shown that 72% of hamsters developed lymphomas when inoculated with SV40 intravenously, compared with none in the control un-inoculated group (Diamandopoulos, 1972). The histological type of the resulting tumours was consistent with diffuse large cells and the lymphomas were shown to be B-cell in origin, expressing cell surface antigen (Coe and Green, 1975). Other studies have also shown that lymphomas were one of the most common malignancies induced by SV40 in animals (Cicala *et al*, 1992). These studies supported a causative role for the virus in lymphomagenesis because SV40 T-ag was expressed in all tumour cells, the animals with tumours developed antibody against SV40 T-ag and neutralisation of infectious SV40 with specific antibody before virus inoculation prevented lymphoma development (Vilchez *et al*, 2002).

Not surprisingly, knowledge of these animal studies initiated consideration of a role for SV40 in human lymphomagenesis. In humans, SV40 as well as the human polyomaviruses BKV and JCV, have been found in the peripheral blood mononuclear cells of normal human donors (Martini *et al*, 1996; Martini *et al* 1998*a*; David *et al*, 2001). A recent study has also detected SV40 in the B cell rich tonsillar tissue of immunocompetent children (Patel *et al*, 2008). This implies that SV40 could have a tropism for the lymphatic system, a factor that would be very significant in trafficking the virus around the body and in pathogenesis.

In the investigation of human lymphomas, SV40 was found to be significantly associated with Non Hodgkin's Lymphoma (NHL). NHL includes a group of more than 20 different malignant lymphoproliferative diseases arising from B and T lymphocytes and NK cells (Grulich and Vadic, 2005). Although the exact aetiology of NHL is unknown, some infectious agents are known to cause NHL by lymphocyte transformation, as is the case with EBV and Burkitt's lymphoma, KSHV and primary effusion lymphoma and Human T Lymphotropic virus type 1 (HTLV-1) and adult T-cell leukaemia/lymphoma. Furthermore, it has been suggested that viruses such as hepatitis C may also increase risk of NHL through chronic immune stimulation in a chronic infection (Engels, 2007). However because commonly associated infectious agents such as EBV, KSHV and HTLV-1 are not present in all NHL cases, it is possible that other oncogenic viruses are involved. Immunodeficiency is considered a major risk factor for the development of NHL, and it is a common malignancy in HIV-infected patients as a result of deficient immunosurveillance of oncogenic viruses.

In 2002, two independent studies investigating human lymphomas found a significant association between SV40 and NHL, with the finding of SV40 T-ag DNA in 42% and 43% of specimens tested (Vilchez *et al*, 2002; Shivapurkar *et al*, 2002). In the study by Vilchez *et al* lymphoma samples were screened for the polyomaviruses, SV40, BKV and JCV, as well as EBV and KSHV using PCR, Southern blot hybridisation and subsequent DNA sequence analysis. The sample population tested consisted of systemic lymphoma samples from 76 HIV-positive and 76 HIV-negative patients and included controls from other cancer types and healthy lymphoid tissue. SV40 sequences were found in forty-two percent of the lymphoma samples compared with none in the control samples (Vilchez *et al*, 2002). Interestingly, of the SV40-positive samples, 50% were from HIV-

negative and 33% from HIV-positive individuals. In contrast, detection of EBV was more commonly associated with HIV-positive patients, correlating with previous reports, which found that EBV-lymphoma was mostly associated with immunodeficiency. While it has previously been suggested that immunosuppressed patients may be at risk of SV40-related disease similar to the human polyomaviruses BKV and JCV, these data indicate that SV40 positive NHL does not appear to be dependent on pronounced immunodeficiency in the host (Vilchez *et al*, 2002). Although the natural history and dynamics of SV40 infections in HIV infection and other immune-deficiencies is not yet understood (Vilchez *et al*, 2006), these observations may be explained by the semi-permissive nature of human cells to SV40 infection, whereby viral replication restrictions may remain in place, even in an immunocompromised host (Martini *et al*, 2007).

Since the initial establishment of SV40-NHL association, more reports have followed in which SV40 T-ag DNA sequences or protein were detected in human NHL samples (Table 1.2). In these studies, SV40 was most often found in diffuse large B cell lymphoma and follicular lymphoma, two of the most common histologic types of B cell lymphomas accounting for approximately 50-60% of all cases of NHL (Vilchez and Butel, 2003*a*). The finding of SV40 in these particular types of NHL raises the question about the significance of the developmental stage of B cells in the progression to lymphoma and suggests that mature B cells may be more susceptible than precursor cells to the transforming potential of SV40. Furthermore, SV40 has been found in the germinal centre B-cell like (GCB) type of diffuse large B cell lymphoma. As these GC B cells are poised for apoptosis, SV40 may function to induce transformation through apoptosis inhibition, a common mechanism used by oncogenic viruses (Vilchez *et al*, 2005).

Table 1.2: PCR detection of SV40 DNA in human lymphoma samples

Study	Country	Detection of SV40 DNA No. positive / no. tested (%)	
		Lymphoma	Control
Amara *et al.*, 2007	Tunisia	63/108 (56)	4/60 (6)
Zekri *et al.*, 2007	Egypt	85/158 (54)	4/34 (12)
Shivapurkar *et al.*, 2002	US	29/68 (43)	5/120 (4.2)
Vilchez *et al.*, 2002	US	64/154 (42)	0/240 (0)
Shivapurkar *et al.*, 2004	US	33/90 (36)	1/56 (1.2)
Meneses *et al.*, 2005	Costa Rica	30/125 (24)	0/91 (0)
Vilchez *et al.*, 2005	US	12/55 (22)	0/19 (0)
David *et al.*, 2001	US	15/79 (19)	19/187 (10)
Martini *et al.*, 1998*b*	Italy	11/79 (14)	3/50 (6)
Chen *et al.*, 2006	Taiwan	13/91 (14)	0/106 (0)
Nakatsuka *et al.*, 2003	Japan	14/122 (11)	3/64 (4.7)
Capello *et al.*, 2003	Spain, Italy	17/500 (3)	0/15 (0)
Daibata *et al.*, 2003	Japan	3/125 (2)	0/31 (0)
MacKenzie *et al.*, 2003	UK	0/152 (0)	0/45 (0)
Sui *et al.*, 2005	Tasmania	0/50 (0)	0/50 (0)
Schüler *et al.*, 2006	Germany	0/77 (0)	0/61 (0)

Studies are ranked based on the percentage positive samples positive for SV40, indicated in brackets.
*Control = non-malignant lymphoid samples and cancer controls - samples from cancer types other than lymphoma

Despite this evidence, some other researchers have failed to detect SV40 in human lymphoma samples (MacKenzie *et al*, 2003, Sui *et al*, 2005, Schüler *et al*, 2006). It is speculated that this negative data could be due to technical difficulties in laboratory detection of SV40 or geographic variation according to the distribution of SV40-contaminated polio vaccines. Another possibility is that this variability in SV40 detection could be due to the characteristics of a particular population, with existence of variation in the ethnic susceptibility to SV40.

As for other SV40-associated cancers, there has been a dramatic increase in NHL incidence in the last 30 years, with an 80% increase in the US noted between 1973 and 1997 (Staudt and Wilson, 2002). Although the role of some viral agents such as EBV have been firmly implicated in certain lymphoma types, questions arise regarding the possibility of SV40 being linked to this increase, and whether it is a causative agent of NHL. As yet, studies investigating the role of SV40 in NHL have raised more questions than answers; is the association of SV40 with NHL causal or incidental? Does SV40 initiate tumourigenic events in NHL or do tumours offer a microenvironment that favours viral replication in humans with latent SV40 infection? (White and Khalili, 2004). These are important questions that have yet to be addressed experimentally.

Although a significant body of research has investigated the presence of SV40 in human lymphoma samples, few studies have focused on the mechanism of SV40 interaction with human lymphocytes. In one small-scale study, Dolcetti *et al* described the presence and persistence of SV40 in EBV-immortalised B-lymphocyte cell lines for a time period of about 4-6 months (Dolcetti *et al*, 2003). Few experimental methods are detailed, however, and the sensitivity of the SV40 detection method used is questionable. In

addition, the presence of EBV in some cell lines examined raises concern about the contribution of EBV to the cellular effects observed and its ability to perhaps limit SV40 replication. In another brief study by Shaikh, SV40-negative B-lymphocyte cell lines were infected with SV40 and monitored for productive infection after two days (Shaikh *et al*, 2004). In this study, virus levels were examined and found to be low, but samples for SV40 detection were taken at only one early time point when little effects would be expected. Nevertheless, despite the limitations of these studies, the results indicated the potential role for SV40 in lymphomagenesis and encouraged much needed investigation to examine the relationship of SV40 with lymphocytes and the effect of the virus on this type of human cell.

1.8 Methods used for the study of SV40 lymphomagenesis

To date conventional methods used to study viral-lymphocyte interaction rely on the monitoring of cell growth following *in vitro* viral infection. More recently, the application of molecular biology techniques has increased specificity and sensitivity for detecting and quantifying a viral genome and its expression.

1.8.1 Cell culture

As with all viruses, the interaction of SV40 with human cells can be examined by the use of a cell culture system. Early tissue culture studies carried out after initial discovery of SV40 showed that the virus was capable of transforming a number of cell types *in vitro,* including human cells (Schein and Enders, 1962). These studies proved invaluable in investigating the effect of the virus on human cells. Cell culture analysis is, however, limited when used in isolation and much more information can be gained by the more sensitive molecular technology currently available.

When studying lymphocytes, primary cells or immortalised cell lines can be used. A primary lymphoid cell culture comprises a heterogeneous group of cells isolated from a human that have a finite life span in *ex vivo* culture. Primary cells are useful because they are normal cells that have not been passaged extensively in culture and these cells carry the same genetic complement as the host from which they were derived (Ahuja *et al*, 2005). Therefore, they may be more representative of an *in vivo* viral-cell interaction. However, primary cells are difficult to work with because they can only be cultured for a limited time before the cells stop dividing, meaning that it is not feasible to use them in studies over a period of time. In addition, primary cells consist of a mixture of cell types and samples differ between donors. These mixed cells may respond differently to

oncogenic signals, complicating the interpretation of experimental results (Ahuja *et al*, 2005).

To avoid the problems of primary lymphoid cell cultures, cloned lymphoid cell lines are used in viral-lymphomagenesis studies. In contrast to primary cells, tumour cells or normal cells that have undergone chemical or viral transformation, referred to as cell lines, can be propagated indefinitely in tissue culture and are said to be immortal (Kindt *et al*, 2007). The great advantages of cloned lymphoid cell lines are that they can be grown for extended periods in tissue culture, abundant samples of cells may be obtained at any time and because the cells are homogeneous this allows experiments to be reproducible and enables the development and optimisation of experimental techniques. Of course, since cell lines are derived from tumour cells or transformed cells, they may have unknown genetic contributions characteristic of the tumour or of the transformed state. Caution must therefore be exercised when extrapolating results obtained with cell lines to *in vivo* viral-host cell interaction (Kindt *et al*, 2007). Nevertheless, cell lines have made a major contribution to the study of virology and immune system responses, and many molecular events discovered in experiments using transformed cell lines have been shown to mirror events in normal lymphocytes *in vivo* (Kindt *et al*, 2007).

To date, there have been limited studies of SV40 lymphomagenesis using lymphocyte cell lines. In particular, studies have lacked a controlled optimised design approach in which viral-lymphocyte interaction is monitored over time. Such a time course experiment could offer novel insights into the mechanism of interaction between this monkey virus and human lymphocytes.

1.8.2 Flow Cytometry

Up until the 1980s, the lymphocyte cell surface was largely uncharacterised. The advent of monoclonal antibodies allowed the identification of lymphocyte specific surface molecules. These markers were designated as 'clusters of differentiation' (CD) by the World Health Organisation (WHO). Among the functions of these molecules is the regulation of lymphocyte development and in facilitating communication with the extracellular environment via a network of cytokines and transcription factors (LeBien and Tedder, 2008). Flow cytometry is a valuable technique for lymphocyte characterisation, enabling the investigation of cell surface markers and cellular protein expression. This method allows the simultaneous measurement and analysis of multiple physical characteristics of a single cell as it flows in a fluid stream through a beam of light (BD Biosciences, 2000). It is a quickly expanding technology that has increased in popularity since the 1970s and is now used frequently in the investigation of the immune response to infectious agents.

A flow cytometer consists of three main systems: fluidics, optics and electronics. The fluidics system transports cells in single file in suspension to the optics system, which consists of lasers to illuminate the cells. The light scattered and fluorescence emitted by the cells is then filtered and collected and the resulting light signals are directed to the appropriate detectors. The electronics system then converts the detected light signals into signals that can be processed by a computer using specialised software (BD Biosciences, 2000).

Light scattering occurs when laser light strikes a cell/particle causing the incident light to be deflected. The extent to which this occurs depends on the physical properties of a

particle, namely its size and internal complexity. Forward-scattered light (FSC) is light that is scattered in the forward direction, along the same axis as the laser is travelling, and is detected in the forward scatter channel. The intensity of this signal is proportional to the cell-surface area or size. Laser light that is scattered at 90° to the axis of the laser path is termed side-scattered light (SSC) and is detected in the side scatter channel. The intensity of this signal is attributed to cell granularity or internal complexity (Figure 1.8).

In flow cytometry, cell surface marker expression on lymphocytes is measured using fluorochrome-labelled target specific antibodies. These fluorophores absorb light energy at one wavelength (excitation) and emit light at another wavelength (emission) that is characteristic for that compound. A number of different fluorescent labels can be used simultaneously as long as the peak emission wavelengths do not overlap.

Flow cytometry is commonly used in the diagnostic laboratory for immunophenotyping of leukaemia and lymphoma cases, where the severity of disease can correlate to the cell surface markers expressed (Kwong, 2007). In addition, flow cytometry can be used to analyse cell surface and intracellular markers in virally infected cells. Cell surface expression of proteins such as MHC and co-stimulatory molecules is required to initiate and sustain an antigen-specific immune response. Ablation or alteration of the surface expression of these molecules involved in forming an immunological synapse between virus-infected and immune system cells is exploited by viruses for immune evasion (Tortorella *et al*, 2000). Co-stimulatory markers such as CD80 and CD86 (also known as B7-1 and B7-2) are present on the surface of antigen presenting cells (APCs), which include B-lymphocytes. Interaction of APCs with T cells is required for T cell activation

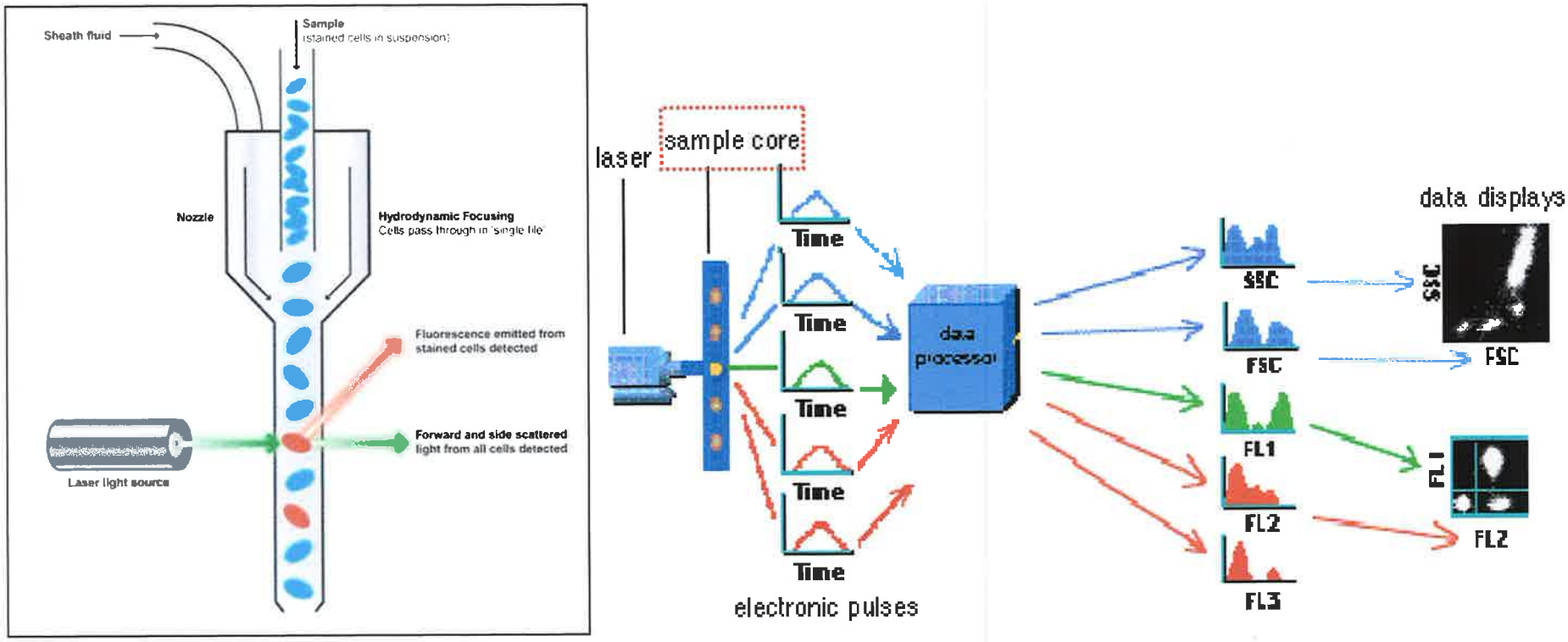

Figure 1.8: Principle of flow cytometry

A stained cell suspension is shown entering sample core in single file and then being transported to the optics system where lasers illuminate the cells. The resulting scattered and emitted light signals are detected and converted to electronic pulses that can be processed by the computer to produce data displays of side scattered light (SSC), relating to cell granularity, forward scattered light (FSC), attributed to cell size, and fluorescence emission from fluorochrome labelled antibody (FL-1, FL-2 and FL-3).

Figure adapted from BD Biosciences, 2000

in the generation of a specific immune response. In T cell-APC interaction, the T cell receptor (TCR) engages with antigenic peptides presented by MHC molecules on the APC. This MHC-TCR interaction alone is insufficient for T cell activation and co-stimulatory signals are required generated by the interaction of CD28 on the T cell with CD80 and CD86 on the APC (Figure 1.9).

Other cell surface markers commonly examined in lymphocyte interactions are activation markers such as CD25 and CD69. CD69 is one of the earliest molecules to be expressed following stimulation and is therefore used as a marker of lymphocyte activation *in vivo* and *in vitro* (Ziegler *et al*, 1994). CD69 is an early membrane receptor transiently induced on B and T lymphocytes in addition to many other haematopoietic cells (Marzio *et al*, 1999). Although the precise role of CD69 is unknown, with its specific ligand also yet to be identified, expression of CD69 is thought to activate cytokine gene expression and lymphocyte proliferation (Marzio *et al*, 1999). It is thought that CD69 is likely to be a pleiotropic immune regulator involved in the activation of a wide variety of haematopoietic cells and may act as a regulatory molecule in the modulation of an inflammatory response (Sancho *et al*, 2005).

Although the ability of other viruses to modulate these cell surface molecules has been documented, this phenomenon has not yet been examined in human lymphocytes infected with SV40. Unlike other SV40-cancer associations, since the target lymphocytes are immune cells, this provides the opportunity of studying SV40 lymphocyte-interaction in terms of viral effect on an array of surface markers and immune mediators involved in the immune response. This analysis could offer clues to understanding SV40 persistence and lymphomagenesis.

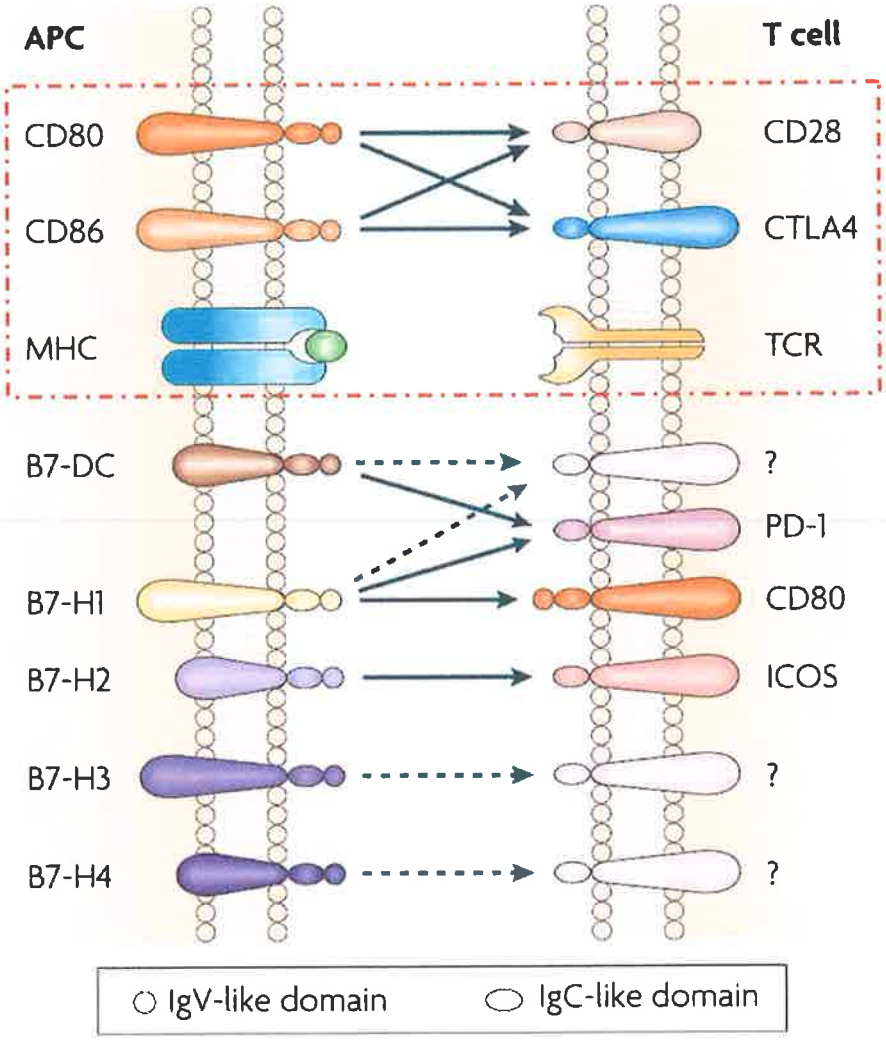

Figure 1.9: Interaction of co-stimulation molecules CD80 and CD86 with T cells
Diagram of immunological synapse structure showing interaction of surface markers CD80 and CD86 on antigen presenting cells (B cells, dendritic cells or macrophages) with CD28 and CTLA-4 on T cells. Antigen presenting cells present a specific antigen on MHC molecules to the T cell receptor of T cells. Co-stimulatory signals are required for optimal T cell activation and are generated by binding of CD80 and CD86 on antigen presenting cells to CD28 on T cells. CTLA-4 is the co-inhibitory counterpart of CD28.

APC; antigen presenting cell, CD; cluster of differentiation, MHC; major histocompatibility complex, TCR; T cell receptor, CTLA-4; cytotoxic T lymphocyte-associated-4

Figure taken from Zou and Chen, 2008.

In addition to surface marker interactions, flow cytometry can be used to investigate intracellular viral proteins. A recent study investigating SV40-lymphomagenesis in the Syrian golden hamster model demonstrated the usefulness of flow cytometry in characterising populations of lymphoid cells and also in the detection of intracellular SV40 large T-ag (McNees *et al*, 2009). SV40 T-ag is the major viral oncoprotein and a necessary component for viral replication. T-ag expression in human and animal tissues has been performed using immunohistochemical and immunofluorescent staining. Flow cytometry offers the advantages of generating quantitative data in multiple parameters simultaneously.

1.8.3 Nucleic acid detection of SV40 DNA

Prior to the introduction of nucleic acid amplification methods, SV40 molecular detection methods were largely based on DNA hybridisation strategies. Whilst these probe-based methods offered a high level of specificity, they lacked equivalent levels of sensitivity. The advent of conventional PCR-based techniques in the early 1990s provided a more sensitive method of viral nucleic acid detection and soon became the preferred diagnostic method (Garcea and Imperiale, 2003). In more recent years, PCR-based methods have been further developed to offer improved performance and greater potential in the field of virology.

In the last ten years, real-time PCR has emerged in the field of molecular biology and is now used in an increasing number of applications. In contrast to conventional or end-point PCR, in real-time PCR systems the target DNA is amplified and detected on an automated analytical platform. Amplicon accumulation is detected in real time using a fluorescent reporter instead of conventional gel electrophoresis. The target DNA is measured during each PCR cycle rather than standard end-point detection. This real-time detection of PCR product not only facilitates exquisite detection sensitivity and confirmation of product, but most importantly it facilitates quantification of target DNA i.e. real time quantitative PCR (RQ-PCR).

Principle of RQ-PCR

An RQ-PCR reaction contains all the components used for conventional PCR with the addition of a fluorescent reporter. Since the reporter only fluoresces when associated with the amplicon, the increase in recorded fluorescence signal during amplification is in direct proportion to the amount of amplification product in the reaction. During the early

cycles of the amplification reaction, background fluorescence is measured. Detection of a target gene occurs at the threshold cycle, C_T, the cycle in which the normalised reporter fluorescence increases ten standard deviations above the mean background fluorescence in the first 15 cycles. Test samples are analysed in the same assay as external standard controls, and quantification of genes is then extrapolated from a standard curve generated by plotting C_T versus copy number of target gene.

Some commonly used fluorogenic oligonucleotide probes rely on fluorescence resonance energy transfer (FRET) between two fluorogenic labels or between one fluorophore and a dark or non-fluorescent quencher (NFQ). FRET is a spectroscopic process where there is transfer of energy from high to low when a high-energy dye is in close proximity to a low-energy dye. The general principle of amplicon detection using such probes is based on the principle that if a fluorescent dye is in close proximity to a quencher dye in the same probe molecule (which disperses energy as heat rather than fluorescence) the fluorescent signal generated by the fluorescent dye in response to excitation is 'adsorbed' by the nearby quenching dye, resulting in no fluorescent signal. However, upon PCR amplification, the fluorescent dye and the quenching dye become spatially separated by probe displacement, resulting in loss of FRET between the fluorescent and quenching dyes, ultimately producing a fluorescent signal. Of the range of dye chemistries used in FRET probes, dual-labelled or TaqMan probes are most commonly employed in molecular detection methods. These target-specific hydrolysis probes contain both a fluorogenic reporter dye e.g. FAM and a quencher dye e.g. TAMRA and are designed to hybridise to the target gene at a location between two oligonucleotide primers used for the PCR amplification. During each PCR cycle the 3-5' nuclease activity of the *Taq*

polymerase results in cleavage of the probes and subsequent fluorescence (Applied Biosystems, Figure 1.10).

A more recent development in target-specific hydrolysis probes involves the use of the TaqMan probe with a 'minor groove binding' (MGB) molecule. An MGB probe is a short sequence probe (18-22 bp) where the standard quencher is replaced with a proprietary NFQ and incorporates a molecule that stabilises the probe-target duplex by folding into the minor groove of the dsDNA. Since MGB probes are very short, they are ideal for detecting small areas of conserved sequence and single nucleotide polymorphisms (SNPs). The NFQ offers the advantage of lower background signal, which results in better precision in quantitation.

Despite the obvious advantage of RQ-PCR systems in terms of sensitivity, specificity, target quantification and speed of detection, a number of important issues must be considered to ensure quality performance. Prior to the PCR assay, an optimal nucleic acid extraction step is essential to guarantee adequate yield and quality of target DNA. To ensure the presence of amplifiable DNA and removal of PCR inhibitors it is also necessary to incorporate a second heterologous PCR to target DNA from an internal control in the assay. For example, a human cellular gene can be targeted as an internal control to establish the suitability of a sample for PCR analysis. Given the high sensitivity of RQ-PCR, precautions must also be taken to prevent laboratory contamination of samples and reactions during processing or testing. These measures include setting up reactions in a restricted 'PCR Clean Facility' in which work with plasmid DNA or other samples with template does not occur. Test samples and positive

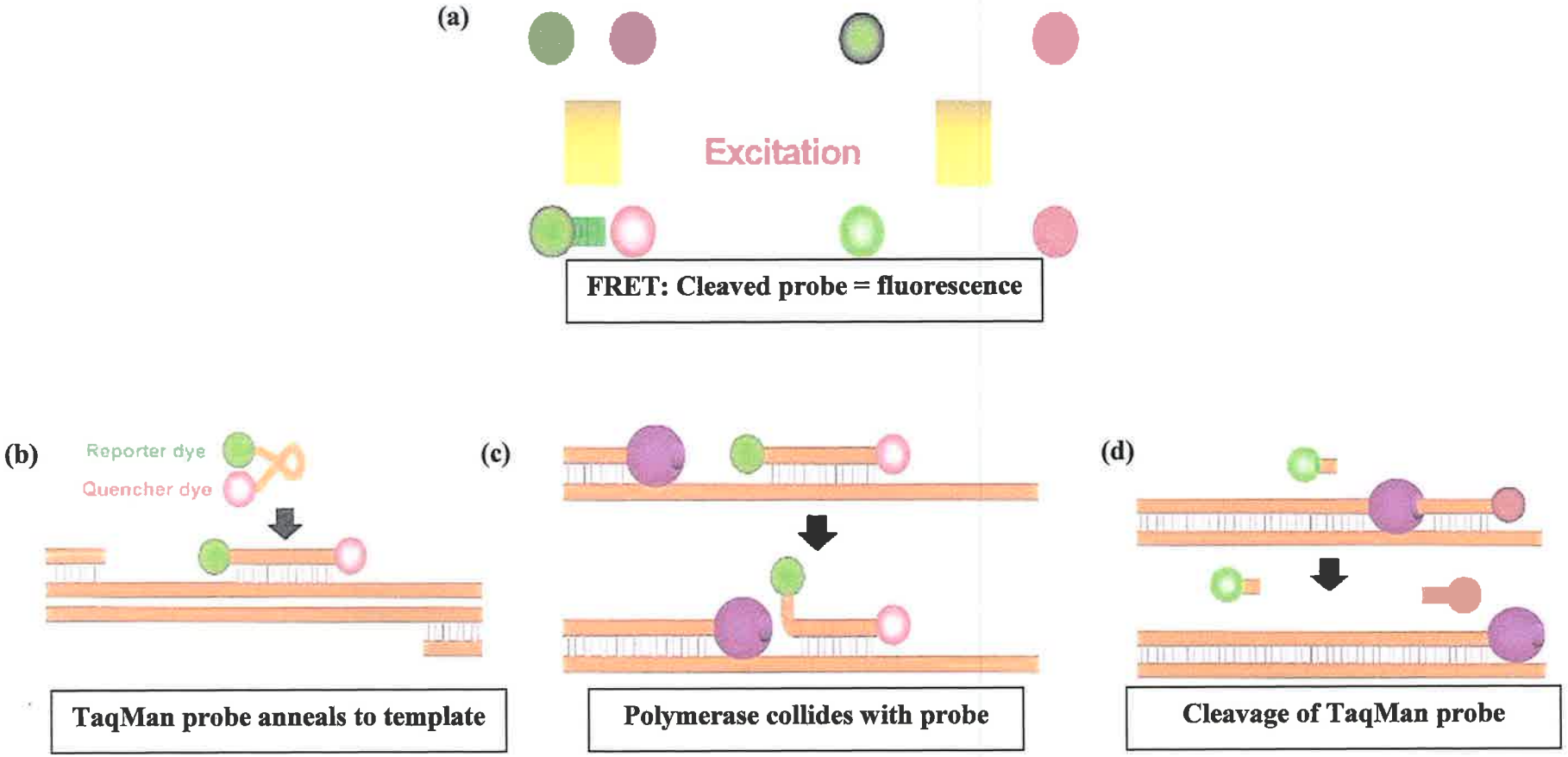

Figure 1.10: Principle of real-time quantitative PCR (RQ-PCR). RQ-PCR is based on (a) fluorescence resonance energy transfer (FRET) between fluorophore and non-fluorescent quencher labels TaqMan probe whereby fluorescence only occurs when probe is cleaved and fluorophore and quencher are spatially separated (b) The fluorogenic probe is designed to anneal to a specific template sequence between the forward and reverse primers. (b) The probe sits in the path of the enzyme as it starts to copy DNA. (c) When the enzyme reaches the annealed probe, the 5' exonuclease activity of the enzyme cleaves the probe. (d) Cleavage of Taqman probe results in fluorescence

Figure adapted from www.applied biosystems.com/support/tutorials/pdf/rtpcr_vs_tradpcr.pdf

control samples are each added to reactions in different laboratory areas. Additionally, appropriate negative controls should be included in each experiment to monitor for reagent contamination (Vilchez and Butel, 2003*a*).

Previous studies have detected SV40 at a low level using both conventional and real-time PCR assays. The high number of PCR cycles required (40-60) for SV40 detection in these studies suggests that SV40 is present in low copy numbers in human tumours, including NHL (Shivapurkar *et al*, 2002). Similar low levels of SV40 DNA have been observed in SV40-infected B cell lines (Dolcetti *et al*, 2003). This apparent low-level infection of B-lymphocytes necessitates the need for an extremely sensitive technique such as RQ-PCR in the evaluation of the role of SV40 in lymphocyte infection.

1.9 Research aims

Whilst debate on the role/association of SV40 in NHL has continued for almost a decade, thorough investigation of the interaction between lymphocytes and SV40 has not yet been described. The aim of this research was to analyse the effect of SV40 infection on human lymphocytes, and gain insights into the pathogenesis of SV40 in human disease. The project was therefore designed to characterise infection of three different strains of SV40 virus, 776-1E, 776-2E and 776-2E-SM, a microRNA deletion mutant, in two human B lymphocyte cell lines and one T lymphocyte cell line. Continuous analysis of SV40-infected lymphocytes then allowed:

- Examination of the effect of SV40 infection on the cell proliferation and viability of B-lymphocytes.

- Analysis of lymphocyte cell surface marker expression to show what changes, if any, virus infection has on the activation state of lymphocytes. The surface markers analysed included CD69, an early marker of lymphocyte activation and CD80 and CD86, co-stimulatory molecules important for the generation of a specific immune response.

- Measurement of the expression of the major transforming protein SV40 T-ag in infected cell lines by flow cytometry.

- Quantification of SV40 T-ag DNA using RQ-PCR assays to establish whether the virus infects or persists in lymphocytes and if viral replication occurs.

It was expected that analysis of these three virus strains in human lymphocytes would reveal the role of T-ag expression in viral replication or maintenance in lymphocytes and how viral features may contribute to pathogenesis and lymphomagenesis. Differences in the viral regulatory region of these three viruses would also provide an insight into the role of single or duplicated enhancer elements in viral pathogenesis.

Hypothesis: SV40 is capable of infecting human lymphocytes and this cell tropism may play an important role in the pathogenesis and/or tumourigenesis of SV40 infection in humans (Figure 1.11).

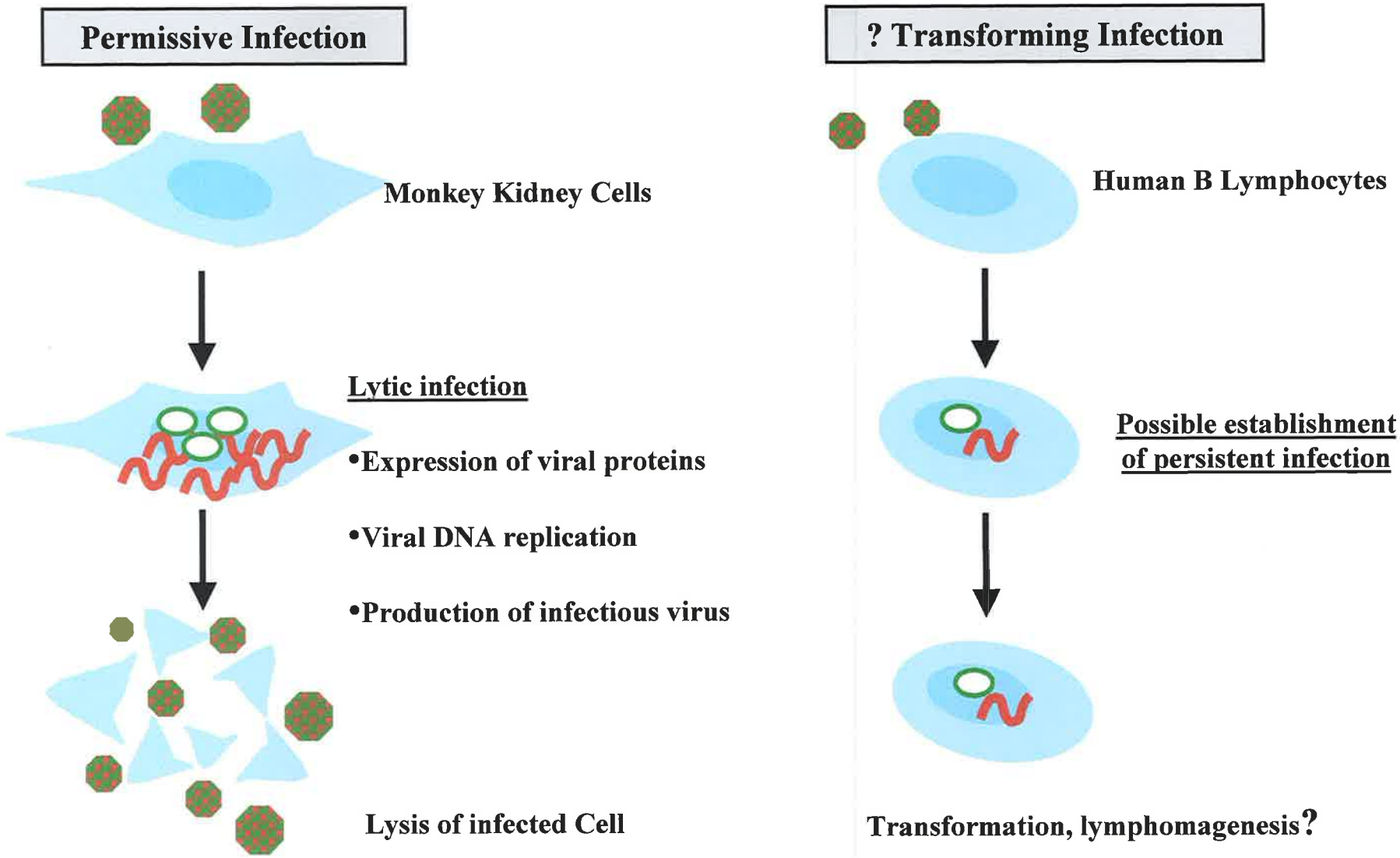

Figure 1.11: Proposed model of SV40 infection in human lymphocytes
Figure shows SV40 life cycle in permissive monkey kidney cells and the proposed model of SV40 lymphomageneis in non-permissive human B-lymphocytes

2.0 Materials and Methods

2.1 Cell culture

Cell culture work was carried out in a class II biohazard cabinet (SterilGARD hood, The Baker Company, Sanford, ME). Aseptic technique was employed at all times to minimise the risk of environmental contamination and to protect the worker against contact with potential pathogens. Sterile work conditions were maintained through the use of 70% ethanol and germicidal ultraviolet light (UV) to decontaminate all surfaces. Gloves were worn at all times and changed frequently throughout procedures.

2.1.1 Cell lines

2.1.1.1 Lymphocyte cell lines

Three American Type Culture Collection (ATCC)-characterised lymphocyte cell lines were used to investigate the effects of SV40 infection on human lymphocytes. These cell lines, BJAB, DG75 and CEM, were obtained from Dr. Linda R. Gooding (Department of Microbiology and Immunology, Emory University, Atlanta, GA). BJAB is an EBV-negative B-lymphoblastoid cell line, which was established from an African Burkitt's lymphoma patient (Menezes *et al*, 1975). The second B cell line, DG75, also EBV-negative, was derived from the pleural effusion of a child with primary abdominal lymphoma (Ben-Bassat *et al*, 1977). The T cell line, CEM, originated from the peripheral blood of a child with acute leukaemia (Foley *et al*, 1965). Lymphocyte cell lines were grown in complete 1X RPMI 1640 medium with L-glutamine (Cellgro® Mediatech Inc, Manassas, VA), supplemented with 10% foetal bovine serum (FBS, Hyclone, Logan, Utah), an additional 5 ml of 3%

glutamine (Baylor College of Medicine, Lot 5736) and 1 ml penicillin-streptomycin (pen-strep, Baylor College of Medicine, Lot 6422).

Vials of each cell line; BJAB, DG75 and CEM were retrieved from the vapour phase of liquid nitrogen storage, taking note of the passage number and flask size in which the cells originated. In this way the cells could be cultured in a tissue culture flask of the same volume as the original stock. The vial, containing 1 ml of cells, was thawed in a 37°C water bath and added to a 25 cm^2 tissue culture flask (Corning® Inc. NY) along with 9 ml of RPMI complete media. Each culture was incubated at 37°C in the CO_2 incubator (Steri-cult 200, Forma Scientific Inc., Marietta, OH) and maintained by passage every 3-4 days, by addition of fresh medium or replacement of medium, until the infection time course commenced. The viability of the culture was checked frequently by observing the microscopic cell morphology and the appearance of the culture medium. Viable cells were rounded in shape and the RPMI growth media remained pink.

2.1.1.2 Control cell lines

TC7 Monkey kidney cell line

The cell line, TC7, a clone of CV-1 cells derived from monkey kidneys, was used as a control cell line (Robb and Huebner, 1973). TC7 cells are fully permissive to SV40 cytopathic replication and were therefore used as a positive control for viral replication and expression of T-antigen, the major transforming protein of SV40. The TC7 cell line had been obtained from Dr. James Robb (Department of Pathology, University of California,

CA). TC7 cells were plated in 60 mm dishes and maintained in enriched minimum essential medium, E-MEM, Gibco (Robb and Heubner 1973; Brugge and Butel 1975).

SV40-transformed hamster cell line S1113

The hamster cell line S1113 was established from the spleen of a Syrian golden hamster that was inoculated intravenously with SV40 as described (McNees *et al*, 2009). The S1113 cell line has been characterised as a lymphoma of histiocytic origin induced *in vivo* by SV40. The S1113 cell line was maintained in 1X RPMI 1640 complete media supplemented with insulin-transferrin-sodium selenite (Sigma, St. Louis, MO). These cells were processed in parallel with test samples from lymphocyte cultures as a control for detection of SV40 T-ag.

2.1.2 SV40 Virus Stocks

Three SV40 viral strains were used to infect the lymphocyte cell lines; SV40 776-1E, SV40 776-2E and SV40 776-2E-SM. The SV40 strain 776-2E (Genbank accession number J02400) is considered to be the reference strain of the SV40 virus. This strain was originally isolated from an adenovirus type 1 vaccine seed stock (Sweet and Hilleman, 1960). The SV40 776-2E virus was obtained from Dr. James Pipas (Department of Biological Sciences, University of Pittsburgh, Pittsburgh, PA). SV40 776-1E, an SV40 776 variant, was previously constructed by Dr. John Lednicky (Department of Molecular Virology and Microbiology, Baylor College of Medicine, Houston, TX) by deletion of one of the 72-bp repeat elements of the enhancer region of the SV40 776-2E reference strain. SV40 776-2E-SM is a mutant viral strain that lacks SV40 microRNA (Sullivan *et al*, 2005). This mutant was obtained from Dr. Christopher Sullivan (Howard Hughes Medical Institute and

Departments of Microbiology and Medicine, University of California, San Francisco, CA). SV40 virus stocks were previously prepared by growth in the permissive TC7 monkey kidney cell line and virus stocks were quantified by plaque assay in the same cells (Butel *et al*, 1999).

2.2 Infection of cell lines with SV40 viral strains

The biological safety hood was set up for cell culture work as described previously (Section 2.1), but additional precautions were taken when working with virus stocks and infected cell lines. Two pairs of gloves were worn when handling live virus stocks and cultures of infected cells. All viral liquid waste was disposed of using 6% hypochlorite and viral-contaminated material was autoclaved. Tissue culture flasks containing SV40-infected cells were clearly labelled and caution was exercised when opening.

2.2.1 SV40-infection time course of lymphocyte cell lines

Cultures of each lymphocyte cell line, BJAB, DG75 and CEM, were passaged to produce sufficient cell culture volumes (approx. 30 ml) for infection with all three SV40 viruses and also to include an uninfected mock cell culture. Twenty-four hours prior to viral infection, each cell culture was fed by adding complete RPMI medium to promote log phase growth. On the day of viral infection, the cells were transferred to 50 ml conical tubes (Sarstedt, Newton, NC), centrifuged for 5 min at 2,000 rpm in the cell culture centrifuge (International Equipment Company, Needham Heights, MA) and the supernatant was removed. The cell pellet was resuspended in 5 mls of serum-free (SF) RPMI (RPMI 1640 1X with L-glutamine), which lacked the FBS, pen-strep and glutamine additives. The purpose of using

SF medium was to prevent protein in the medium interfering with viral adherence and subsequent infection of the cells. A cell count (cells/ml) was then performed using a haemocytometer (Hausser Scientific, Horsham, PA). This cell count was used to collect a specific number of cells to establish the multiplicity of infection (m.o.i.) and to calculate the volume of cells required to achieve the desired cell density for infection (e.g. 1 x 10^6 cells/ml). The m.o.i. is defined as the ratio of viral agents to cells (cells/ml).

Virus strains were then added to each cell suspension at the chosen m.o.i. In preliminary infection experiments of B cell lines, the volume of virus stock added to cells was normalised among the virus strains based on virus titre measured in plaque forming units (PFU), which had been determined by plaque assays. For example, the two B cell lines BJAB and DG75 were infected at 2 PFU/cell for each virus strain (Figure 2.1). Follow up data indicated that there was a wide range of the genome/PFU ratios among the stocks, which resulted in large variations of the input viral genomes. The SV40 genomes of each virus stock were quantified using a real-time quantitative PCR assay as described in following sections (Section 2.5) and the data are listed in Table 2.1. Hence, for the data discussed herein, unless otherwise stated, experiments were conducted by normalising the amount of virus added to cells based on the quantity of input viral genomes. Table 2.1 lists the virus stocks, and their corresponding titres, genome/PFU ratios, and amount of input virus in both genomes and infectious particles.

Following the addition of the viruses to the cell lines, the three infected lymphocyte cell cultures and the uninfected mock sample were incubated for 90 min at 37°C, washed

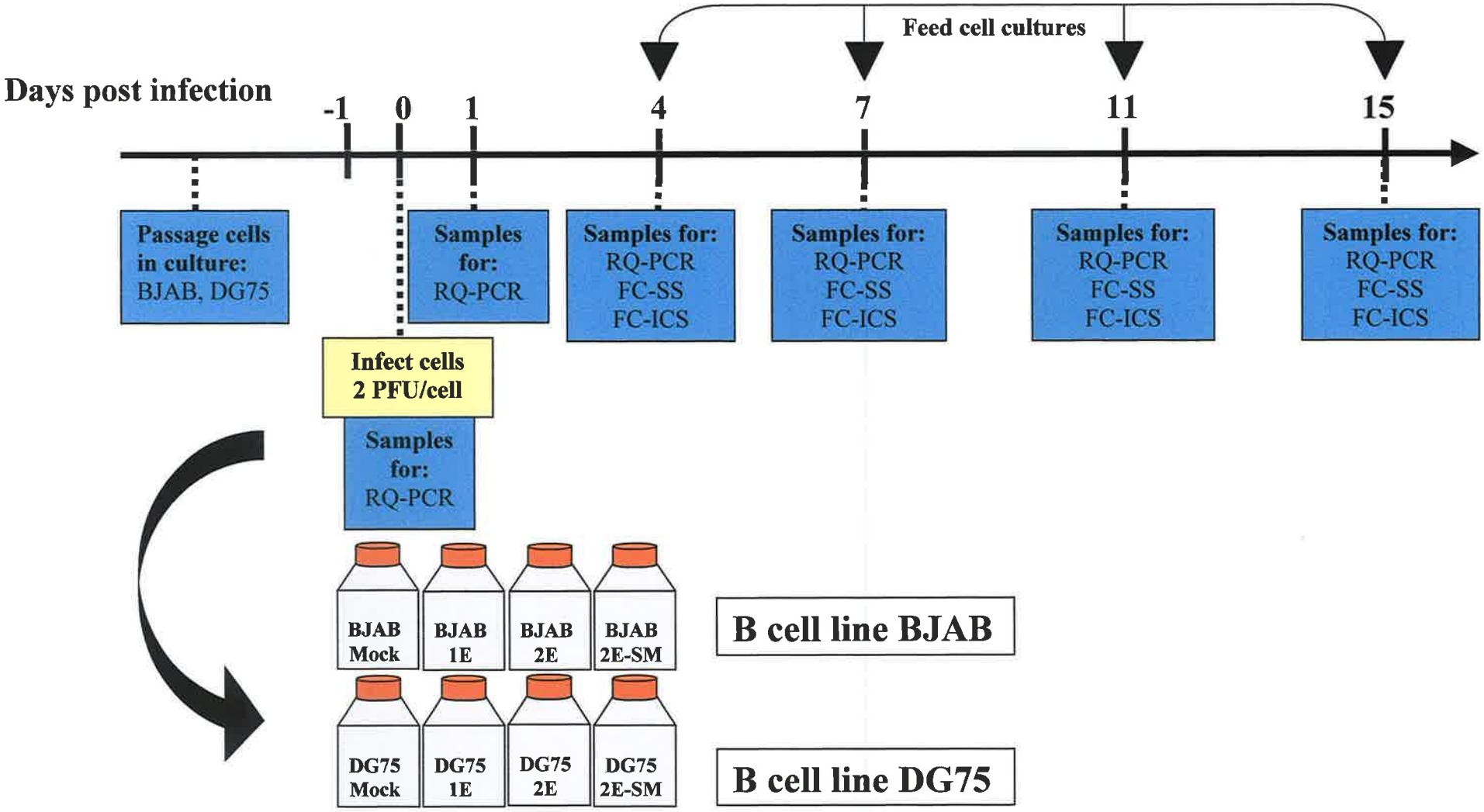

Figure 2.1: Initial infection time course experiment
Two B cell lines, BJAB and DG75, were infected with three SV40 776 virus variants, SV40 776-1E, -2E and -2E-SM and sample collection at time points 0, 1, 4, 7, 11 and 15 days post infection (d.p.i.) for RQ-PCR; real-time quantitative PCR, FC-SS; flow cytometry surface staining, FC-ICS; flow cytometry intracellular staining. Fresh media was added to cultures to replace sample collection volume on days 4, 7, 11 and 15.

Table 2.1: Calculations for SV40 virus stocks used in the optimised infection experiment

SV40 virus strain	Virus titre PFU/ml†	Genomes/ml‡	Genome/PFU ratio	Volume of virus stock used (ml)*	Genomes/cell used to infect cell lines	M.o.i. equivalent
776-1E	1.4×10^7	4.1×10^{10}	2929	1.894	15,400	5.2
776-2E	1.1×10^7	6.2×10^{10}	5636	1.260	15,600	2.8
776-2E-SM	1.1×10^8	7.1×10^{10}	645	1.116	15,800	24.5

† Measured using plaque assay, ‡ Measured using RQ-PCR assay, * Volume for infecting 5×10^6 cells.

three times with RPMI complete medium to remove any unbound viral particles, and resuspended. The infected cell cultures were then transferred into twelve tissue culture flasks and incubated in at 37°C for the two-week infection time course. During the time course cell samples were collected on 0, 2, 4, 6, 8, 10 and 13 days post infection (d.p.i.) for use in the following analysis (Figure 2.2):

- Flow cytometry cell surface marker expression
- Detection of SV40 T-ag by intracellular staining and flow cytometry
- Real-time quantitative PCR (RQ-PCR)

The cell density of the infected cell cultures was re-adjusted to 1 x 10^6 cells/ml before each sample collection time point.

2.2.2 Infection of the TC7 Monkey Kidney cell line with SV40 (positive control)

The monkey kidney cell line TC7 (described in Section 2.1.1) was used as a positive control in analyses for T-ag and RQ-PCR samples collected in the time course. SV40-infection of the TC7 cell monolayers in 60 mm dishes was carried out by removing the culture media using aspiration, washing the monolayer with tris buffered saline (TBS), then adding virus stock in 0.2 ml TBS. Virus was adsorbed during 90 min incubation. The monolayer was washed again three times with 1 ml TBS. Three ml maintenance media (Eagles MEM, 2% FBS) was added and cells were incubated until harvest as described later.

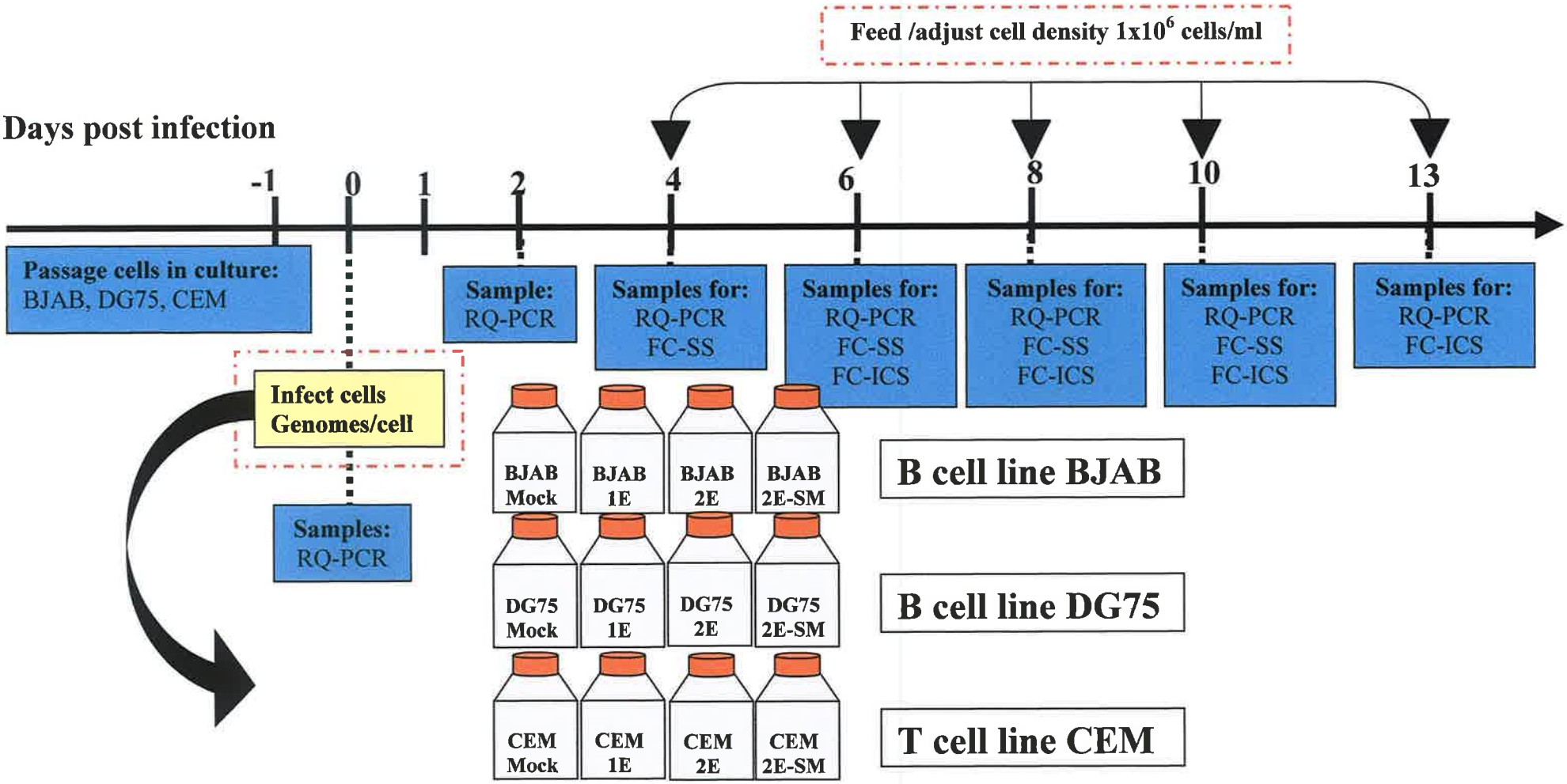

Figure 2.2: Optimised infection time course experiment
Two B cell lines, BJAB and DG75, and a T cell line, CEM, were infected with SV40 776-1E, -2E and -2E-SM and samples were collected at time points 0, 2, 4, 6, 8, 10 and 13 days post infection (d.p.i.). Changes from the initial infection experiment, including the infection of cells based on genomes/cell rather than PFU/cell and adjustment of the cell density to 1 x 10^6cells/ml as indicated on days 4, 6, 8 10 and 13, are highlighted in red.
RQ-PCR; real-time quantitative PCR, FC-SS; flow cytometry surface staining, FC-ICS; flow cytometry intracellular staining.

2.3 Cell proliferation and viability

Daily cell counts were performed to investigate the effect of SV40 viral infection on cell proliferation and viability of lymphocyte cell lines. The trypan blue exclusion assay was used for cell counts. In this assay, dead cells are distinguished by the uptake of the blue dye. A 10 µl aliquot of cells was mixed with 10 µl of 0.4% trypan blue (Gibco BRL® Life Technologies®, Carlsbad, CA) and added to a haemocytometer. Each cell culture was counted in duplicate. From this data, the cell viability was then calculated by expressing the number of live cells as a percentage of the total number of cells counted. Cell counts were also necessary to calculate the amount of media to be added to re-adjust the cell density at each sample collection time point.

2.4 Cell surface marker expression by flow cytometry analysis

Cell surface marker expression was investigated on aliquots from B cell lines, BJAB and DG75, and the T cell line, CEM, from cell cultures collected at 4, 6, 8 and 10 d.p.i. of the time course using fluorescent-labelled CD-specific monoclonal antibodies (BD Biosciences Pharmingen™, San Jose, CA). Cell surface molecules selected for analysis included the lymphocyte early activation marker, CD69, and the co-stimulation markers, CD80 and CD86 (Table 2.2).

Surface marker staining was carried out on cells in a class II biohazard cabinet (Section 2.1) immediately after sample collection, with cells and reagents held on ice during the staining procedure. Samples (1 ml) were collected from the culture flasks, transferred into low retention polymer 1.6 ml micro centrifuge tubes (Neptune™, Biotix Inc., San Diego, CA) and centrifuged at 1,000 rpm for 5 min (Eppendorf centrifuge 5415C). The supernatant was removed and the cell pellets resuspended in 160 µl of ice-cold Fluorescence Activated Cell Sorting (FACS) buffer, comprised of 0.01M Phosphate Buffered Saline (PBS), 5 ml FBS and 5 ml sodium azide. Resuspended cells were then divided into two aliquots, with 80 µl of resuspended cells used for each test reaction and 80 µl used for a control reaction. An isotype control antibody matched to the CD-specific monoclonal antibodies was used to assess the level of background staining on cells.

A three-colour staining protocol was set up using monoclonal antibodies conjugated to the fluorochromes phycoerythrin (PE), fluorscein isothiocyanate (FITC), and allophycocyanin (APC). Per the manufacturer's recommendations, a 15 µl aliquot of antibody was added to

Table 2.2: List of antibodies used in analysis of cell surface marker expression by flow cytometry

Antibody	Catalogue number	Lot number	Expiration date
CD69-PE	555531	31391	30/09/2014
CD80-FITC	557226	96060	31/07/2013
CD86-APC	555660	10990	28/02/2011
IC-FITC	555748	28391	31/08/2014
IC-PE	555749	27920	31/08/2014
IC-APC	555751	30447	30/09/2011

IC; Isotype control, PE; phycoerythrin, FITC; fluorscein isothiocyanate, APC; allophycocyanin

each reaction. For each of the 12 samples, a corresponding isotype control reaction was set up for each fluorochrome (Table 2.3). Following addition of antibodies, the samples were allowed to incubate on ice in darkness by covering with aluminium foil for 30-45 min. After two washes with 1 ml cold FACS buffer, the cells were fixed in 2% paraformaldyde and stored at 4°C until analysis. The 2% paraformaldehyde was made fresh from a 37% stock solution (Fischer Scientific, Pittsburgh, PA) by diluting with PBS. Before flow cytometry analysis, the samples were centrifuged to remove the paraformaldehyde and then resuspended in 500 µl PBS before being transferred to 5 ml polystyrene round-bottom tubes for flow cytometry analysis (Becton Dickinson, Franklin Lakes, NJ).

Stained samples were analysed at the Cytometry and Cell Sorting Core facility at Baylor College of Medicine using the Canto II flow cytometer (Becton Dickinson). A total of 10,000 events were acquired for each sample. Analysis of the data was then performed using FlowJo software (FlowJo, LLC, Ashland, OR). Using a dot plot display of FSC *versus* SSC, the cells were gated to include the majority of cells together in a dense population and exclude any cellular debris and dead cells. From this gated population, a daughter population was displayed in histogram format. By overlaying the histograms from infected cell lines with the histogram from the uninfected samples for a particular surface marker at each d.p.i., changes in fluorescence emission and therefore increases or decreases in surface marker expression could be observed. A shift in the histogram was recorded as the percentage upregulation or downregulation of the surface marker measured, compared to the uninfected mock sample for each cell line (Figure 2.3).

Table 2.3: Three-colour surface staining of SV40-infected lymphocyte cell lines for flow cytometric analysis

Cell culture sample	Fluorescent antibody	Isotype control	Cell volume (µl)	Antibody volume (µl)
BJAB - Mock	CD69-PE, CD80-FITC, CD86-APC	PE-IC, FITC-IC, APC-IC	80	15
BJAB - 776-1E	CD69-PE, CD80-FITC, CD86-APC	PE-IC, FITC-IC, APC-IC	80	15
BJAB - 776-2E	CD69-PE, CD80-FITC, CD86-APC	PE-IC, FITC-IC, APC-IC	80	15
BJAB - 776-2E SM	CD69-PE, CD80-FITC, CD86-APC	PE-IC, FITC-IC, APC-IC	80	15
DG75 - Mock	CD69-PE, CD80-FITC, CD86-APC	PE-IC, FITC-IC, APC-IC	80	15
DG75 - 776-1E	CD69-PE, CD80-FITC, CD86-APC	PE-IC, FITC-IC, APC-IC	80	15
DG75 - 776-2E	CD69-PE, CD80-FITC, CD86-APC	PE-IC, FITC-IC, APC-IC	80	15
DG75 - 776-2E SM	CD69-PE, CD80-FITC, CD86-APC	PE-IC, FITC-IC, APC-IC	80	15
CEM - Mock	CD69-PE, CD80-FITC, CD86-APC	PE-IC, FITC-IC, APC-IC	80	15
CEM - 776-1E	CD69-PE, CD80-FITC, CD86-APC	PE-IC, FITC-IC, APC-IC	80	15
CEM - 776-2E	CD69-PE, CD80-FITC, CD86-APC	PE-IC, FITC-IC, APC-IC	80	15
CEM - 776-2E SM	CD69-PE, CD80-FITC, CD86-APC	PE-IC, FITC-IC, APC-IC	80	15

For each cell culture, an aliquot was stained with CD69-PE, CD80-FITC and CD86-APC and a separate aliquot was stained with PE, FITC and APC IC antibodies
PE; phycoerythrin, FITC; fluorscein isothiocyanate, APC; allophycocyanin, IC; isotype control

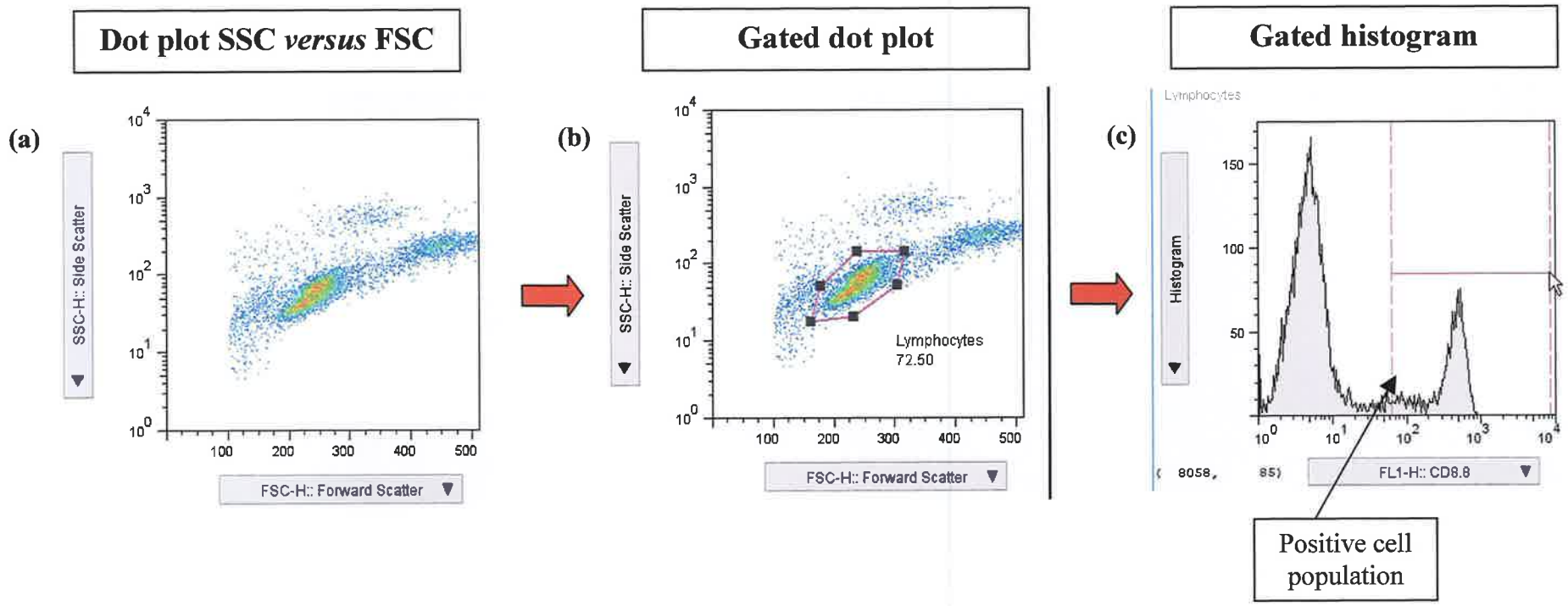

Figure 2.3: Method of flow cytometric analysis of lymphocyte surface marker expression.
(a) Flow cytometric analysis of infected cell cultures generates a dot-plot display of side-scatter (SSC) *versus* forward scatter (FSC), relating to cell size *versus* granularity. (b) A gate is drawn around this initial dot plot to include the majority of the cell population and exclude cellular debris. Only cells within this gate are analysed further. (c) The gated dot plot is switched to a histogram display of frequency *versus* fluorescence (FL1-H). A range of fluorescent values that will define the positive cell population is selected using gating tool on computer program, with cells falling to the right this gate being defined as positive.

Figures adapted from FlowJo online tutorial: http://offsite.treestar.com/downloads/BasicTutorial0709web.pdf

2.5 Detection of SV40 T-ag by flow cytometry

2.5.1. Sample collection and treatment

Detection of intracellular expression of SV40 large T-antigen (T-ag), the major transforming protein of SV40, was carried out by flow cytometry as described previously (McNees *et al*, 2009). SV40 T-ag expression was investigated on aliquots of infected-B cell lines, BJAB and DG75, and T cell, CEM, cell cultures collected at 6, 8, 10 and 13 d.p.i. T-ag expression was also measured in aliquots of SV40-infected TC7 cells collected at the designated 24, 48 and 96 hours post infection (h.p.i.). As TC7 is a permissive cell line for SV40 infection, this serves as a positive control for T-ag expression during the infection time course. Another cell line established by *in vivo* SV40-transformation, S1113, was also included as a positive control for the intracellular staining process. This cell line is known to stably express high levels of T-ag and was used to compare to test samples.

On each collection day, 1-4 ml from each culture flask was added to 15 ml conical tubes (Sarstedt) and centrifuged at 2,000 rpm for 5 min. Using 10 ml glass pipettes, the supernatant was collected and discarded, taking care not to disrupt the cell pellet. The pellets were resuspended in PBS and centrifuged again at 2,000 rpm for 5 min. After the supernatant was removed, the cells were fixed by resuspending the cell pellet in 200 µl of 2% paraformaldehyde and incubating in a 37°C incubator for at least 10 min. The samples were then stored at 4°C where they were expected to remain stable for two weeks. To permeabilise cells, the paraformaldehyde was removed following centrifugation and the cells were resuspended in 100 µl PBS and overlaid with 900 µl of methanol. The methanol had been stored at -20°C and was added slowly down the side of tube. The samples were then

stored in the -20°C freezer, where they can remain for up to six months. For each batch of test samples, positive control samples S1113 cells were included to validate the intracellular staining protocol. S1113 samples included: unstained cells, cells stained with secondary antibody only, and stained with both the primary and secondary antibody.

2.5.2 Intracellular staining for T-ag

The permeabilised cells were removed from storage at -20°C and intracellular staining was carried out to detect large T-antigen. The primary antibody SVTAg Pab416, a mouse monoclonal antibody (Santa Cruz Biotechnology, Santa Cruz, CA), was prepared by diluting 1:50 in stain buffer (1% BSA in PBS). An aliquot of approx. 250-300 µl of each permeablised cell sample was transferred into low retention polymer 1.6 ml flat cap micro centrifuge tubes (Neptune™) and centrifuged at 2,000 rpm for 5 min. Stain buffer (1 ml) was added to each sample and centrifuged at 1,000 rpm for 5 min. The cell pellet was resuspended in 100 µl diluted primary antibody and incubated at room temperature (RT) for 30 min. The cells were washed twice in 500 µl of stain buffer and then the cell pellet was resuspended in 100 µl of secondary antibody. The secondary antibody, Goat F (ab') $_2$ anti-mouse IgG_{2a} (γ_{2a} chain specific, Southern Biotech, Birmingham, AL), was diluted 1:100. Samples were incubated at RT for greater than 30 min in darkness by covering with aluminium foil. Stain buffer (500 µl) was added, the samples were centrifuged and supernatant removed. Two washes with 500 µl stain buffer were then performed. Finally, the cell pellets were fixed in 100 µl of 2% paraformaldehyde, incubated for 10 min at 37°C and stored at 4°C, covered with aluminium foil, until flow cytometric analysis. Paraformaldehyde was removed by centrifugation prior to analysis, as described previously.

The cell pellets were resuspended in 500 µl PBS and transferred to appropriate 5 ml tubes (Beckon Dickinson) for analysis. Samples were analysed at the Flow Cytometry Core Facility at Baylor College of Medicine using the Canto II flow cytometer (Becton Dickinson) and FlowJo software. Following the acquisition of 10,000 events for each sample, a dot plot of cell FSC *versus* SSC was displayed. From this initial plot, a daughter population was displayed following debris exclusion. A square gate was set on the uninfected mock sample, defined as being negative for T-ag expression. When this mock gate was copied to sample dot plots, changes in the -PE fluorescence of the secondary antibody, indicating binding to the primary anti-Tag antibody, were evident by a shift to the right which was measured as percentage positive for SV40 T-ag.

2.6 Real-time Quantitative PCR measurement of SV40

SV40 DNA was quantified in infected BJAB and DG75 B cell lines and the CEM T cell line, using a real time quantitative PCR (RQ-PCR) assay. This RQ-PCR assay was designed as a TaqMan hydrolysis probe assay, and was previously shown to be a sensitive and specific method for the detection and quantification of SV40 virus (McNees *et al*, 2005).

2.6.1 Nucleic acid extraction

Previous studies in SV40-infected cell lines have shown that DNA extraction may be dependent on cell culture density (McNees *et al*, 2005). It was therefore necessary to optimise a suitable extraction protocol for this study. Total DNA was extracted from the SV40-infected cell culture samples using two methods: a commercially available kit and a cell lysis method.

2.6.1.1 QIAamp® DNA blood mini kit

The QIAamp® DNA Blood Mini Kit (Qiagen Inc., Valencia, CA) is designed for the isolation of total DNA, both cellular and viral. In this method, DNA binds specifically to the QIAamp column membrane while other components are washed through and removed in two wash steps. The bound nucleic acid is then eluted in the elution buffer supplied with the kit. To evaluate this commercial kit, a 1 ml sample was taken from B cell culture flasks at 0, 1, 4, 7, 11 and 15 d.p.i. Samples were centrifuged at 1,000 rpm for 4-6 min, the supernatant removed and the cell pellets were stored by freezing at -20°C. Once the infection time course was completed, the frozen samples were thawed and 100 µl of sterile PBS was added to dilute the sample. A 60 µl aliquot of the diluted sample was made up to 200 µl with PBS

in accordance with the manufacturer's instructions. Briefly, an 80 µl aliquot of lysis buffer AL was added to 20 µl of QIAGEN Protease and 200 µl of diluted sample and incubated at 56°C for 10 min. Pure ethanol (200 µl) was added to the sample, which was then applied to the QiaAmp column and centrifuged at 8,000 rpm for 1 min. Successive washes of 500 µl of wash buffers AW1 and AW2 were applied before centrifugation at 8,000 rpm for 1 min and 14,000 rpm for 3 min respectively. DNA was eluted in 200 µl of buffer AE and stored at -20°C for use in RQ-PCR reaction.

2.6.1.2 Cell lysis DNA extraction

To evaluate the cell lysis K DNA extraction method, a 250 µl sample of each B and T cell line culture was collected in duplicate at 0, 2, 4, 6, 8, 10 and 13 d.p.i., into 1.5 ml screw cap tubes (Sarstedt) and stored at -20°C until analysis. Samples were then processed by adding 62.5 µl of 5X lysis buffer (50 mM Tris-HCL, 2.5 % Tween-20, Proteinase K 0.4 mg/ml) and incubating in a 55°C water bath for 60 min, followed by 10 min incubation at 95°C to inactivate the proteinase K enzyme. Samples were then ready to use in the RQ-PCR assay or could be stored at -20°C for future analysis.

2.6.2 Real-time quantitative PCR (RQ-PCR) assay

Viral DNA was quantified in the SV40-infected cell lines using a real time quantitative PCR assay designed to target the T-ag DNA sequences as described previously (McNees *et al*, 2005). A second RQ-PCR assay to measure the single copy human RNAse P gene was also performed on each sample (McNees *et al*, 2005). The parallel detection of the RNAse P gene

allows SV40 viral gene copy numbers to be normalised to cell numbers and also serves as an internal control to monitor the DNA extraction process and the presence of PCR inhibitors.

2.6.2.1 Primers and probe design

SV40-specific oligonucleotide primer/probe sets were previously designed using Primer Express software and were synthesized by and purchased from Applied Biosystems (Foster City, CA). The primers and probe were selected to target the conserved N-terminal region of the T-ag gene in the SV40 genome. The DNA sequence of the T-ag gene from viral test strains SV40 776-2E (Genbank accession number J02400.1), SV40 776-1E and SV40 776-2E-SM (Sullivan *et al*, 2005) were aligned using Clustal w software (http://www.ebi.ac.uk) and examined for suitable conserved primer and probe sites (Figure 2.4). Details of SV40 T-ag-specific primer and probe nucleic acid sequences used in this assay are included in Table 2.4. The T-ag-specific probe was labelled with FAM (6-carboxyfluorescein) at the 5'end and MGB (minor groove binder) at the 3' end. Upon receipt, the oligonucleotides were resuspended in sterile water (Gibco) to a stock concentration of 100 μM and stored at -20°C in small volumes. TaqMan® RNAse P Control Reagent (Applied Biosystems), contained the patented primers and probe (VIC-labelled) for amplification of the RNAse P gene.

CLUSTAL 2.0.11 nucleotide sequence alignment of T-antigen gene of SV40 strains 776-1E, -2E and -2E-SM

```
776-2E      TTATGTTTCAGGTTCAGGGGGAGGTGTGGGAGGTTTTTTAAAGCAAGTAAAACCTCTACA 60
776-1E      TTATGTTTCAGGTTCAGGGGGAGGTGTGGGAGGTTTTTTAAAGCAAGTAAAACCTCTACA 60
776-2E-SM   TTATGTTTCAGGTTCAGGGGGAGGTGTGGGAGGTTTTTTAAAGCAAGTAAAACCTCTACA 60
            ************************************************************

776-2E      AATGTGGTATGGCTGATTATGATCATGAACAGACTGTGAGGACTGAGGGGCCTGAAATGA 120
776-1E      AATGTGGTATGGCTGATTATGATCATGAACAGACTGTGAGGACTGAGGGGCCTGAAATGA 120
776-2E-SM   AATGTGGTATGGCTGATTATGATCATGAACAGACTG GA GACTG GG GC TGAAA GA 120
            ************************************  ** ***** ** ** ***** **

776-2E      GCCTTGGGACTGTGAATCAATGCCTGTTTCATGCCCTGAGTCTTCCATGTTCTTCTCCCC 180
776-1E      GCCTTGGGACTGTGAATCAATGCCTGTTTCATGCCCTGAGTCTTCCATGTTCTTCTCCCC 180
776-2E-SM    CC TG GACTG GAATCAATACCGGTCTCATGACCAGAATCCTCCATATTCTTCTCCCC 180
             ** ** ***** ******** ** ** ***** ** ** ** ***** **********

776-2E      ACCATCTTCATTTTTATCAGCATTTTCCTGGCTGTCTTCATCATCATCATCACTGTTTCT 240
776-1E      ACCATCTTCATTTTTATCAGCATTTTCCTGGCTGTCTTCATCATCATCATCACTGTTTCT 240
776-2E-SM   ACCATCTTCATTTTTATCAGCATTTTCCTGGCTGTCTTCATCATCATCATCACTGTTTCT 240
            ************************************************************

776-2E      TAGCCAATCTAAAACTCCAATTCCCATAGCCACATTAAACTTCATTTTTTGATACACTGA 300
776-1E      TAGCCAATCTAAAACTCCAATTCCCATAGCCACATTAAACTTCATTTTTTGATACACTGA 300
776-2E-SM   TAGCCAATCTAAAACTCCAATTCCCATAGCCACATTAAACTTCATTTTTTGATACACTGA 300
            ************************************************************

776-2E      CAAACTAAACTCTTTGTCCAATCTCTCTTTCCACTCCACAATTCTGCTCTGAATACTTTG 360
776-1E      CAAACTAAACTCTTTGTCCAATCTCTCTTTCCACTCCACAATTCTGCTCTGAATACTTTG 360
776-2E-SM   CAAACTAAACTCTTTGTCCAATCTCTCTTTCCACTCCACAATTCTGCTCTGAATACTTTG 360
            ************************************************************

776-2E      AGCAAACTCAGCCACAGGTCTGTACCAAATTAACATAAGAAGCAAAGCAATGCCACTTTG 420
776-1E      AGCAAACTCAGCCACAGGTCTGTACCAAATTAACATAAGAAGCAAAGCAATGCCACTTTG 420
776-2E-SM   AGCAAACTCAGCCACAGGTCTGTACCAAATTAACATAAGAAGCAAAGCAATGCCACTTTG 420
            ************************************************************

776-2E      AATTATTCTCTTTTCTAACAAAAACTCACTGCGTTCCAGGCAATGCTTTAAATAATCTTT 480
776-1E      AATTATTCTCTTTTCTAACAAAAACTCACTGCGTTCCAGGCAATGCTTTAAATAATCTTT 480
776-2E-SM   AATTATTCTCTTTTCTAACAAAAACTCACTGCGTTCCAGGCAATGCTTTAAATAATCTTT 480
            ************************************************************

776-2E      GGGCCTAAAATCTATTTGTTTTACAAATCTGGCCTGCAGTGTTTTAGGCACACTGTACTC 540
776-1E      GGGCCTAAAATCTATTTGTTTTACAAATCTGGCCTGCAGTGTTTTAGGCACACTGTACTC 540
776-2E-SM   GGGCCTAAAATCTATTTGTTTTACAAATCTGGCCTGCAGTGTTTTAGGCACACTGTACTC 540
            ************************************************************

776-2E      ATTCATGGTGACTATTCCAGGGGGAAATATTTGAGTTCTTTTATTTAGGTGTTTCTTTTC 600
776-1E      ATTCATGGTGACTATTCCAGGGGGAAATATTTGAGTTCTTTTATTTAGGTGTTTCTTTTC 600
776-2E-SM   ATTCATGGTGACTATTCCAGGGGGAAATATTTGAGTTCTTTTATTTAGGTGTTTCTTTTC 600
            ************************************************************

776-2E      TAAGTTTACCTTAACACTGCCATCCAAATAATCCCTTAAATTGTCCAGGTTATTAATTCC 660
776-1E      TAAGTTTACCTTAACACTGCCATCCAAATAATCCCTTAAATTGTCCAGGTTATTAATTCC 660
776-2E-SM   TAAGTTTACCTTAACACTGCCATCCAAATAATCCCTTAAATTGTCCAGGTTATTAATTCC 660
            ************************************************************

776-2E      CTGACCTGAAGGCAAATCTCTGGACTCCCCTCCAGTGCCCTTTACATCCTCAAAAACTAC 720
776-1E      CTGACCTGAAGGCAAATCTCTGGACTCCCCTCCAGTGCCCTTTACATCCTCAAAAACTAC 720
776-2E-SM   CTGACCTGAAGGCAAATCTCTGGACTCCCCTCCAGTGCCCTTTACATCCTCAAAAACTAC 720
            ************************************************************
```

```
776-2E      TAAAAACTGGTCAATAGCTACTCCTAGCTCAAAGTTCAGCCTGTCCAAGGGCAAATTAAC 780
776-1E      TAAAAACTGGTCAATAGCTACTCCTAGCTCAAAGTTCAGCCTGTCCAAGGGCAAATTAAC 780
776-2E-SM   TAAAAACTGGTCAATAGCTACTCCTAGCTCAAAGTTCAGCCTGTCCAAGGGCAAATTAAC 780
            ************************************************************

776-2E      ATTTAAAGCTTTCCCCCCACATAATTCAAGCAAAGCAGCTGCTAATGTAGTTTTACCACT 840
776-1E      ATTTAAAGCTTTCCCCCCACATAATTCAAGCAAAGCAGCTGCTAATGTAGTTTTACCACT 840
776-2E-SM   ATTTAAAGCTTTCCCCCCACATAATTCAAGCAAAGCAGCTGCTAATGTAGTTTTACCACT 840
            ************************************************************

776-2E      ATCAATTGGTCCTTTAAACAGCCAGTATCTTTTTTTAGGAATGTTGTACACCATGCATTT 900
776-1E      ATCAATTGGTCCTTTAAACAGCCAGTATCTTTTTTTAGGAATGTTGTACACCATGCATTT 900
776-2E-SM   ATCAATTGGTCCTTTAAACAGCCAGTATCTTTTTTTAGGAATGTTGTACACCATGCATTT 900
            ************************************************************

776-2E      TAAAAAGTCATACACCACTGAATCCATTTTGGGCAACAAACAGTGTAGCCAAGCAACTCC 960
776-1E      TAAAAAGTCATACACCACTGAATCCATTTTGGGCAACAAACAGTGTAGCCAAGCAACTCC 960
776-2E-SM   TAAAAAGTCATACACCACTGAATCCATTTTGGGCAACAAACAGTGTAGCCAAGCAACTCC 960
            ************************************************************

776-2E      AGCCATCCATTCTTCTATGTCAGCAGAGCCTGTAGAACCAAACATTATATCCATCCTATC 1020
776-1E      AGCCATCCATTCTTCTATGTCAGCAGAGCCTGTAGAACCAAACATTATATCCATCCTATC 1020
776-2E-SM   AGCCATCCATTCTTCTATGTCAGCAGAGCCTGTAGAACCAAACATTATATCCATCCTATC 1020
            ************************************************************

776-2E      CAAAAGATCATTAAATCTGTTTGTTAACATTTGTTCTCTAGTTAATTGTAGGCTATCAAC 1080
776-1E      CAAAAGATCATTAAATCTGTTTGTTAACATTTGTTCTCTAGTTAATTGTAGGCTATCAAC 1080
776-2E-SM   CAAAAGATCATTAAATCTGTTTGTTAACATTTGTTCTCTAGTTAATTGTAGGCTATCAAC 1080
            ************************************************************

776-2E      CCGCTTTTTAGCTAAAACAGTATCAACAGCCTGTTGGCATATGGTTTTTTGGTTTTTGCT 1140
776-1E      CCGCTTTTTAGCTAAAACAGTATCAACAGCCTGTTGGCATATGGTTTTTTGGTTTTTGCT 1140
776-2E-SM   CCGCTTTTTAGCTAAAACAGTATCAACAGCCTGTTGGCATATGGTTTTTTGGTTTTTGCT 1140
            ************************************************************

776-2E      GTCAGCAAATATAGCAGCATTTGCATAATGCTTTTCATGGTACTTATAGTGGCTGGGCTG 1200
776-1E      GTCAGCAAATATAGCAGCATTTGCATAATGCTTTTCATGGTACTTATAGTGGCTGGGCTG 1200
776-2E-SM   GTCAGCAAATATAGCAGCATTTGCATAATGCTTTTCATGGTACTTATAGTGGCTGGGCTG 1200
            ************************************************************

776-2E      TTCTTTTTTAATACATTTTAAACACATTTCAAAACTGTACTGAAATTCCAAGTACATCCC 1260
776-1E      TTCTTTTTTAATACATTTTAAACACATTTCAAAACTGTACTGAAATTCCAAGTACATCCC 1260
776-2E-SM   TTCTTTTTTAATACATTTTAAACACATTTCAAAACTGTACTGAAATTCCAAGTACATCCC 1260
            ************************************************************

776-2E      AAGCAATAACAACACATCATCACATTTTGTTTCCATTGCATACTCTGTTACAAGCTTCCA 1320
776-1E      AAGCAATAACAACACATCATCACATTTTGTTTCCATTGCATACTCTGTTACAAGCTTCCA 1320
776-2E-SM   AAGCAATAACAACACATCATCACATTTTGTTTCCATTGCATACTCTGTTACAAGCTTCCA 1320
            ************************************************************

776-2E      GGACACTTGTTTAGTTTCCTCTGCTTCTTCTGGATTAAAATCATGCTCCTTTAACCCACC 1380
776-1E      GGACACTTGTTTAGTTTCCTCTGCTTCTTCTGGATTAAAATCATGCTCCTTTAACCCACC 1380
776-2E-SM   GGACACTTGTTTAGTTTCCTCTGCTTCTTCTGGATTAAAATCATGCTCCTTTAACCCACC 1380
            ************************************************************

776-2E      TGGCAAACTTTCCTCAATAACAGAAAATGGATCTCTAGTCAAGGCACTATACATCAAATA 1440
776-1E      TGGCAAACTTTCCTCAATAACAGAAAATGGATCTCTAGTCAAGGCACTATACATCAAATA 1440
776-2E-SM   TGGCAAACTTTCCTCAATAACAGAAAATGGATCTCTAGTCAAGGCACTATACATCAAATA 1440
            ************************************************************
```

```
776-2E      TTCCTTATTAACCCCTTTACAAATTAAAAAGCTAAAGGTACACAATTTTTGAGCATAGTT 1500
776-1E      TTCCTTATTAACCCCTTTACAAATTAAAAAGCTAAAGGTACACAATTTTTGAGCATAGTT 1500
776-2E-SM   TTCCTTATTAACCCCTTTACAAATTAAAAAGCTAAAGGTACACAATTTTTGAGCATAGTT 1500
            ************************************************************

776-2E      ATTAATAGCAGACACTCTATGCCTGTGTGGAGTAAGAAAAAACAGTATGTTATGATTATA 1560
776-1E      ATTAATAGCAGACACTCTATGCCTGTGTGGAGTAAGAAAAAACAGTATGTTATGATTATA 1560
776-2E-SM   ATTAATAGCAGACACTCTATGCCTGTGTGGAGTAAGAAAAAACAGTATGTTATGATTATA 1560
            ************************************************************

776-2E      ACTGTTATGCCTACTTATAAAGGTTACAGAATATTTTTCCATAATTTTCTTGTATAGCAG 1620
776-1E      ACTGTTATGCCTACTTATAAAGGTTACAGAATATTTTTCCATAATTTTCTTGTATAGCAG 1620
776-2E-SM   ACTGTTATGCCTACTTATAAAGGTTACAGAATATTTTTCCATAATTTTCTTGTATAGCAG 1620
            ************************************************************

776-2E      TGCAGCTTTTTCCTTTGTGGTGTAAATAGCAAAGCAAGCAAGAGTTCTATTACTAAACAC 1680
776-1E      TGCAGCTTTTTCCTTTGTGGTGTAAATAGCAAAGCAAGCAAGAGTTCTATTACTAAACAC 1680
776-2E-SM   TGCAGCTTTTTCCTTTGTGGTGTAAATAGCAAAGCAAGCAAGAGTTCTATTACTAAACAC 1680
            ************************************************************

776-2E      AGCATGACTCAAAAAACTTAGCAATTCTGAAGGAAAGTCCTTGGGGTCTTCTACCTTTCT 1740
776-1E      AGCATGACTCAAAAAACTTAGCAATTCTGAAGGAAAGTCCTTGGGGTCTTCTACCTTTCT 1740
776-2E-SM   AGCATGACTCAAAAAACTTAGCAATTCTGAAGGAAAGTCCTTGGGGTCTTCTACCTTTCT 1740
            ************************************************************

776-2E      CTTCTTTTTTGGAGGAGTAGAATGTTGAGAGTCAGCAGTAGCCTCATCATCACTAGATGG 1800
776-1E      CTTCTTTTTTGGAGGAGTAGAATGTTGAGAGTCAGCAGTAGCCTCATCATCACTAGATGG 1800
776-2E-SM   CTTCTTTTTTGGAGGAGTAGAATGTTGAGAGTCAGCAGTAGCCTCATCATCACTAGATGG 1800
            ************************************************************

776-2E      CATTTCTTCTGAGCAAAACAGGTTTTCCTCATTAAAGGCATTCCACCACTGCTCCCATTC 1860
776-1E      CATTTCTTCTGAGCAAAACAGGTTTTCCTCATTAAAGGCATTCCACCACTGCTCCCATTC 1860
776-2E-SM   CATTTCTTCTGAGCAAAACAGGTTTTCCTCATTAAAGGCATTCCACCACTGCTCCCATTC 1860
            ********************  ********************  ********************
                 SVPENT1 FP            SV40 PROBE            SVPENT2 RP
776-2E      ATCATTCCATAGGTTGGAATCTCAGTTGCATCCCAGAAGCCTCCAAAGTCAGGTTGATGA 1920
776-1E      ATCATTCCATAGGTTGGAATCTCAGTTGCATCCCAGAAGCCTCCAAAGTCAGGTTGATGA 1920
776-2E-SM   ATCATTCCATAGGTTGGAATCTCAGTTGCATCCCAGAAGCCTCCAAAGTCAGGTTGATGA 1920
            ************************************************************

776-2E      GCATATTTTACTCCATCTTCCATTTTCTTGTACAGAGTATTCATTTTCTTCATTTTTTCT 1980
776-1E      GCATATTTTACTCCATCTTCCATTTTCTTGTACAGAGTATTCATTTTCTTCATTTTTTCT 1980
776-2E-SM   GCATATTTTACTCCATCTTCCATTTTCTTGTACAGAGTATTCATTTTCTTCATTTTTTCT 1980
            ************************************************************

776-2E      TCATCTCCTCCTTTATCAGGATGAAACTCCTTGCATTTTTTTAAATATGCCTTTCTCATC 2040
776-1E      TCATCTCCTCCTTTATCAGGATGAAACTCCTTGCATTTTTTTAAATATGCCTTTCTCATC 2040
776-2E-SM   TCATCTCCTCCTTTATCAGGATGAAACTCCTTGCATTTTTTTAAATATGCCTTTCTCATC 2040
            ************************************************************

776-2E      AGAGGAATATTCCCCCAGGCACTCCTTTCAAGACCTAGAAGGTCCATTAGCTGCAAAGAT 2100
776-1E      AGAGGAATATTCCCCCAGGCACTCCTTTCAAGACCTAGAAGGTCCATTAGCTGCAAAGAT 2100
776-2E-SM   AGAGGAATATTCCCCCAGGCACTCCTTTCAAGACCTAGAAGGTCCATTAGCTGCAAAGAT 2100
            ************************************************************

776-2E      TCCTCTCTGTTTAAAACTTTATCCAT 2126
776-1E      TCCTCTCTGTTTAAAACTTTATCCAT 2126
776-2E-SM   TCCTCTCTGTTTAAAACTTTATCCAT 2126
            *************************
```

Figure 2.4: Alignment of the sequence of the T-antigen gene from SV40 strains 776-1E, -2E (Genbank accession number J02400.1) and -2E-SM (Sullivan *et al*, 2005) showing forward primer (FP), reverse primer (RP) and probe

Table 2.4: Nucleic acid sequence of SV40 T-ag specific primers and probes used in the RQ-PCR assay

Primer set	Primer / Probe name [a]	Primer / Probe sequence (5' to 3')	Nucleotide position [b]
T-ag-specific	SVPENT1 FP	GATGGCATTTCTTCTGAGCAAA	1796-1817
T-ag-specific	SVPENT2 RP	GAATGGGAGCAGTGGTGGAA	1860-1841
T-ag-specific	SV40 probe	FAM-CAGGTTTTCCTCATTAAA-MGB	1819-1836

[a] FP; forward primer, RP; reverse primer
[b] Reference nucleotide positions in T-antigen gene of SV40 strain 776 (Genbank accession number J02400.1)
(Table adapted from McNees *et al*, 2009)

2.6.2.2 RQ-PCR quantification standards

Quantification of the SV40 T-ag and human RNAse P genes was performed, by generating a dilution series using quantification standards with known gene copy numbers ranging from 10^7 to 10^0 copies. Quantification standards were prepared by making serial 10-fold dilutions of plasmid DNA encoding the target genes. For the SV40 T-ag quantification standards, a previously prepared plasmid encoding the full-length SV40 genome, pSV40-B2E strain Baylor was used (Lednicky and Butel, 1997). RNAse P standards had been prepared by cloning RNAse P gene amplicons from human placental DNA into a pUC19 plasmid (McNees *et al*, 2005). The RNAse P insert was then confirmed by restriction digestion and nucleic acid sequence analysis. Plasmid concentrations were determined spectrophotometrically, and dilutions were made accordingly. Accurate preparation of the standard dilution series was confirmed by RQ-PCR analysis and the plasmid standards were then stored in small-volume aliquots at -20°C. Quantification standards were analysed in duplicate in each RQ-PCR assay.

2.6.2.3 RQ-PCR assay

RQ-PCR reactions were prepared in the PCR Clean Rooms Core Facility at the Department of Molecular Virology and Microbiology, Baylor College of Medicine. This facility is an area with PCR-preparation dedicated workspaces and equipment. All equipment and reaction reagents used to prepare RQ-PCR reaction mixes were stored in this PCR facility and used in this area. Equipment was allowed to stand under UV light for greater than 15 min before use. Immediately before use, aliquots of PCR reagents were collected from -20°C storage and thawed inside the biological cabinet. Details of all reagents used were recorded.

The two singleplex RQ-PCR assays for the detection of SV40 T-ag and the single copy RNAse P genes were performed in parallel on DNA samples from the infection time course. A master mix of PCR components was prepared separately for both SV40 and RNAse P reactions. The 50 µl SV40 reaction mixture contained 25 µl of 2X TaqMan® Universal PCR Master Mix 2X (Applied Biosystems), 900 nM of SV40 primers SVPENT1 and SVPENT2 and 100 nM of the SV40 probe. The RNAse P reaction mixture consisted of 25 µl of 2X TaqMan® Universal PCR Master Mix 2X (Applied Biosystems) and 2.5 µl TaqMan® FAM-MGB control reagent RNAse P primer and probe, used as per manufacturer's directions. Both master mixes were brought up to 40 µl with distilled water (Gibco). A 40 µl aliquot of the mastermix was added to each PCR tube (MicroAmp™ Optical 8-Tube Strip, Applied Biosystems) and reactions were sealed with optical caps (Applied Biosystems). Outside of the PCR Clean Rooms Core Facility, 10 µl of SV40-infected cell DNA samples or standard plasmid dilutions were added in duplicate to the PCR tubes. A non-template control (NTC) containing all PCR components but lacking test or plasmid DNA was also included in all RQ-PCR reactions as a negative control for DNA amplification. A series of uninfected mock samples, taken at different time points, were analysed with each RQ-PCR run for both SV40 T-ag and human RNAse P as a negative control for SV40 detection. PCR reaction tubes were centrifuged briefly using a microcentrifuge before RQ-PCR analysis.

2.6.2.4 RQ-PCR amplification conditions

Amplification was carried out using the ABI PRISM 7000 Sequence Detection System (Applied Biosystems) according to the manufacturer's recommendations. Reaction conditions for amplification of both target genes were as follows: 50°C for 2 min, 95°C for

10 min to activate hot start *Taq* DNA polymerase, 40 cycles of denaturing at 95°C for 15 s followed by annealing and extension at 60°C for 1 min. Amplification data, measured as an increase in reporter fluorescence, were collected in real time and analysed by Sequence Detection System software (Applied Biosystems).

2.6.2.5 Analysis of RQ-PCR

Absolute quantification of the target SV40 and RNAse P genes was calculated from standard curves generated by plotting the $\log_{10}$ of the known gene copy number of the standard dilution series against the C_T value obtained in the RQ-PCR analysis. The C_T value is defined as the threshold cycle, which is the cycle number calculated by the Sequence Detection Software at which fluorescence is ten standard deviations above the mean background signal in the first 15 cycles. Detection of target genes occurs at threshold cycle. Using the standard curves generated from each assay, mean quantities of the duplicate samples were calculated from the C_T results. To calculate the RNAse P copy number per cell, the RNAse P mean quantity was divided by two to calculate the RNAse P copy number per cell, as there is one gene copy per human genome and human cells are diploid. This figure was then divided by the SV40 mean quantity to give the number of T-ag copies per cell.

3.0 Results

This study was designed to investigate SV40 interaction with human lymphocytes by infecting three lymphocyte cell lines with three different strains of SV40 as illustrated in Figure 2.2. Infected cell cultures were incubated for up to 13 days and during this time period aliquots were taken at time points for analysis of lymphocyte surface marker expression, SV40 T-ag expression and SV40 viral load. In addition, daily cell counts allowed SV40 effect on lymphocyte cell growth to be examined.

3.1 Cell proliferation and viability of SV40-infected cell lines

To investigate the effect of SV40 infection on the cell proliferation and viability of B lymphocyte cell lines BJAB and DG75 and T cell line CEM, a viable cell count was performed daily throughout the infection time course, using the trypan blue exclusion assay. When lymphocyte cell viability was calculated, by expressing the number of live cells as a percentage of the total number of cells counted, the percentage viability of all SV40-infected cell lines remained above 90% similar to the uninfected mock samples, indicating that infection with any of the three viral strains of SV40 was not associated with cell death.

An increase in cell numbers in the DG75 cell line, following infection with 776-1E and 776-2E SV40 strains was observed, suggesting that these particular viruses may, in fact, induce proliferation of this B-lymphocyte cell line (Figure 3.1 a). In DG75 cells infected with the single enhancer virus, SV40 776-1E, there was an increase in cell numbers from 2×10^7 on 6 d.p.i. to 7×10^7 on 13 d.p.i. DG75 cells infected with the virus SV40 776-2E, containing a duplicated enhancer element, displayed cell number increases from 2×10^7 on 7 d.p.i. to 8 x

10^7 by day 13. These increases in cell numbers in both the -1E and -2E infected DG75 cells represent almost a four-fold increase seen over the time course period compared to the uninfected mock cells, which remained at a constant cell number throughout the 13 days (Figure 3.2).

The SV40 776-1E and SV40 776-2E-induced proliferation seen in the DG75 cell line was not mirrored in the other B cell line, BJAB, with the number of live cells in infected cultures remaining constant at 2 x 10^7 cells until the end of the time course (Figure 3.1 b). Unlike the DG75 cell line, the uninfected mock BJAB cells outgrew the infected cultures, with numbers reaching a peak of 5 x 10^7 cells on 10 d.p.i. before decreasing back down to below 3 x 10^7 by 13 d.p.i. In contrast to the SV40 -1E and -2E strains, the miRNA mutant virus 776-2E-SM failed to induce proliferation in either of the two B cell lines, BJAB and DG75, instead appearing to stagnate cell growth, with the number of live cells being reduced following infection (Figure 3.1 a and 3.1 b). The same pattern of growth is seen in the two B cell lines infected with the mutant virus. In both cases, cell growth was comparable to the uninfected mock sample up until 6 d.p.i., after which time, cell numbers decreased and remained between 1 x 10^6 and 2 x 10^7 until 13 d.p.i.

In the SV40-infected T cell line, CEM, no notable change in cell numbers was observed among the different cultures (Figure 3.1 c). The CEM SV40-infected and uninfected mock cells grew at a similar rate. By 13 d.p.i., the CEM mock cell culture reached over 5 x 10^7 cells with the -2E and -1E infected cultures growing to between 2 x 10^7 and 3 x 10^7 cells over the 13 days respectively.

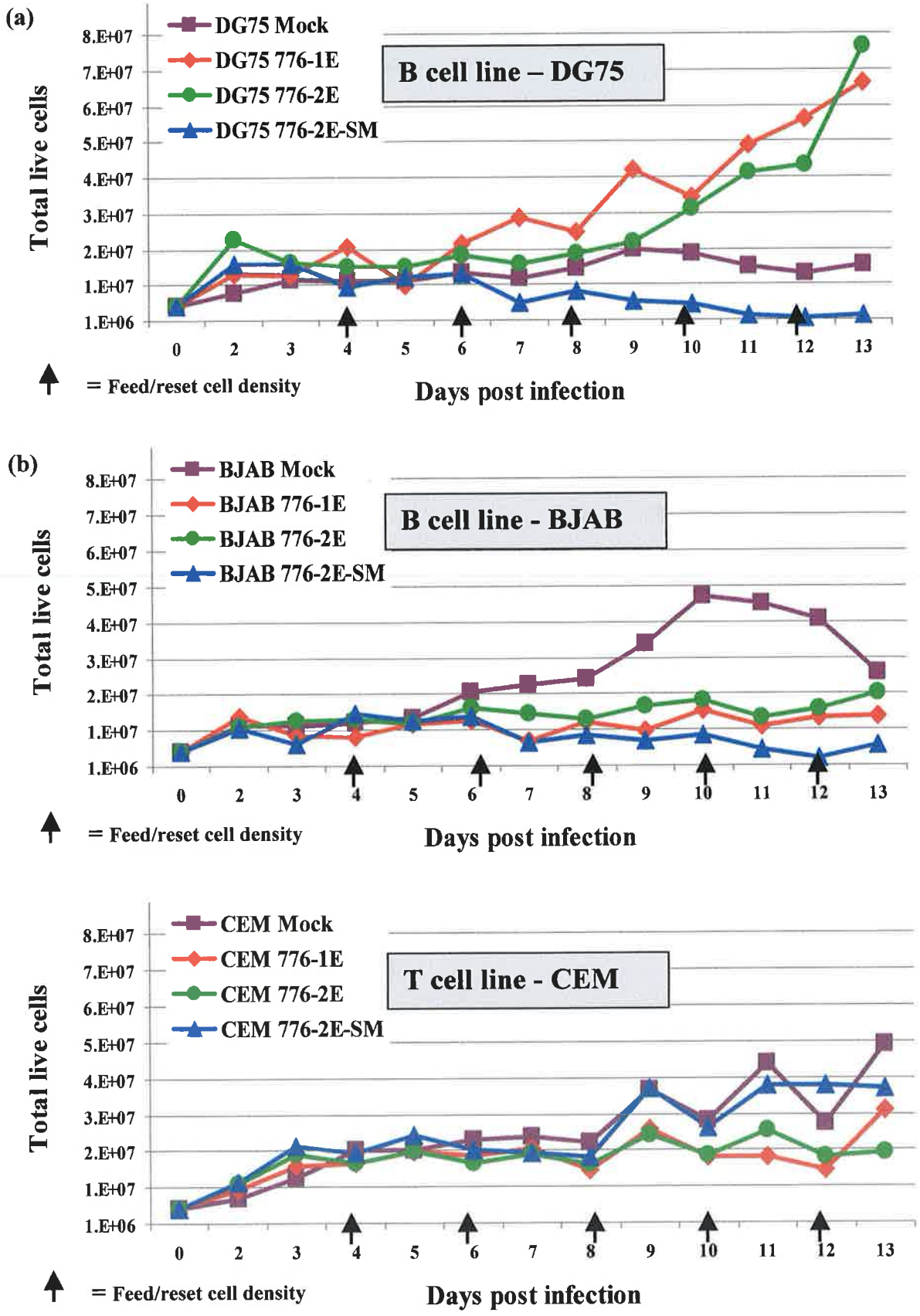

Figure 3.1: Total number of live cells in SV40-infected lymphocyte cell lines
Figures show the total number of live cells in cultures of human lymphocyte B cell lines (a) DG75, (b) BJAB and T cell line (c) CEM, infected with SV40 viruses 776-1E, -2E, and -2E-SM, as measured in duplicate by the trypan blue exclusion assay. Uninfected mock samples are shown in purple.

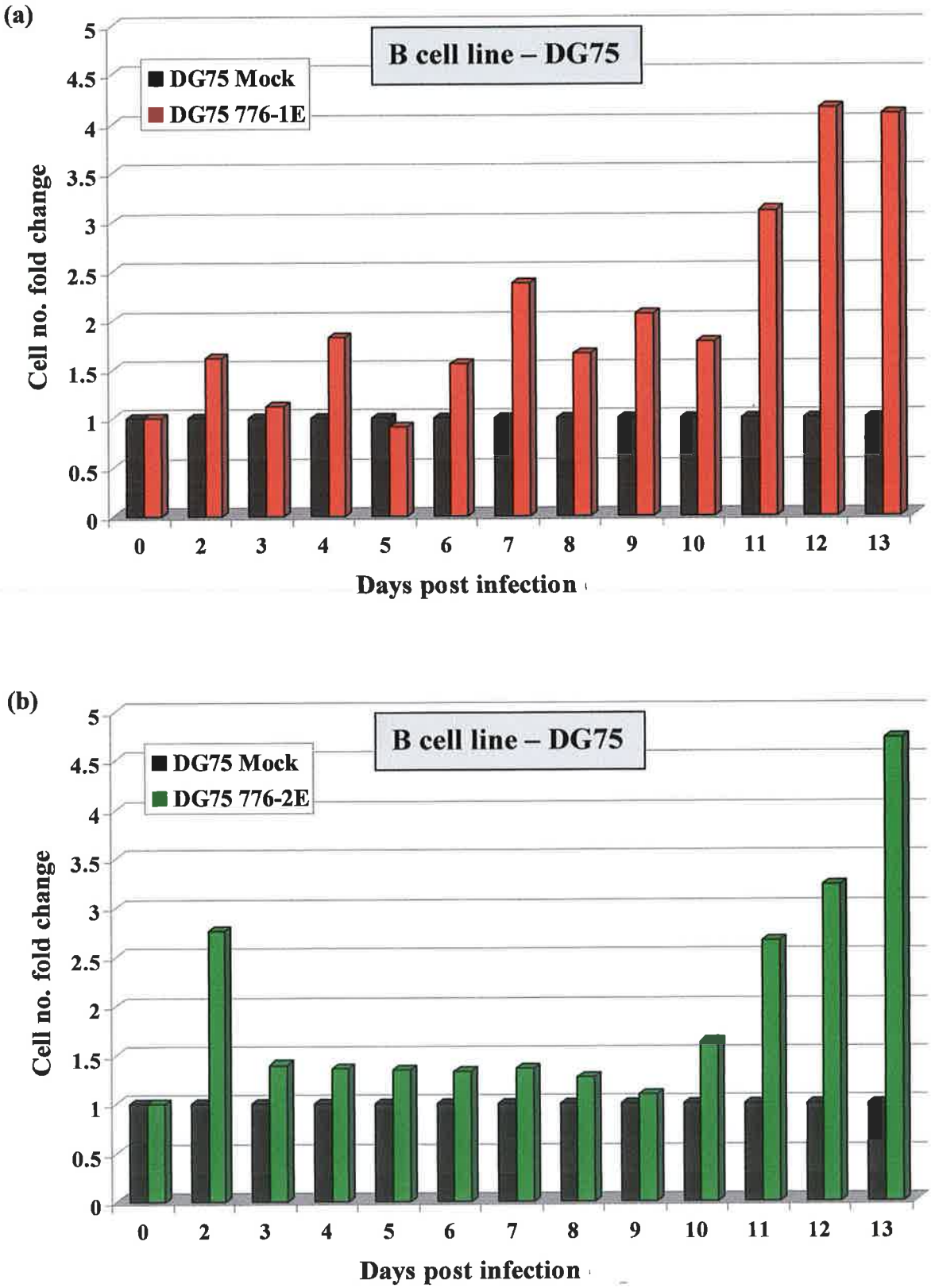

Figure 3.2: Cell number fold change in SV40-infected B cell line DG75
Change in cell numbers in DG75 cell line infected with (a) SV40 776-1E and (b) SV40 776-2E, as compared to uninfected mock cells. Cell number fold change is based on the ratio of virally-infected cells to uninfected cells at each day post infection as calculated using daily viable cell counts performed in duplicate using the trypan blue exclusion assay.

3.2 Cell surface marker expression by flow cytometry analysis

In addition to analysing the effect of SV40 on lymphocytic proliferation and viability, viral effects on surface expression of the activation marker CD69 and co-stimulation markers, CD80 and CD86, were also investigated on SV40-infected cell lines. Surface staining was performed on aliquots collected from the optimised infection time course (Figure 2.2) using fluorescent-labelled monoclonal antibodies and samples were then analysed by flow cytometry.

In the control of this analysis, the isotype-control antibody produced similar background fluorescence for each fluorescent marker (-PE, -FITC and -APC) on uninfected mock samples and cells infected with the SV40 776-1E and -2E viruses. A slight increase in isotype-control staining was, however, noted on cells infected with the SV40 776-2E-SM virus at the later time points. On investigation, comparison of -PE dot plots for the mock and 776-2E-SM isotype controls revealed increased non-specific staining in -2E-SM-infected cells, most likely due to cell death in virally infected cells at later time points (Figure 3.3).

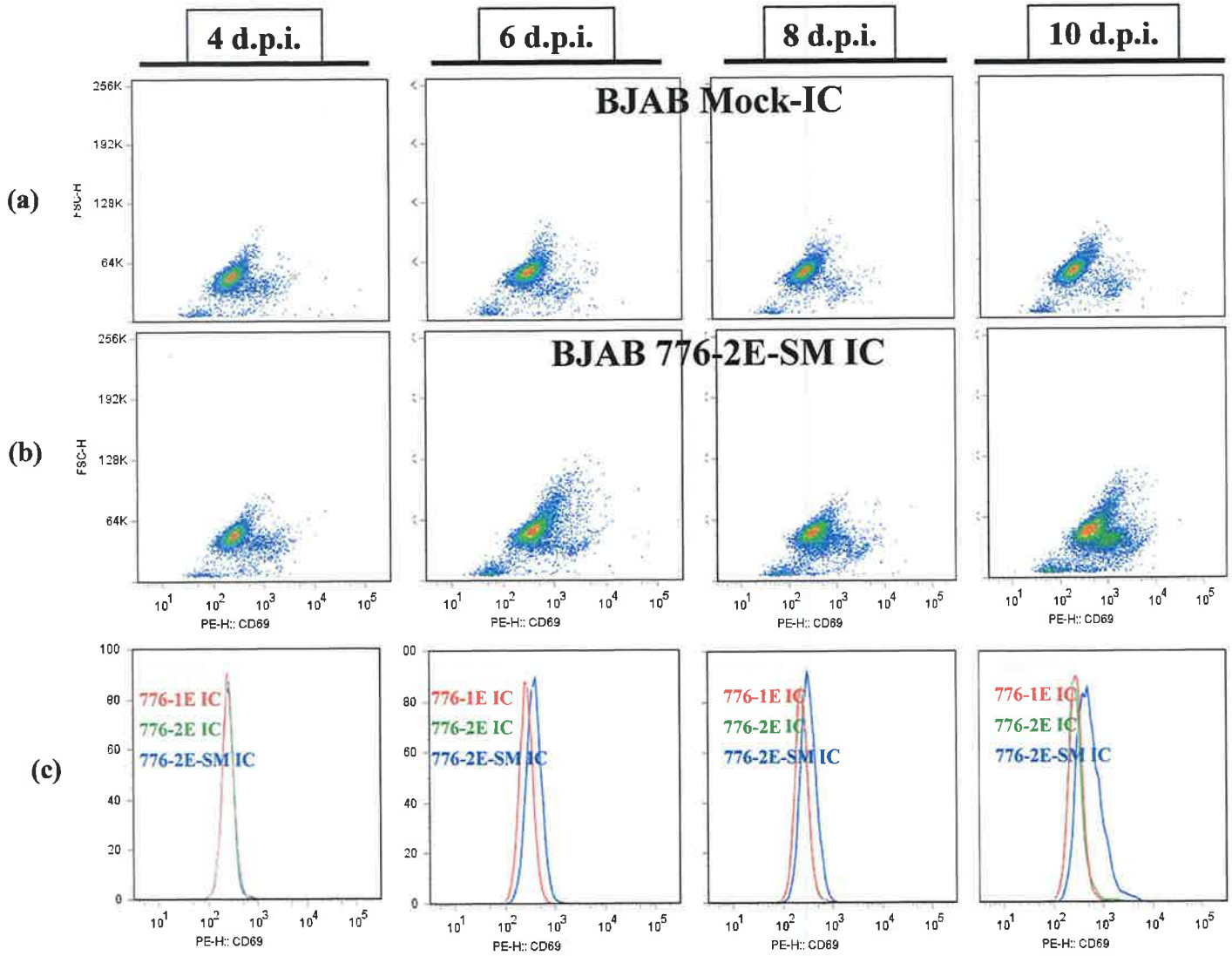

Figure 3.3: Flow cytometric analysis of BJAB mock and SV40 776-2E-SM-infected isotype control samples. Dot plots of FSC-H *versus* PE-H are shown for (a) BJAB uninfected mock cells and (b) SV40 776-2E-SM-infected cells stained with a PE-isotype control (IC) at 4, 6, 8 and 10 days post infection (d.p.i.). Panel (c) shows the histograms of the isotype controls for the mock and cells infected with SV40 776-1E, 776-2E, -2E and 2E-SM infected cells.

When the flow cytometry results of CD80 were analysed using the BJAB cell line, by overlaying histograms from uninfected mock cells and virally-infected cells, changes in the expression of this co-stimulatory marker were evident in cells infected with the SV40 776-2E-SM virus (Figure 3.4). A downward trend in CD80 expression was notable on 2E-SM-infected BJAB cells, beginning at 6 d.p.i. and continuing until the final time point at 10 d.p.i., with a left shift of 4.5% on 8 d.p.i. and 17% on 10 d.p.i (Figures 3.5-3.8). In contrast, minimal changes were observed in cells infected with the other two SV40 strains, with SV40 776-1E and 776-2E-infected cells demonstrating a shift of less than 1% from 4 to 8 d.p.i. in CD80 expression (Figure 3.5-3.7). CD80 downregulation was, however, observed at the final time point by 3.5% and 3.8% on -1E and -2E infected cells respectively (Figure 3.8). Based on the non-specific staining observed in isotype control samples at later time points, it is likely that there was a decrease in cell viability by day 10, making these results a less reliable indicator of surface marker changes (Figure 3.3).

On the other DG75 B cell line and CEM T cell line, this pattern of CD80-downregulation was absent with surface expression being comparable to the uninfected mock samples (Figure 3.9).

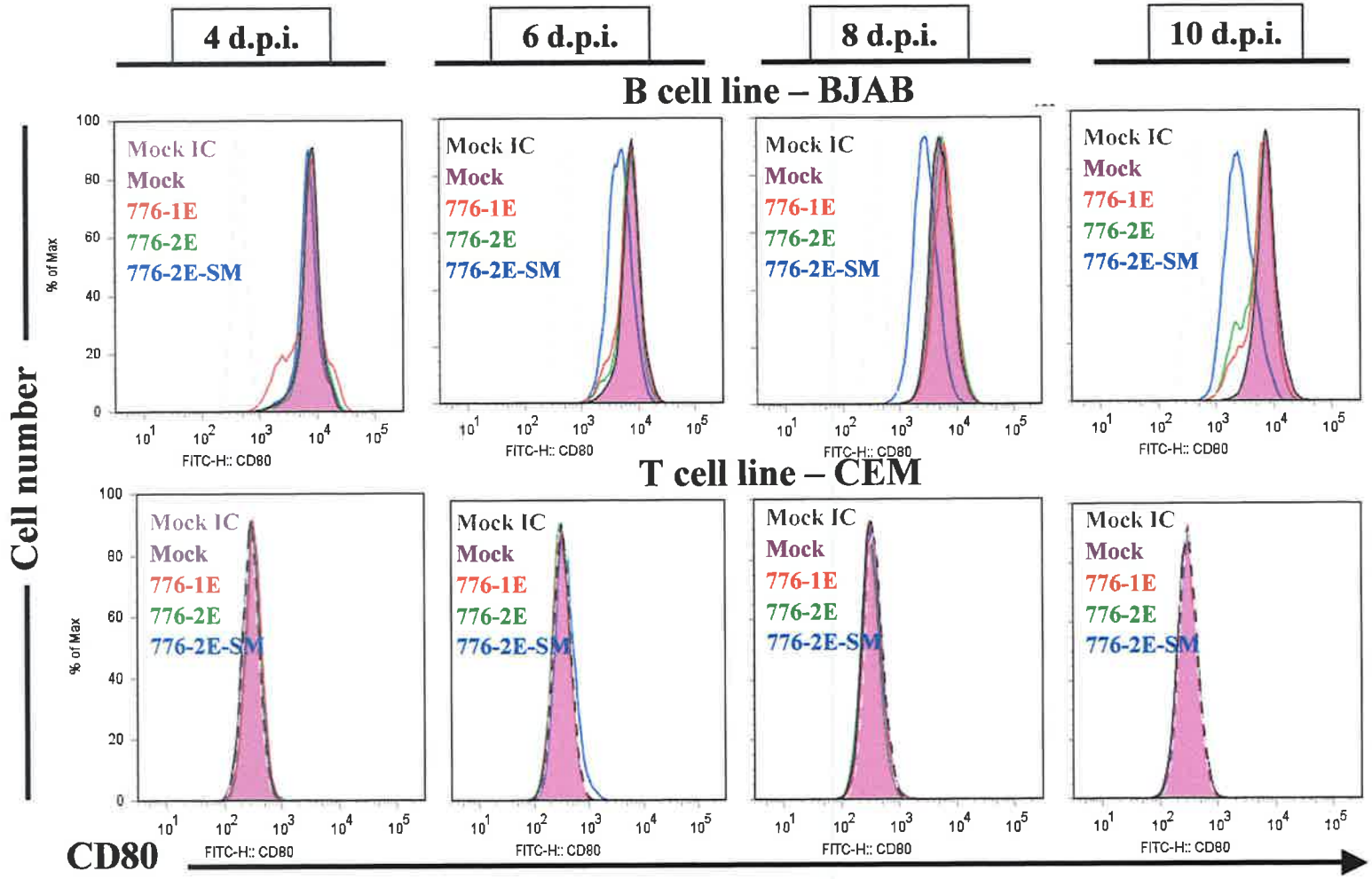

Figure 3.4: CD80 expression on SV40-infected BJAB and CEM cell lines. Histograms show surface expression of CD80 on the B cell line, BJAB, and T cell line, CEM. Both cell lines were either uninfected (solid purple peak), or infected with SV40 776-1E (red), SV40 776-2E (green) and SV40 776-2E-SM (blue) in an optimised infection time course experiment. Aliquots were taken from cell cultures at 4, 6, 8 and 10 days post infection (d.p.i.), stained with anti-CD80-FITC (BD Pharmingen) and analysed by flow cytometry. Grey dashed lines represent the isotype control (IC).

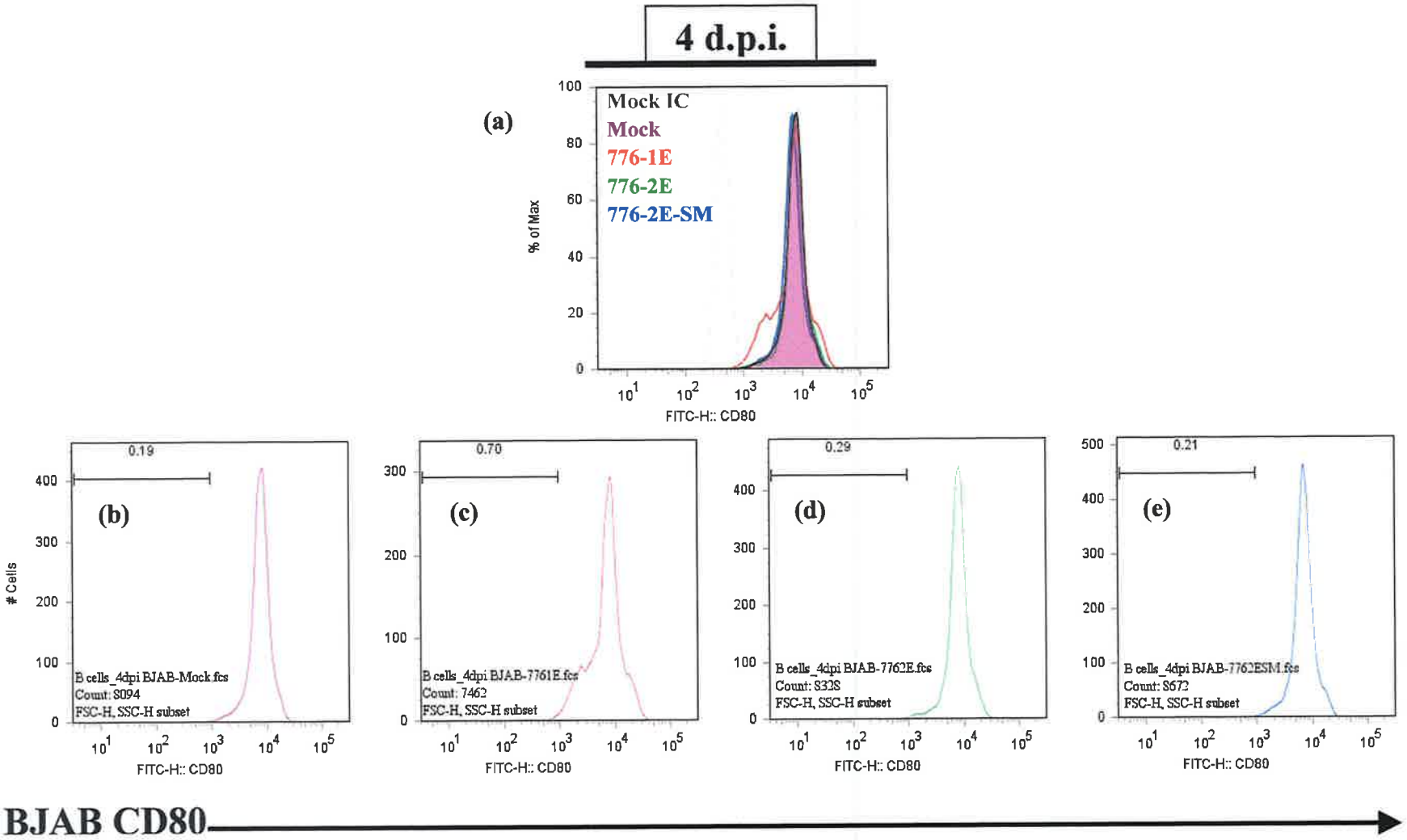

Figure 3.5: CD80 expression on SV40-infected BJAB cell line at 4 d.p.i.
Flow cytometric results of CD80 expression on BJAB cell line at 4 days post infection (d.p.i.) showing (a) overlayed histograms of (b) uninfected mock and cells infected with (c) SV40 776-1E, (d) SV40 776-2E and (e) SV40 776-2E-SM.

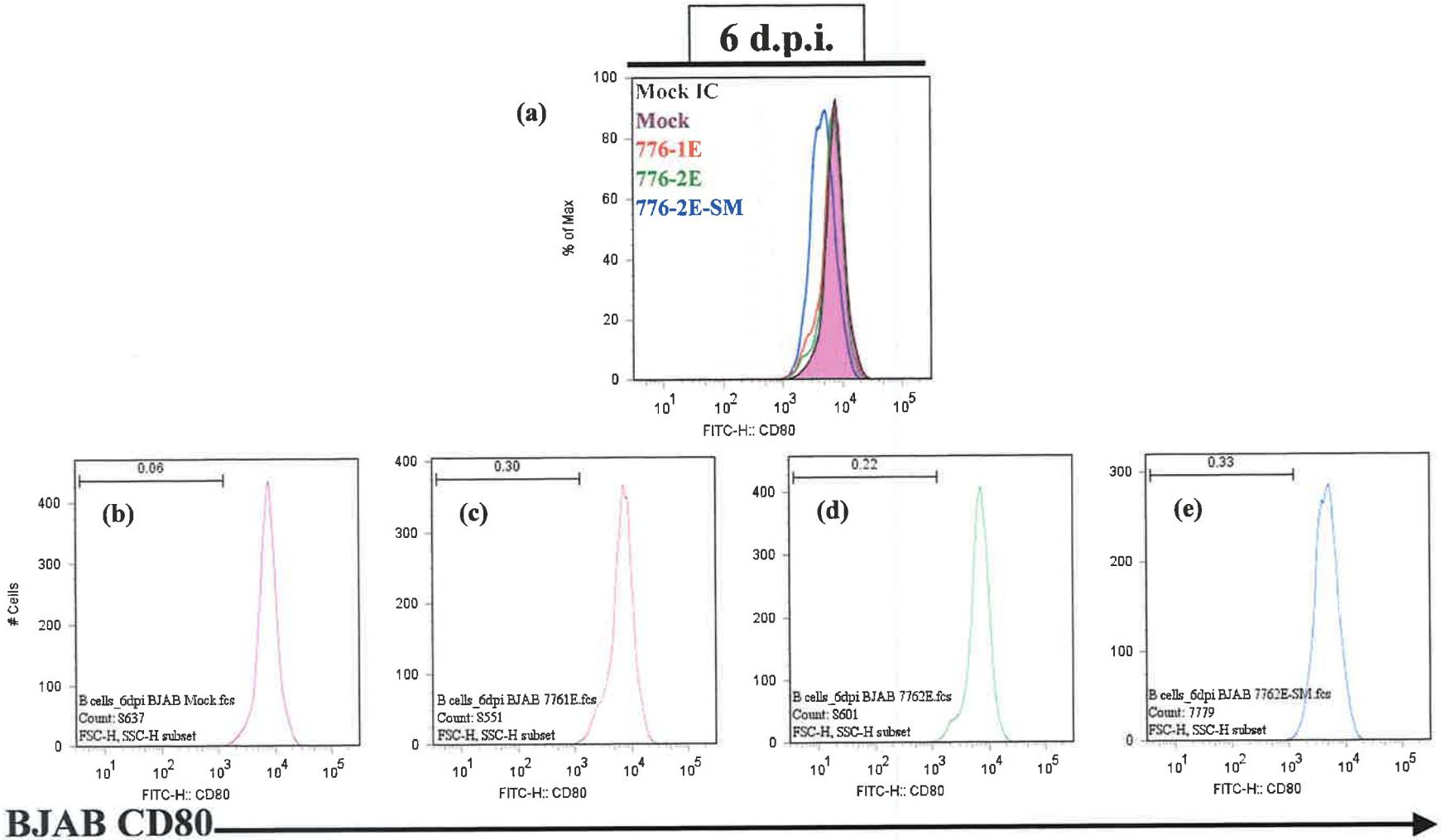

Figure 3.6: CD80 expression on SV40-infected BJAB cell line at 6 d.p.i.
Flow cytometric results of CD80 expression on BJAB cell line at 6 days post infection (d.p.i.) showing (a) overlayed histograms of (b) uninfected mock and cells infected with (c) SV40 776-1E, (d) SV40 776-2E and (e) SV40 776-2E-SM.

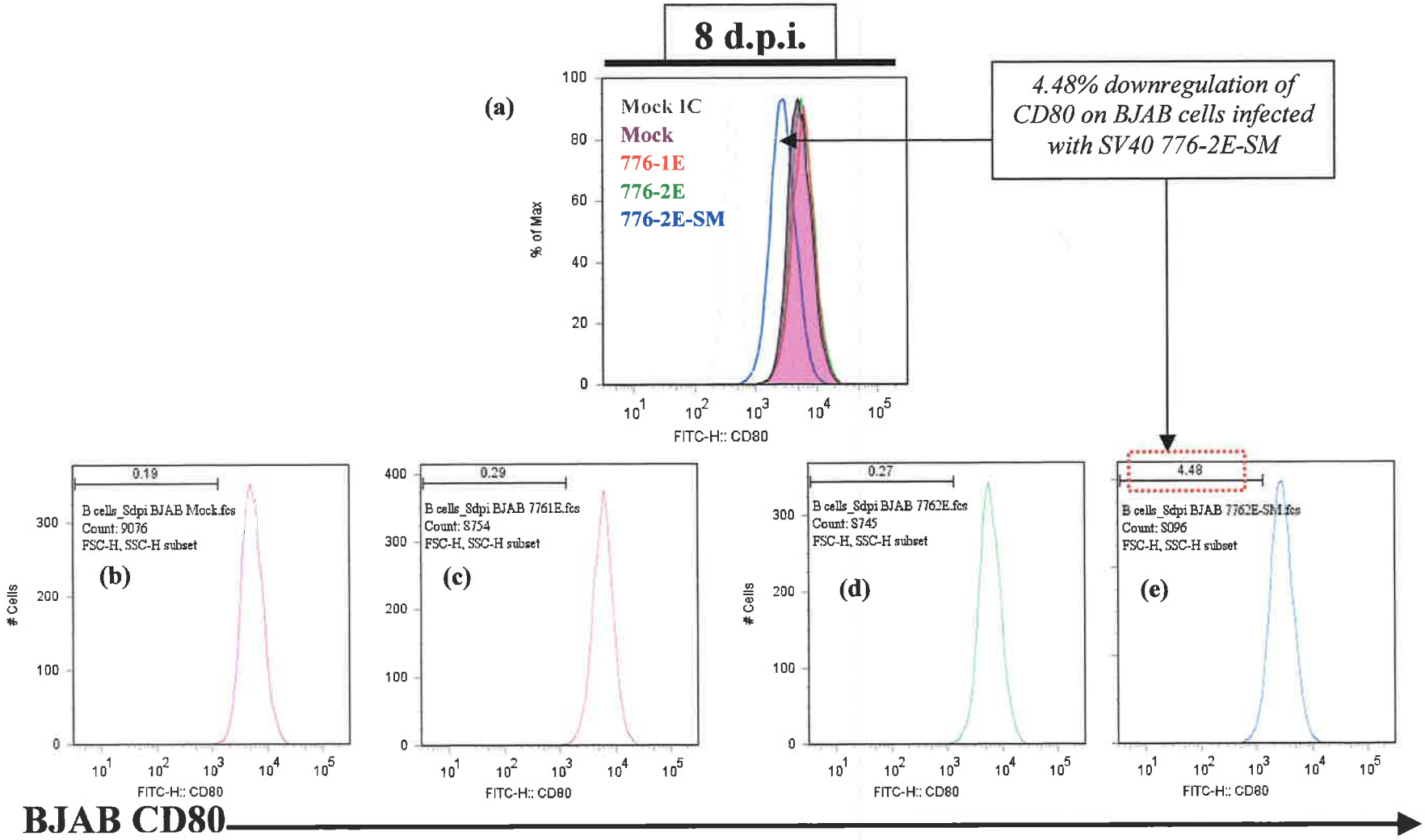

Figure 3.7: CD80 expression on SV40-infected BJAB cell line at 8 d.p.i.
Flow cytometric results of CD80 expression on BJAB cell line at 8 days post infection (d.p.i.) showing (a) overlayed histograms of (b) uninfected mock and cells infected with (c) SV40 776-1E, (d) SV40 776-2E and (e) SV40 776-2E-SM.

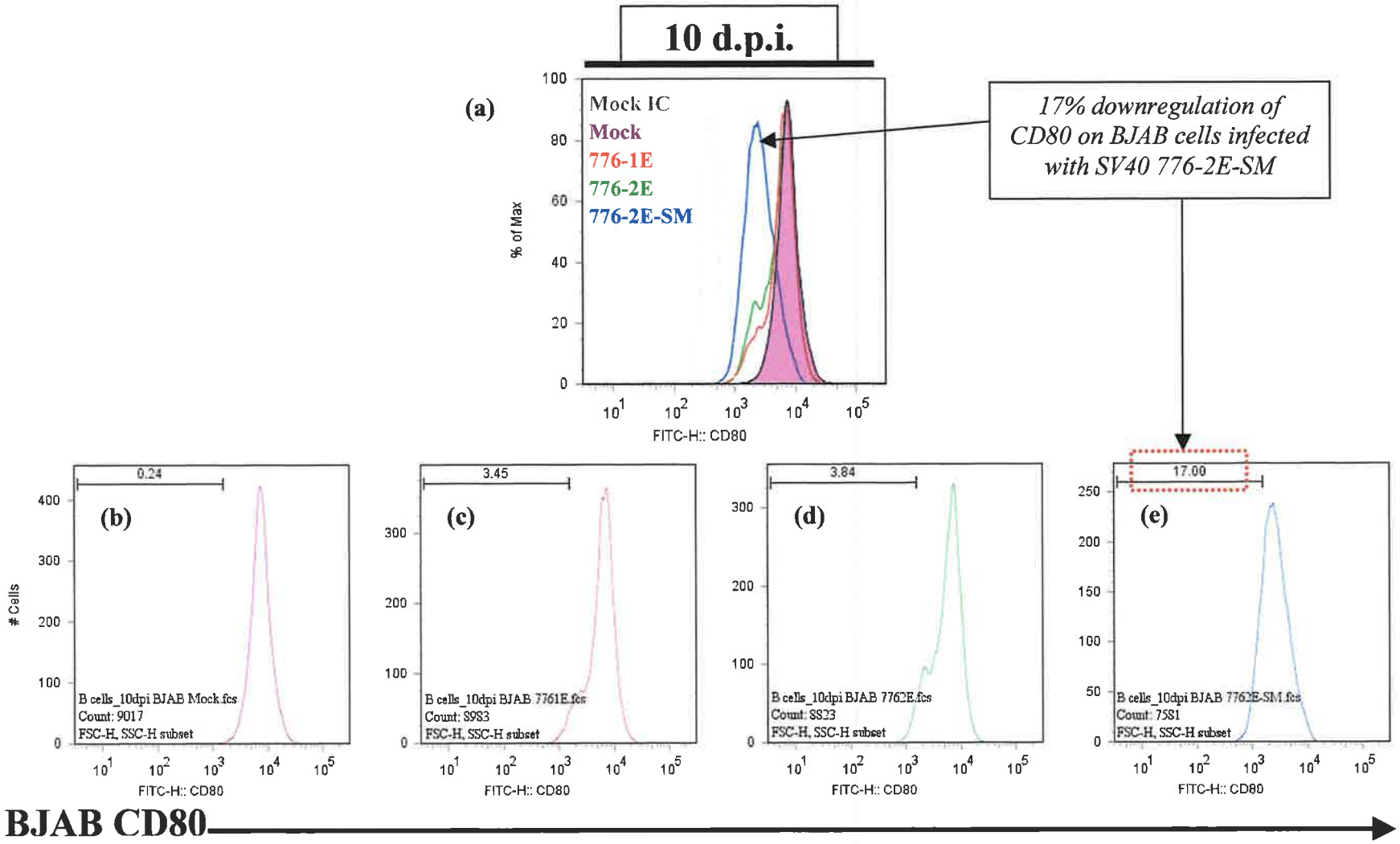

Figure 3.8: CD80 expression on SV40-infected BJAB cell line at 10 d.p.i.
Flow cytometric results of CD80 expression on BJAB cell line at 10 days post infection (d.p.i.) showing (a) overlayed histograms of (b) uninfected mock and cells infected with (c) SV40 776-1E, (d) SV40 776-2E and (e) SV40 776-2E-SM.

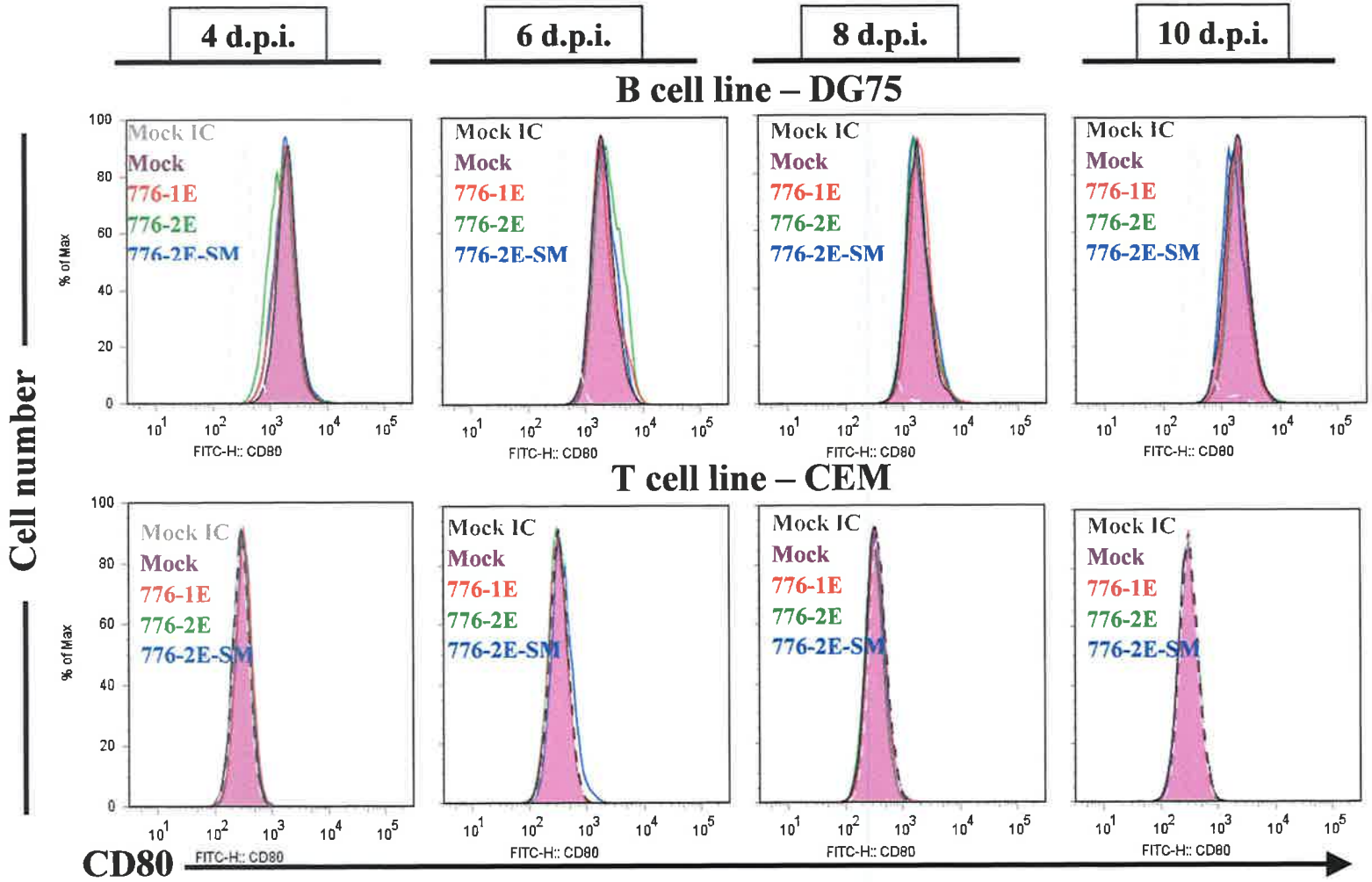

Figure 3.9: CD80 expression on SV40-infected DG75 and CEM cell lines
Histograms show surface expression of CD80 on the B cell line, DG75, and T cell line, CEM. Both cell lines were either uninfected (solid purple peak) or infected with SV40 776-1E (red), SV40 776-2E (green) and SV40 776-2E-SM (blue) in an optimised infection time course experiment. Aliquots were taken from cell cultures at 4, 6, 8 and 10 days post infection (d.p.i.), stained with anti-CD80-FITC (BD Pharmingen) and analysed by flow cytometry. Grey dashed lines represent the isotype control (IC).

When the results of activation marker, CD69, expression were analysed on the BJAB cell line, some changes in the cell surface marker were observed, with a pattern of CD69 upregulation on -2E-SM-infected cells evident over the time course (Figure 3.10). Compared to the uninfected mock cells, samples infected with SV40 776-2E-SM collected on 4, 6 and 8 d.p.i., demonstrated a percentage right-shift of 9.5%, 2.4% and 4% in CD69 expression respectively (Appendix I). For BJAB cells infected with SV40 776-1E and -2E, CD69 expression was largely unchanged over the time course from 4 to 10 d.p.i. Using a gate established from the uninfected mock, the percentage shift of CD69-associated fluorescence for -1E and -2E infected cells remained less than 1% at each time point (Appendix I). The 10 d.p.i. time point differed in that there appeared to be a down regulation of CD69 in cells infected with each of the three viruses, again, most likely due to decreased cell viability at 10 d.p.i. (Figure 3.10).

CD69 expression on the other B cell line, DG75, was slightly upregulated on SV40-infected cells compared to uninfected mock cells at 6, 8 and 10 d.p.i. The CEM cell line once again showed a lack of surface marker changes (Figure 3.11).

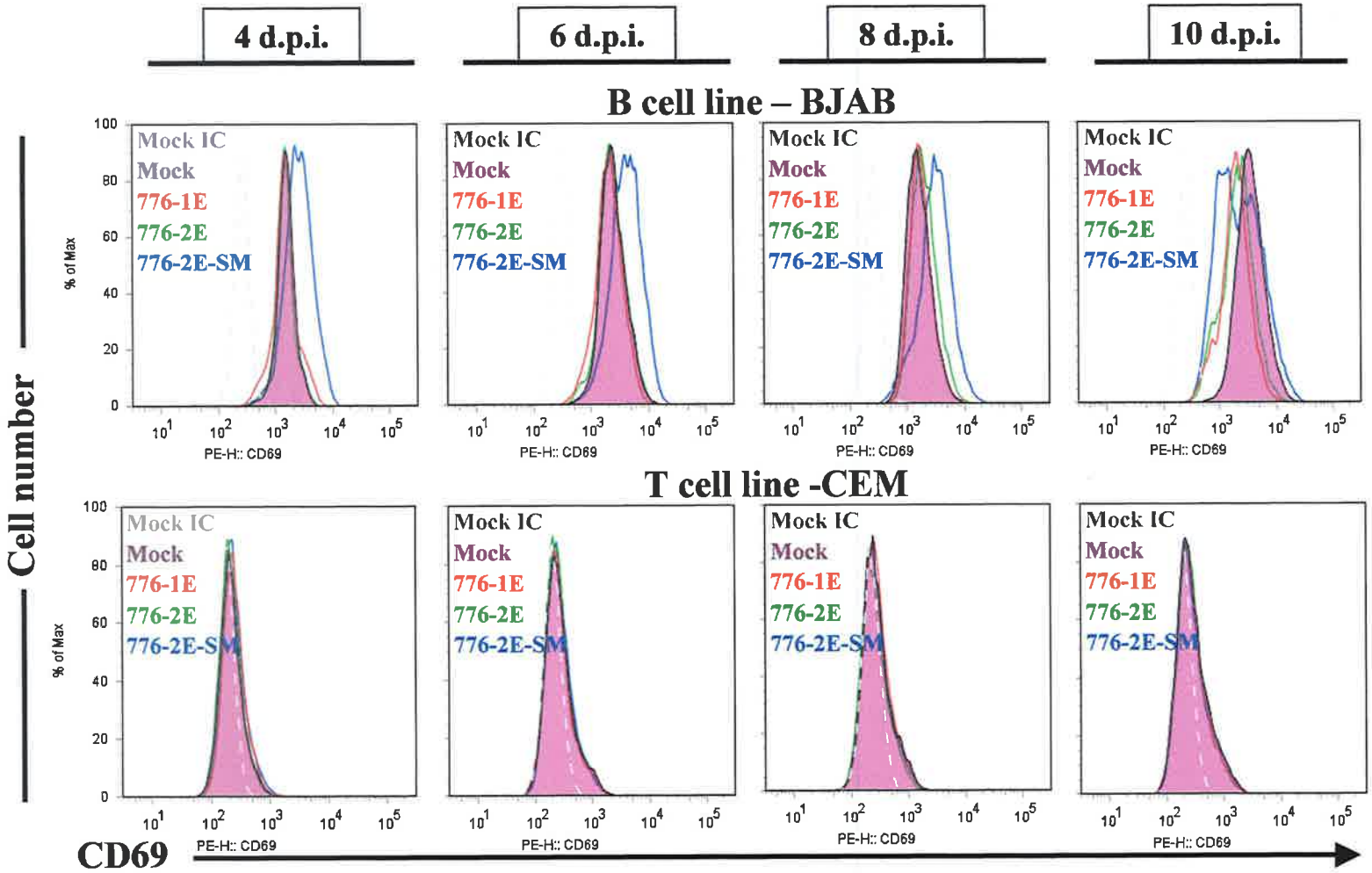

Figure 3.10: CD69 expression on SV40-infected BJAB and CEM cell lines. Histograms show surface expression of lymphocyte activation marker CD69 on the B cell line, BJAB, and T cell line, CEM. Both cell lines were either uninfected (mock, solid purple region) or infected with SV40 776-1E (red), -2E (green) and -2E-SM (blue) in an optimised infection time course experiment. Aliquots were taken from cell cultures at 4, 6, 8 and 10 days post infection (d.p.i.), stained with anti-CD69-PE (BD Pharmingen) and analysed by flow cytometry. Grey dashed lines represent the isotype control (IC).

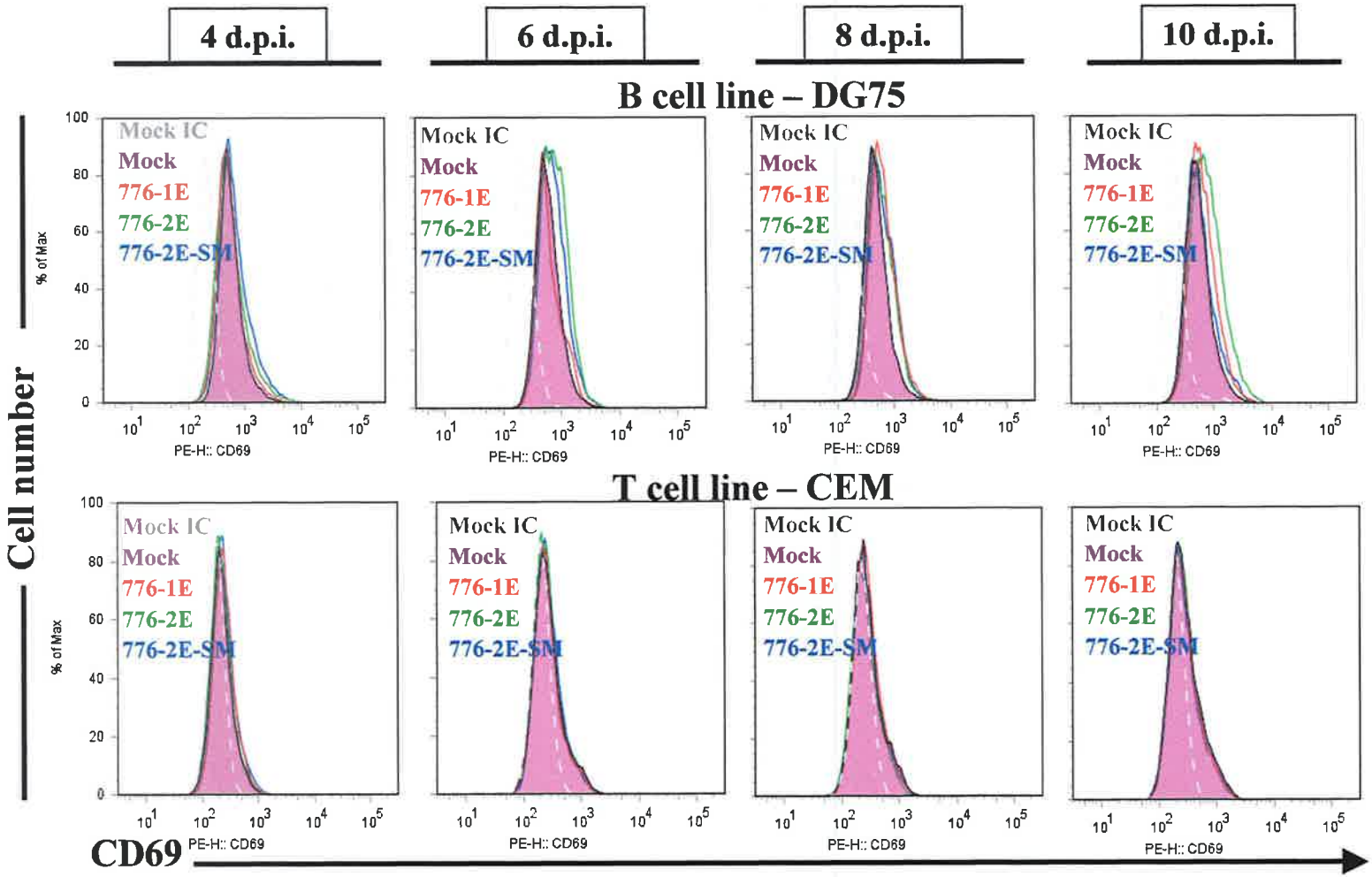

Figure 3.11: CD69 expression on SV40-infected DG75 and CEM cell lines. Histograms show surface expression of lymphocyte activation marker CD69 on the B cell line, DG75, and T cell line, CEM. Both cell lines were either uninfected (mock, solid purple region) or infected with SV40 776-1E (red), SV40 776-2E (green) and SV40 776-2E-SM (blue) in an optimised infection time course experiment. Aliquots were taken from cell cultures at 4, 6, 8 and 10 days post infection (d.p.i.), stained with anti-CD69-PE (BD Pharmingen) and analysed by flow cytometry. Grey dashed lines represent the isotype control (IC).

In contrast to CD69 and CD80, expression analysis of the other co-stimulatory molecule CD86 revealed minimal changes on both B cell lines. In SV40-infected BJAB cells, a moderate level of CD86 downregulation was observed at day 10 post-infection (Figure 3.12). In the DG75 cell line, discernible trends in CD86 surface expression in SV40-infected samples compared to the uninfected mock cell samples were absent (Figure 3.13). CD86 expression remained unchanged on the CEM T cell line relative to the uninfected mock (Figure 3.13).

Having established the lymphoproliferative effect of SV40 on B cell lines and the role of the virus on the modulation of lymphocyte activation and co-stimulatory, the expression of T-ag viral protein was examined. T-ag is known to be essential for viral replication and host cell transformation making T-ag detection an important element of SV40 studies.

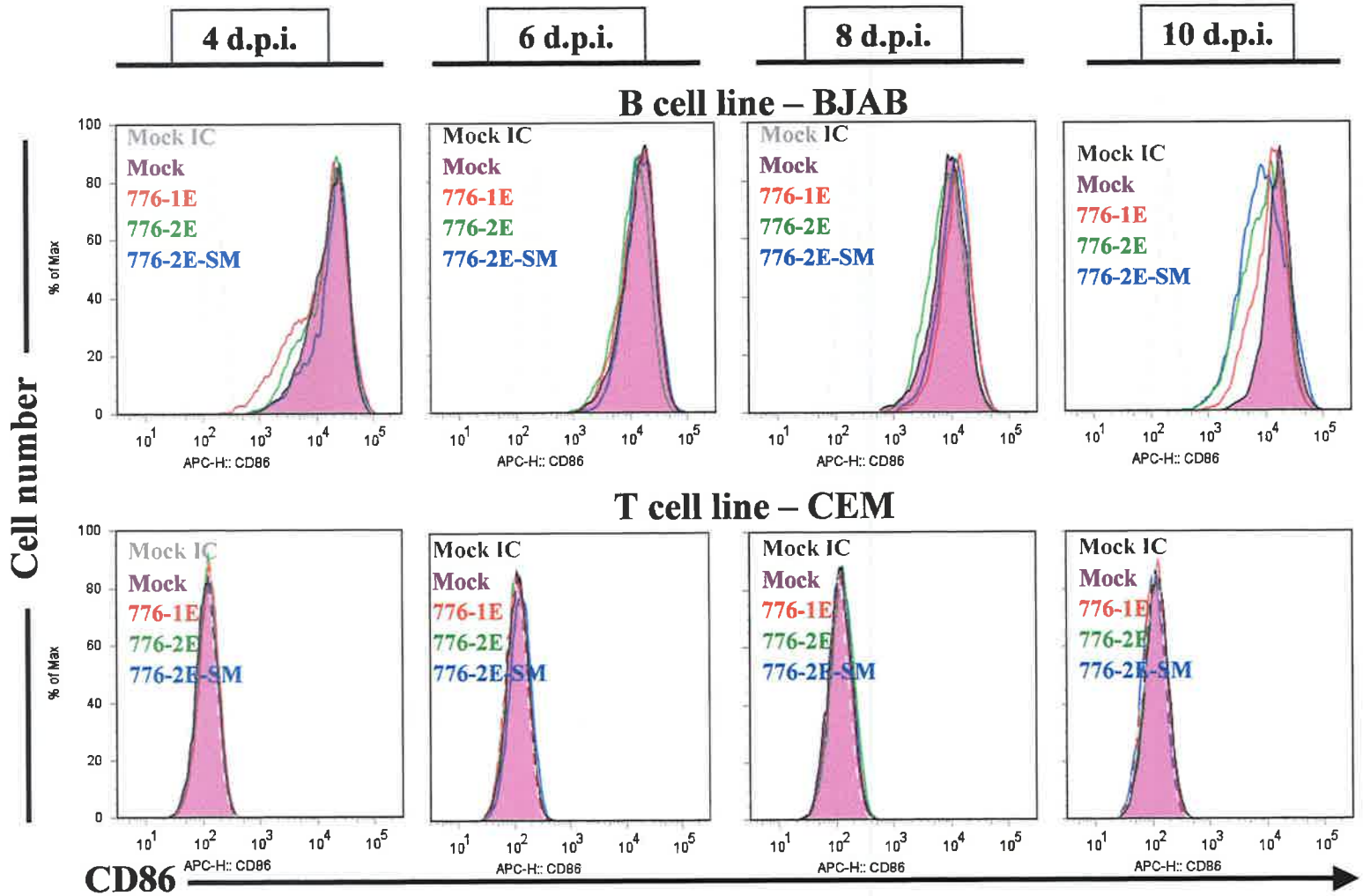

Figure 3.12: CD86 expression on SV40-infected BJAB and CEM cell lines
Histograms show surface expression of CD86 on the B cell line, BJAB, and T cell line, CEM. Both cell lines were either uninfected (solid purple peak) or infected with SV40 776-1E (red), SV40 776-2E (green) and SV40 776-2E-SM (blue) in an optimised infection time course experiment. Aliquots were taken from cell cultures at 4, 6, 8 and 10 days post infection (d.p.i.), stained with anti-CD86-APC (BD Pharmingen) and analysed by flow cytometry. Grey dashed lines represent the isotype control (IC).

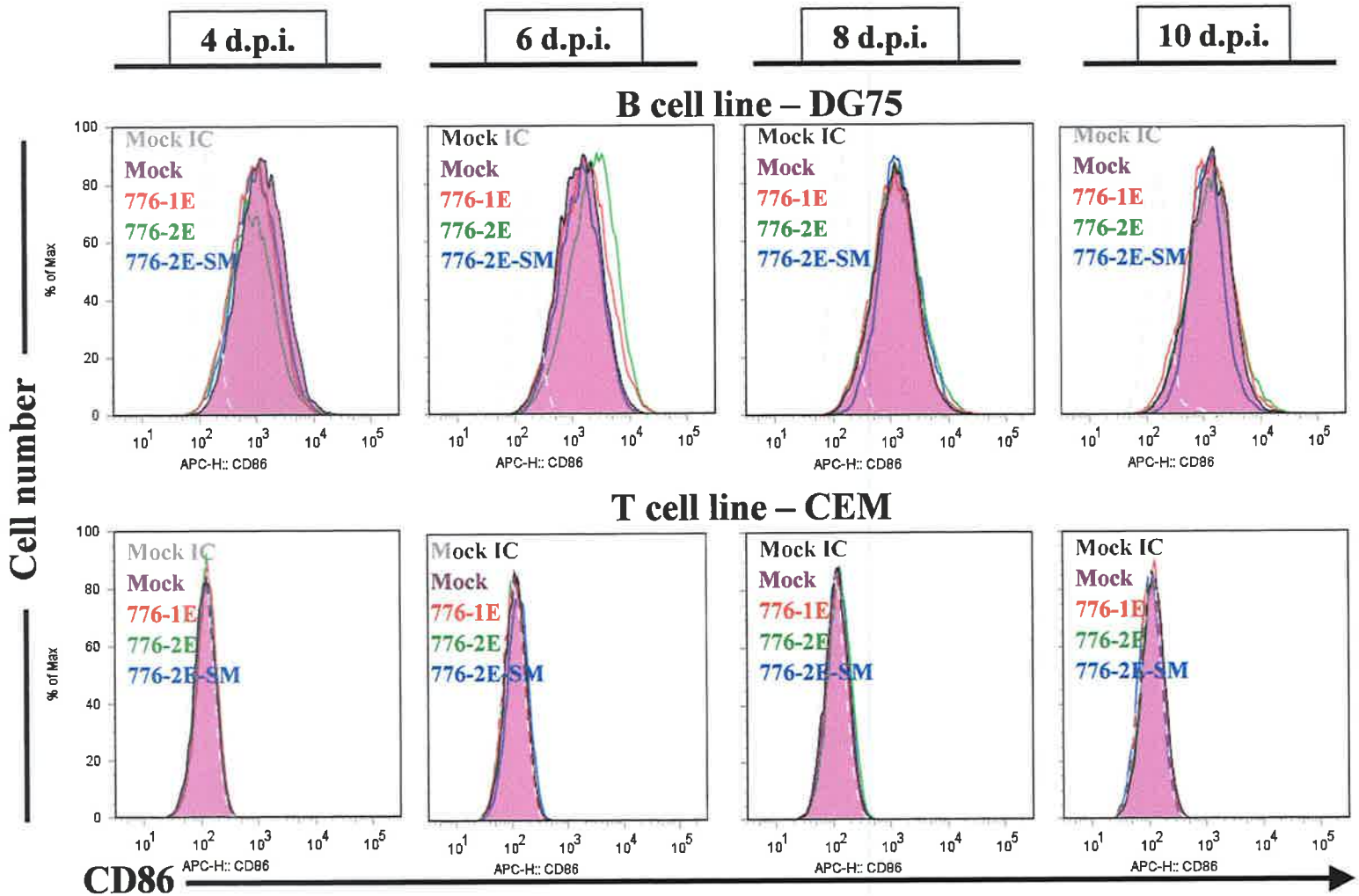

Figure 3.13: CD86 expression on SV40-infected DG75 and CEM cell lines
Histograms show surface expression of CD86 on the B cell line, DG75, and T cell line, CEM. Both cell lines were either uninfected (solid purple peak) or infected with SV40 776-1E (red), SV40 776-2E (green) and SV40 776-2E-SM (blue) in an optimised infection time course experiment. Aliquots were taken from cell cultures at 4, 6, 8 and 10 days post infection (d.p.i.), stained with anti-CD86-APC (BD Pharmingen) and analysed by flow cytometry. Grey dashed lines represent the isotype control (IC).

3.3 Detection of SV40 T-ag by flow cytometry

Flow cytometry was also used to measure expression of large T-ag, the major viral oncoprotein, in the SV40-infected cell lines. In the analysis of the flow cytometric data, a gate was applied to set a fluorescence threshold on the uninfected mock cells at each time point, marking these uninfected mock cells as being negative for -PE fluorescence and thus T-ag expression. When this gate was applied to all SV40-infected cell line samples, the percentage population that shifted to the right lower quadrant was measured as being positive for T-ag. When intracellular staining control results, consisting of the T-ag-positive S1113 cell line, were analysed using a dot plot of SSC *versus* PE fluorescence, 98.3% of stained cells were positive for T-ag expression, with a shift to the right lower quadrant, compared to 0.2% in unstained cells and 0.9% in cells stained with secondary antibody only (Figure 3.14).

SV40-infected TC7 monkey kidney cells were also used as a positive control for the T-ag intracellular staining protocol and flow cytometric analysis. Analysis of the flow cytometric results for these infected-TC7 cells show that the cells were strongly positive for T-ag. In TC7 cells infected with 776-1E, 7% of cells expressed T-ag 24 hours post infection (h.p.i.) and this increased to 20% after 48 hours and 42% at 72 h.p.i. Similarly the percentage of cells expressing T-ag following 776-2E-infection also increased. At 24 h.p.i., 36% of 776-2E-infected TC7 cells expressed T-ag with this figure increasing to 43% and 75% at 48 h.p.i. and 72 h.p.i. respectively, with the percentage expression being twice that in 776-1E-infected cells by 72 h.p.i. The highest rates of T-ag positivity was seen in the TC7 cells infected with the microRNA mutant virus, 776-2E-SM, with cells starting at 52% at 24 h.p.i., 56% at 48 h.p.i. and 97% expression at 72 h.p.i. (Figure 3.15, Figure 3.16, Table 3.1).

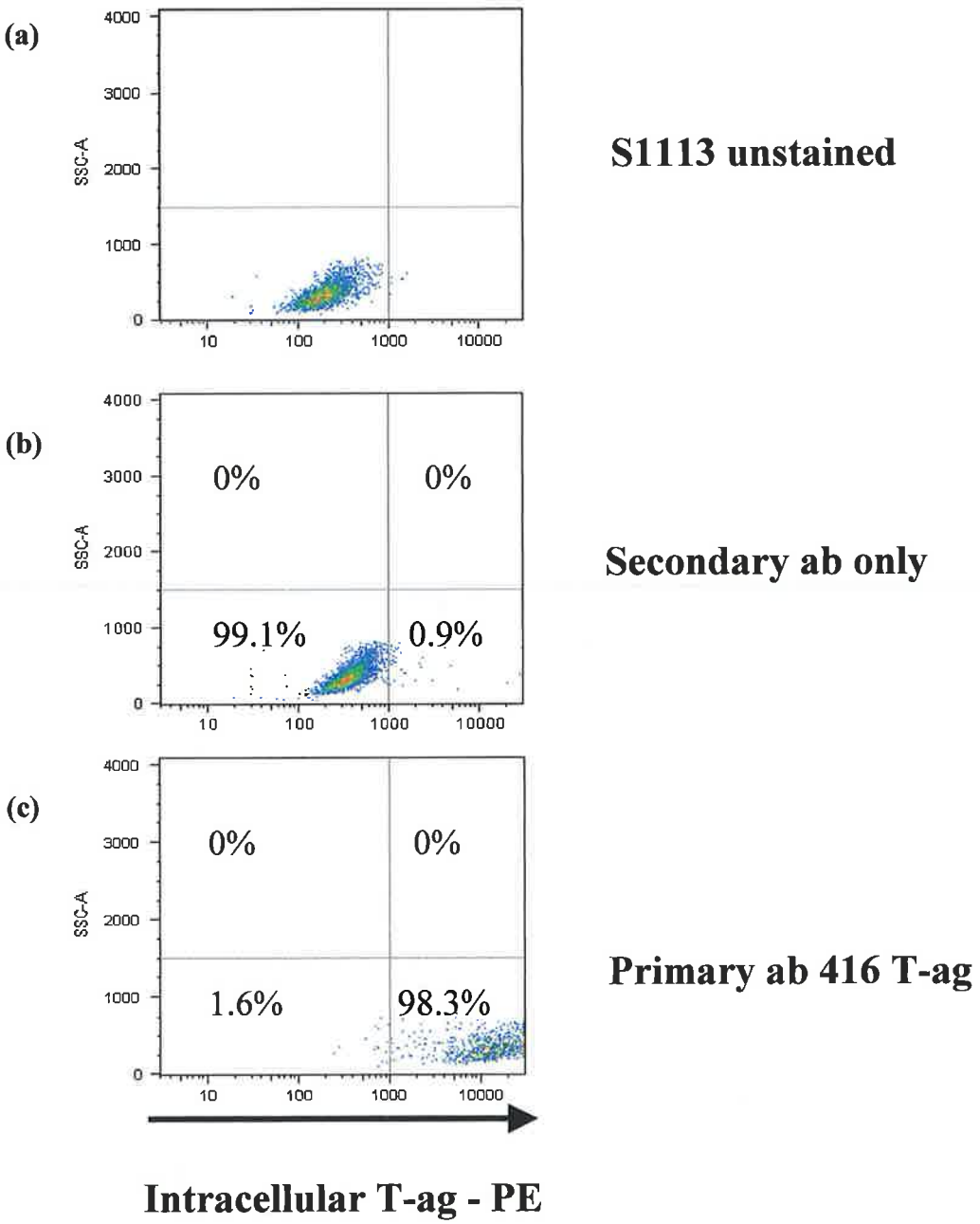

Figure 3.14: T-ag expression in S1113 positive control cell line
S1113 cells were analysed (a) unstained, (b) stained with secondary antibody only, Goat $F(ab')_2$ anti-mouse IgG_{2a} (Southern Biotech), and (c) stained with primary antibody, anti-T-ag 416 (Santa Cruz Biotechnology) and secondary antibody. The total sample cell population was analysed and gated by flow cytometry to exclude cellular debris. A quadrant gate was subsequently applied to the gated cell sub-population allowing positive and negative cell populations to be defined.

SSC; side scatter, PE; phycoerythrin, ab; antibody, T-ag; T antigen

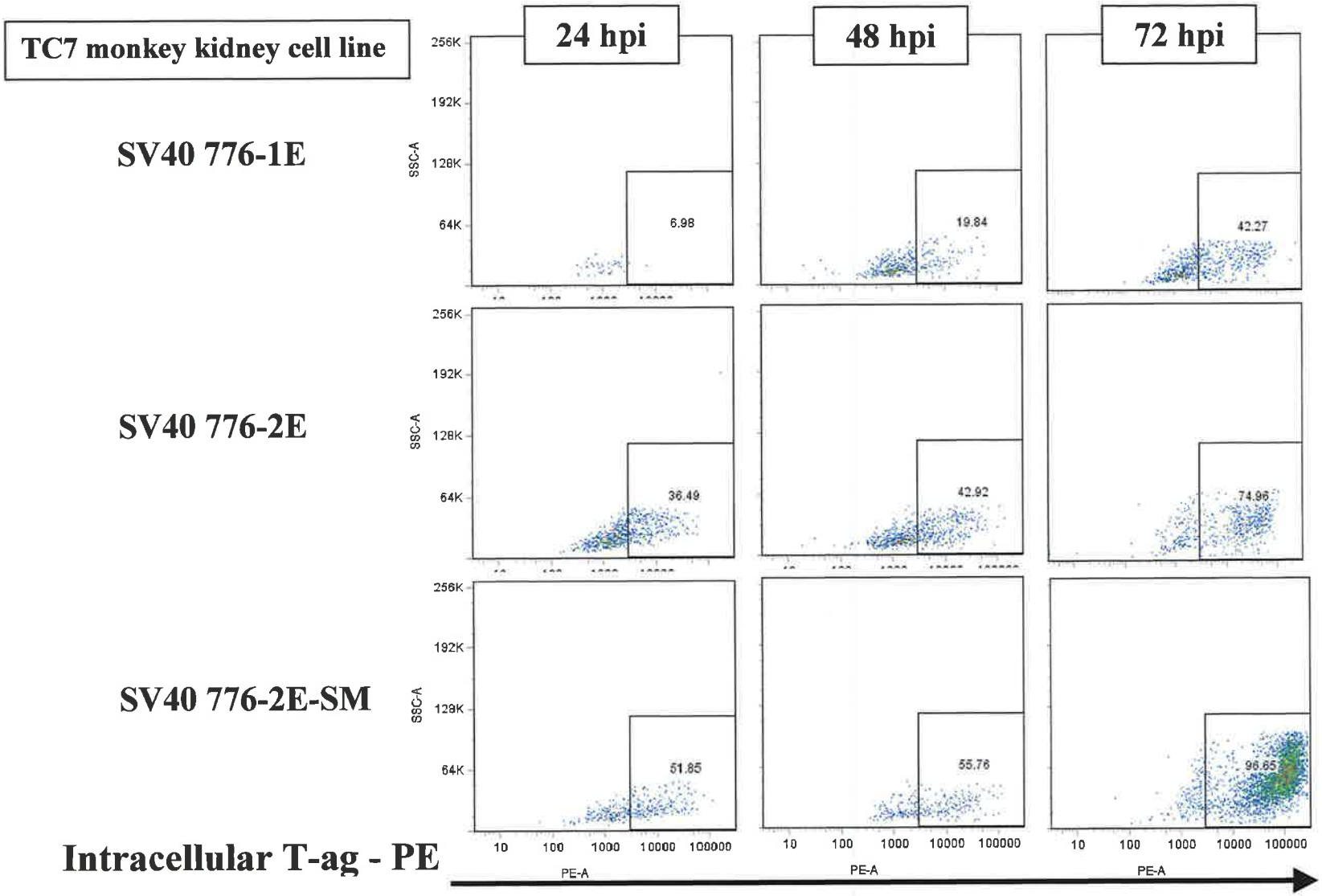

Figure 3.15: T-ag expression in permissive TC7 monkey kidney cell line. Cells were infected with SV40 776-1E, -2E and -2E-SM and cell culture samples harvested at 24, 48 and 72 hours post infection (h.p.i) were analysed by flow cytometry. SSC; side-scatter, PE; phycoerythrin, h.p.i.; hours post infection, T-ag; T-antigen

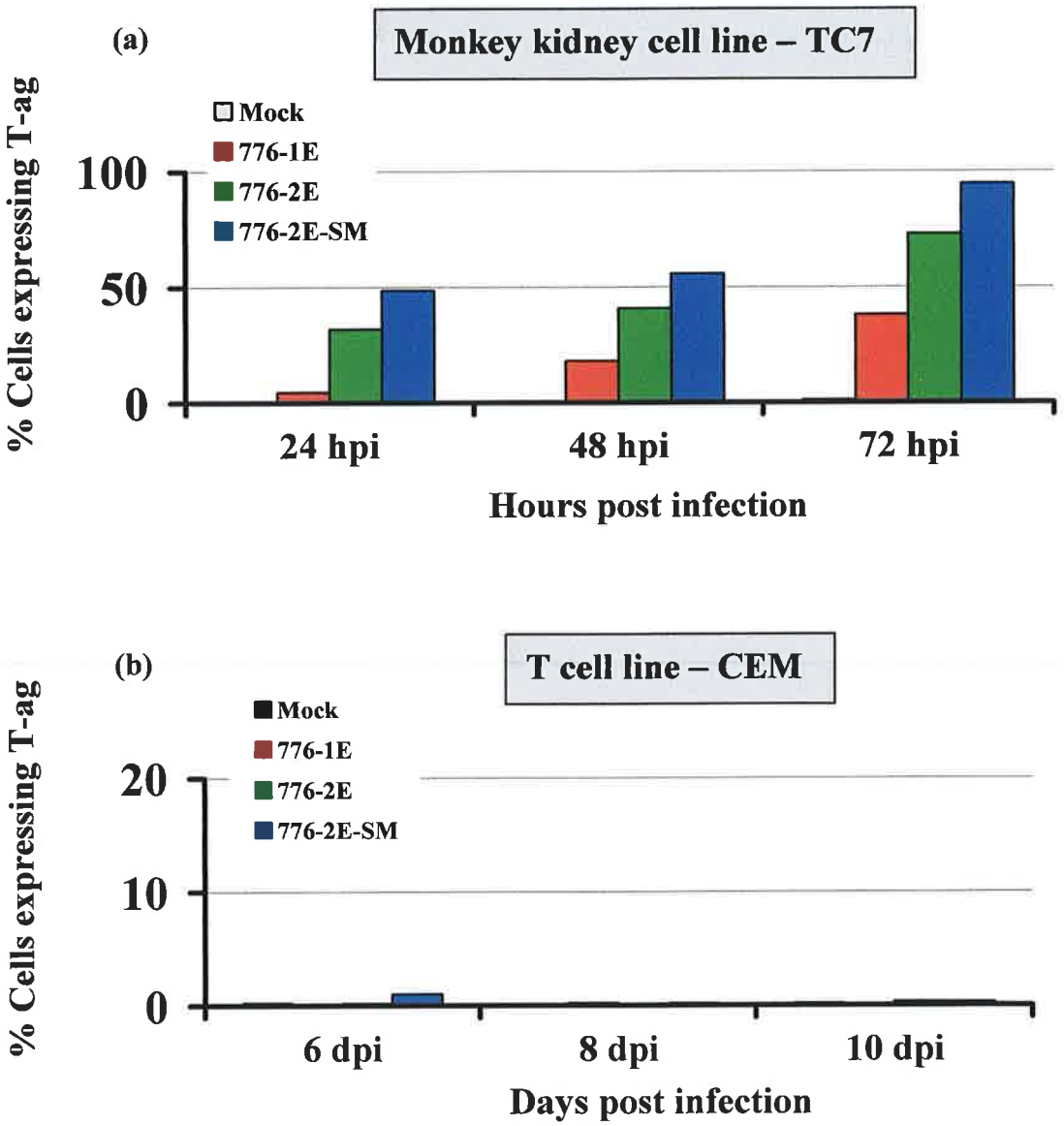

Figure 3.16: Percentage of cells expressing the SV40 large T-ag in TC7 and CEM cell lines

Graphs show the percentage of cells expressing T-ag in SV40-infected (a) monkey kidney cell line, TC7, a permissive cell line for SV40 cytopathic replication and (b) T cell line, CEM. Cell lines were infected with SV40 viruses 776-1E, -2E and –2E-SM, and analysed by flow cytometry using the anti-T-ag antibody 416 (Santa Cruz Biotechnology) and goat anti-mouse F(ab')2-PE (Southern Biotechnology). A mock sample representing an uninfected cell line is shown on each graph.

T-ag; T antigen, h.p.i.; hours post infection, d.p.i.; days post infection, PE; phycoerythrin

Table 3.1: Percentage of T antigen expression in TC7 and lymphocyte cell lines as measured by flow cytometry

Cell line	Cells infected with:	24 h.p.i.	48 h.p.i.	72 h.p.i.
TC7 monkey kidney	Mock	0	0	1
cell line	776-1E	7	20	43
Positive control	776-2E	36	43	75
	776-2E-SM	52	56	97

Cell line	Cells infected with:	6 d.p.i.	8 d.p.i.	10 d.p.i.	13 d.p.i.
CEM T cell line	Mock	0.2	0.1	0.2	0.1
Negative control	776-1E	0.1	0.2	0.1	0.1
	776-2E	0.2	0.1	0.3	0.1
	776-2E-SM	1	0.2	0.3	0.04
BJAB B cell line	Mock	1	1	TFTC	1.00
	776-1E	1	0.4	4	1
	776-2E	0.7	0.8	5	2
	776-2E-SM	5	4	13	NS
DG75 B cell line	Mock	0.3	0.8	0.9	0.7
	776-1E	1	2	0.8	0.6
	776-2E	1	3	1	0.5
	776-2E-SM	1	9	17	NS

TFTC = too few to count, NS = no sample, h.p.i. = hours post infection, d.p.i. = days post infection

When flow cytometric analysis was used to detect the expression of T-ag in SV40-infected lymphocyte cell lines, the results showed that the T-ag oncoprotein was expressed in both B cell lines, BJAB and DG75, albeit at a low level (Table 3.1, Figure 3.17). In the BJAB cell line infected with SV40 776-1E and 776-2E, there was low-level expression of T-ag with 1% of 776-1E infected cells positive at 6 d.p.i., reaching a peak of 4% at 10 d.p.i. BJAB cells infected with SV40 776-2E showed a similar pattern, with less than 1% expression at 6 d.p.i. and 8 d.p.i., 5% at 10 d.p.i. In contrast, BJAB cells infected with the 776-2E-SM had a higher percentage of T-ag positive cells, showing 4% by 8 d.p.i. and rising on 10 d.p.i. with 13% of the cells expressing T-ag (Table 3.1, Figure 3.17).

The DG75 B cell line showed a similar pattern of T-ag expression to BJAB with the 776-1E and 776-2E demonstrating 2% and 3% T-ag expression by 8 d.p.i. Again, the 776-2E-SM-infected cells showed the highest percentage of T-ag expression in the DG75 cell line percentage cells at 9% on 8 d.p.i. and 17% on 10 d.p.i. (Table 3.1, Figure 3.17). T-ag levels detected in the T cell line CEM were similar for mock- and SV40-infected cells, indicating this cell line was negative for the SV40 protein (Table 3.1, Figure 3.16).

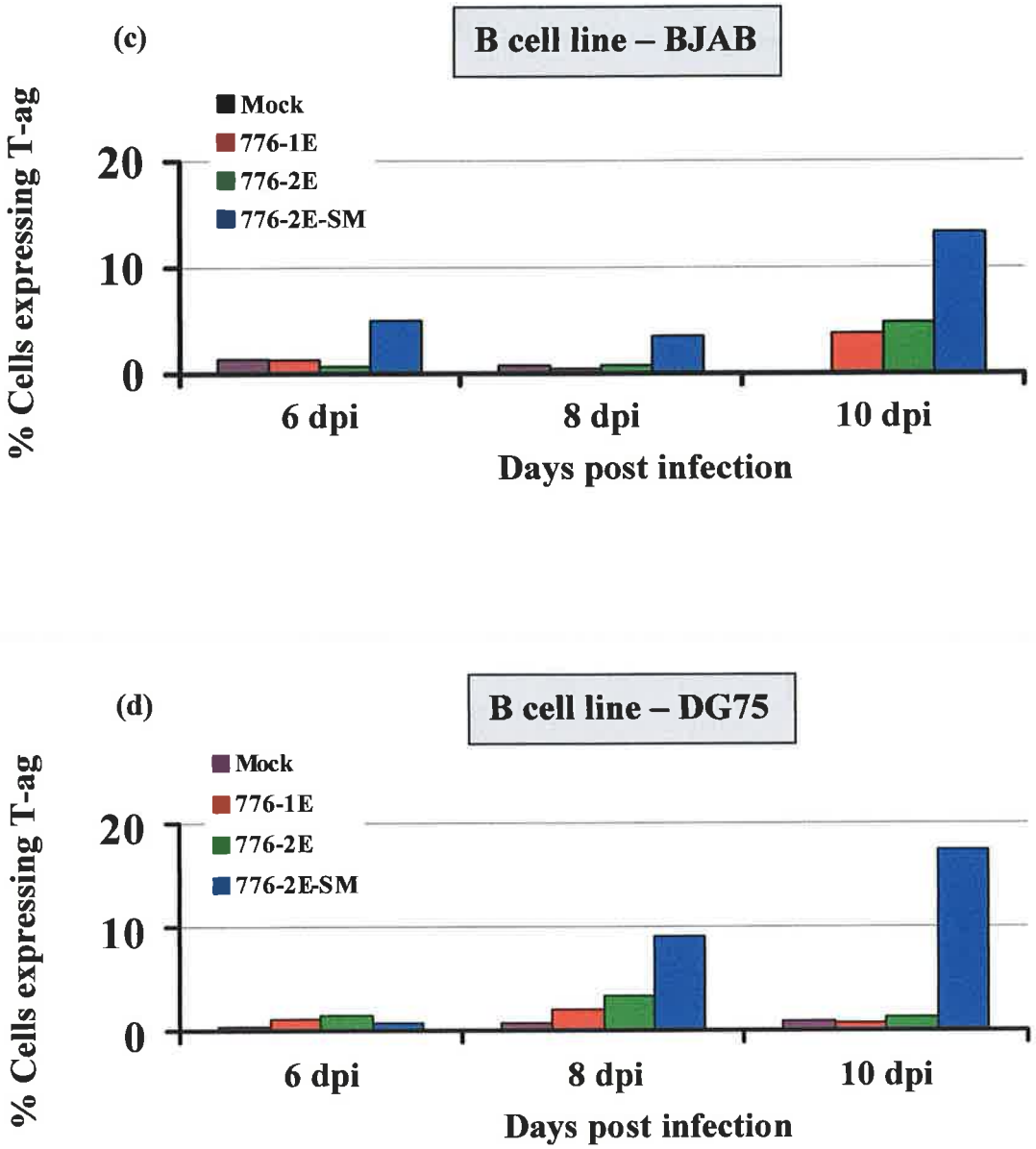

Figure 3.17: Percentage of cells expressing the SV40 large T-ag in BJAB and DG75 cell lines

Graphs show the percentage of cells expressing T-ag in SV40-infected B cell lines (a) BJAB and (b) DG75. Cell lines were infected with SV40 viruses 776-1E, -2E and –2E-SM, and analysed by flow cytometry using the anti-T-ag antibody 416 (Santa Cruz Biotechnology) and goat anti-mouse F(ab')2-PE (Southern Biotechnology). A mock sample representing an uninfected cell line is shown in on each graph.

T-ag; T antigen, h.p.i.; hours post infection, d.p.i.; days post infection, PE; phycoerythrin

3.4 RQ-PCR measurement of SV40 in infected cell lines

Following analysis of T-ag expression, RQ-PCR was employed to measure SV40 viral load in time course samples from the infected lymphocyte cell lines. Prior to performing RQ-PCR analysis, it was necessary to optimise the nucleic acid extraction procedure. Having evaluated both the column-based kit and cell lysis manual method, the cell lysis method was selected as the method of choice because of higher recovery and greater consistency of sample DNA. The cell lysis method was thus used to extract cell culture samples in the optimised infection time course for RQ-PCR analysis.

In the RQ-PCR assay, the parallel detection of the SV40 T-ag gene and the human RNAse P gene allowed viral copy numbers to be normalised to cell numbers (McNees *et al*, 2005). The accuracy and efficiency of the RQ-PCR for SV40 and RNAse P was confirmed using a standard dilution series containing known gene copy numbers for both target genes. In standard curves generated from log copy number *versus* C_T value, the amplification efficiency of the assay, as determined by the slope value of the log-linear phase, was between the recommended –3.1 and –3.6 for both targets, correlating to 90-100% efficient RQ-PCR assays. In addition, the r^2 regression coefficient values remained >0.99 in all PCR assays for both SV40 and RNAse P, ensuring the accuracy of the RQ-PCR assay. The standard dilution series also confirmed the low limit of detection of the assay with both targets detected at concentrations as low as 10^1 DNA copies. The assay also displayed good reproducibility, with duplicate standards and test samples remaining within 1.5 C_T values of each other (Figure 3.18 and 3.19).

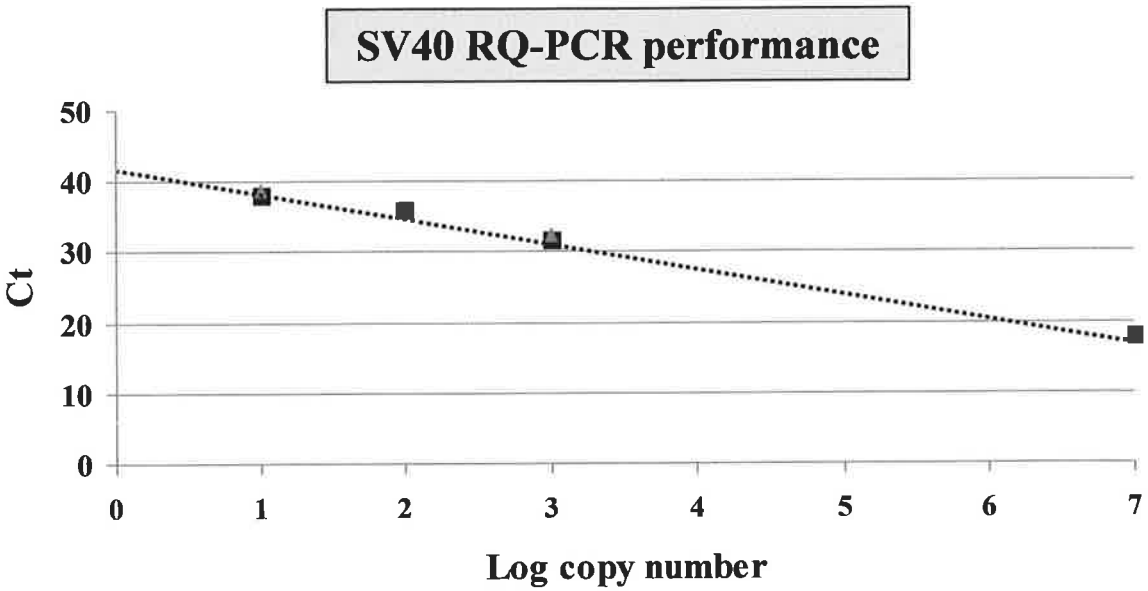

SV40 DNA Copy no.	Duplicate plasmid standards	
	C_T	C_T
10^7	18.07	17.78
10^3	31.86	32.23
10^2	35.99	35.88
10^1	38.04	38.54

r^2	0.9974
Slope	-3.4633

Figure 3.18: Standard curve for target gene SV40 T-ag
The curve was generated by plotting the observed threshold cycle C_T against the $\log_{10}$ of the input copy number of standard plasmid DNA encoding the large T-ag of SV40. These data show C_T values for duplicate samples showing reproducibility as well as r^2 and slope values.

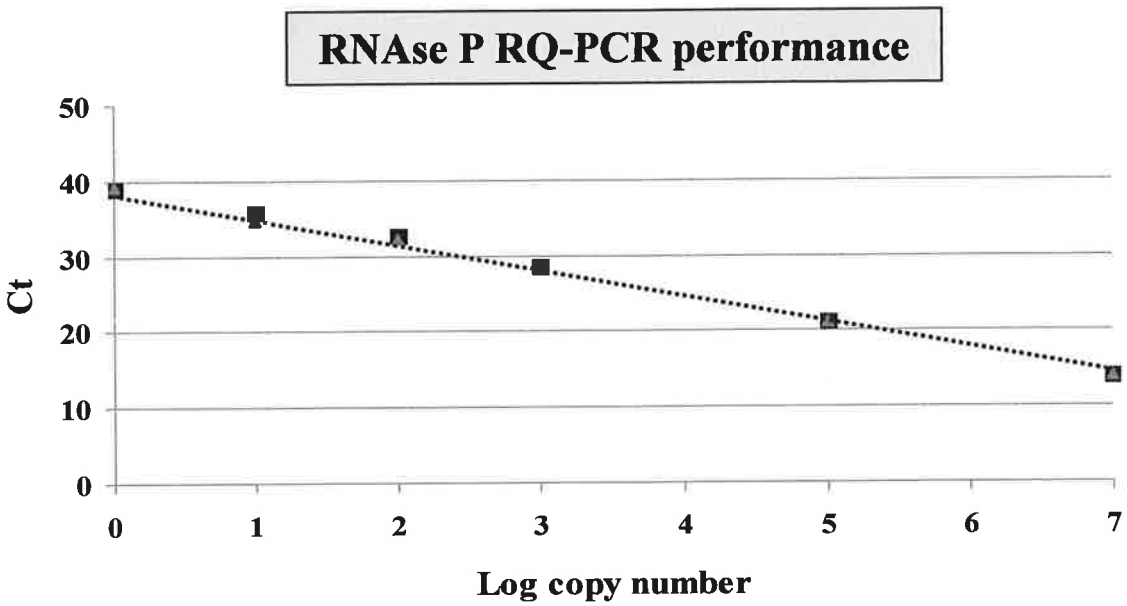

RNAse P DNA Copy no.	Duplicate plasmid standards	
	C_T	C_T
10^7	14.14	14.04
10^5	21.28	21.15
10^3	28.51	28.36
10^2	32.60	32.18
10^1	35.76	34.68
10^0	38.93	39.15

r^2	0.9993
Slope	-3.5647

Figure 3.19: Standard curve for target gene RNAse P
The curve was generated by plotting the observed threshold cycle C_T against the $\log_{10}$ of the input copy number of standard plasmid DNA encoding the human RNAse P gene. These data show C_T values for duplicate samples showing reproducibility as well as r^2 and slope values.

When amplification plots of Δ Rn reporter fluorescence *versus* C_T value for the detection of SV40 were analysed, an exponential rise in fluorescence emission consistent with amplification of T-ag target was observed. In contrast, the uninfected mock samples and non-template control (NTC) failed to show amplification with C_T values remaining undetected. In addition to the role of RNAse P in cell normalisation, the consistent detection of the RNAse P as an internal control in all lymphocyte cell lines confirmed the absence of PCR inhibitors in amplification reactions.

When the relative quantity of SV40 T-ag was calculated by normalisation of viral gene copy number to cell number based on RNAse P quantification, results from the initial time course indicated a decrease in viral load from day 0 to day 15 for both cell lines (Figure 3.20). In addition, viral load was seen to decrease sharply after each sample collection time point with values of 10,000 genomes on day 0 in the case of the -1E and -2E viruses diminishing to 10-100 copies by 15 d.p.i. It therefore appeared that this decreasing viral load may have resulted from the dilution effect of sample removal followed by cell culture feeding with fresh media, thereby diluting the numbers of virus present.

When further analysis of the initial time course revealed a significant difference in SV40 DNA copy number between 776-1E and -2E (10,000 copies/cell) and -2E-SM (1,000) on the day of infection, the validity of the results was further questioned. There appeared to be ten-fold less of viral genomes for SV40 776-2E-SM virus compared with the SV40 776-1E and -2E strains at 0 d.p.i., the day of infection. This was unexpected as all cell lines were infected with the same amount of each virus (2 PFU/cell). Subsequently, an RQ-PCR analysis of the

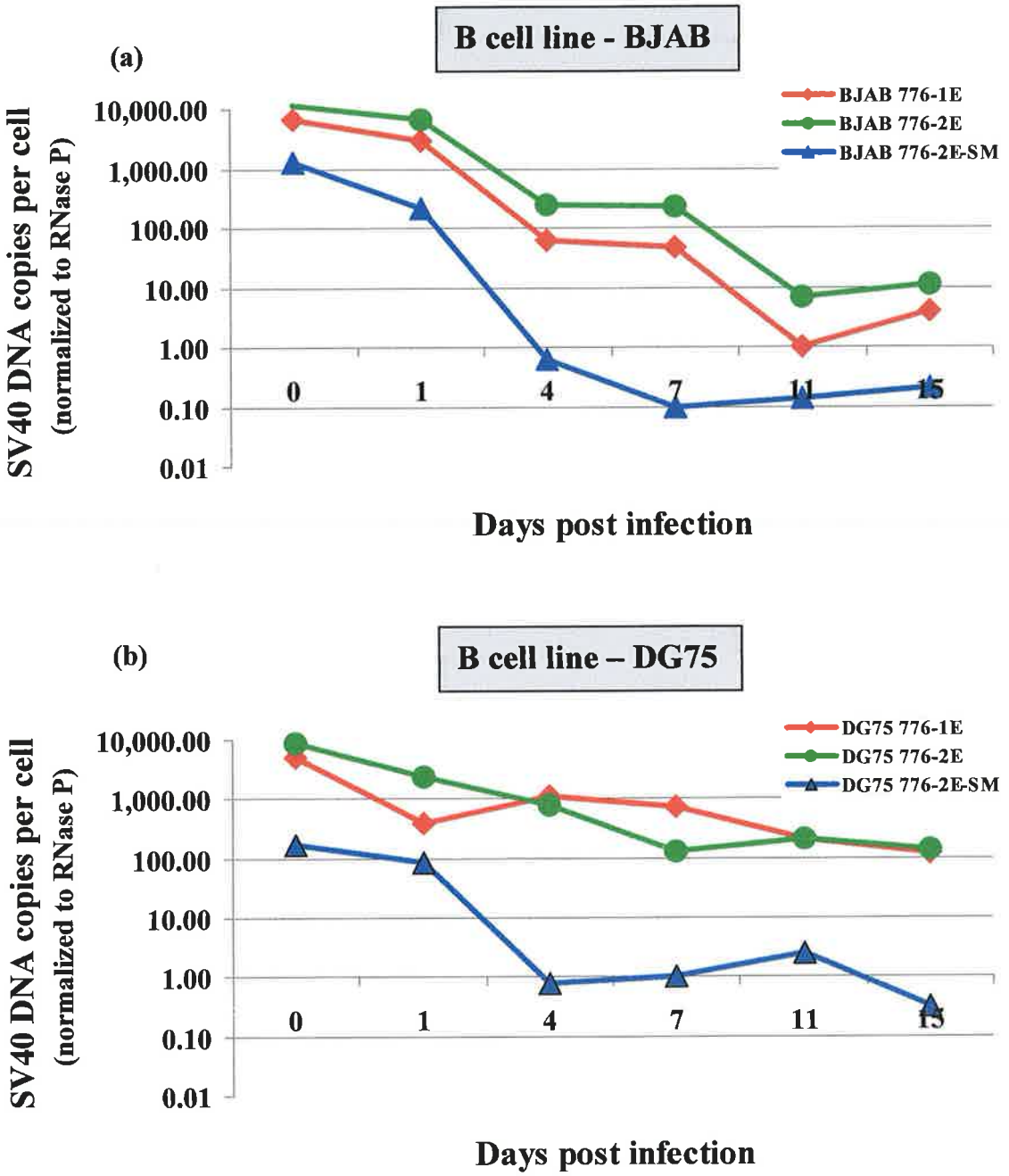

Figure 3.20: RQ-PCR quantification of SV40 genomes per cell in BJAB and DG75 cell lines
SV40 genomes per cell were quantified in (a) BJAB and (b) DG75 B cell lines infected with SV40 776-1E, 776-2E or 776-2E-SM in initial experiment at 0, 1, 4, 7, 11, 15 days post infection (d.p.i.). The values for the time course are shown as the ratio of SV40 DNA mean copy number per cell, assuming two copies of RNAse P per cell.

SV40 virus stocks revealed that the SV40 776-2E-SM stock had a lower number of genomes than the apparent equivalent stocks of -1E and -2E virus. The relatively low number of genomes was confirmed by RQ-PCR analysis of a separate -2E-SM stock. The identification of cell culture dilution and viral inoculum variation prompted the standardisation of the time course in the optimised experiment.

In the optimised experiment, where infection was normalised to input viral genomes rather than infectious particles and cell culture conditions were standardised, sharp decreases in viral load were no longer evident during the time course and the number of genomes/cell on day 0 was the same for each virus on the day of infection indicating standardised inoculum (Figure 3.21). When the relative quantity of SV40 was calculated in this optimised experiment, SV40 was detected throughout the time course for all viruses in both B cell lines (Tables 3.2 - 3.4). Overall, it appeared that the viral genome was maintained at levels of at least 1-10 copies/cell in cells infected with the 776-1E and 776-2E viruses. Even higher viral genome numbers, approximately 100 copies per cell, were observed in the case of the 776-2E-SM virus. This increased T-ag detected in -2E-SM-infected cells is consistent with flow cytometric detection of T-ag where increased levels were apparent compared to the -1E and -2E-infected cells. The SV40 persistence in the B cell lines was in contrast to the steadily decreasing viral load observed with the negative control CEM T cell line (Figure 3.21).

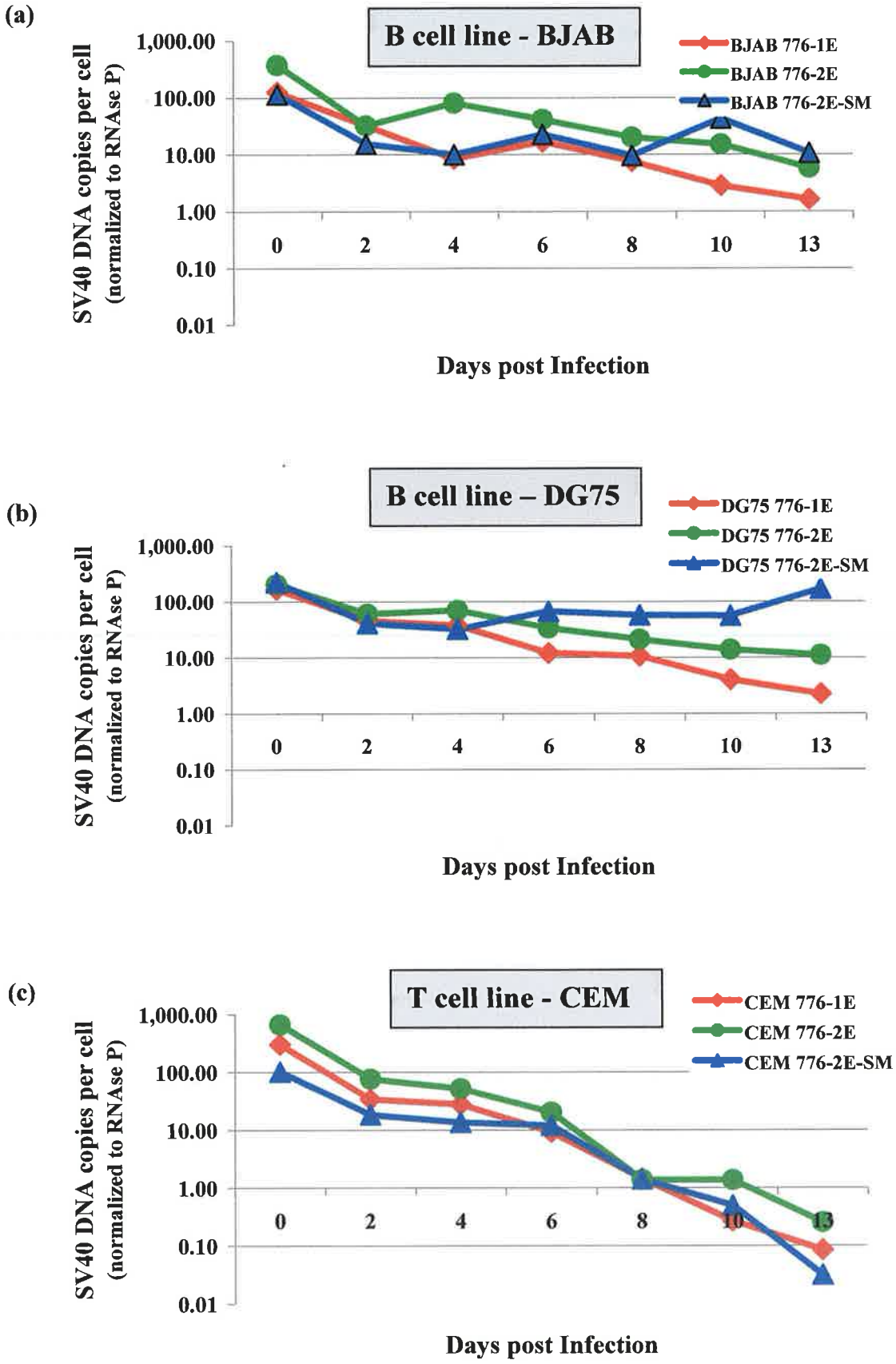

Figure 3.21: RQ-PCR quantification of SV40 genomes per cell in lymphocyte cell lines
SV40 genomes per cell were quantified in (a) BJAB, (b) DG75 and (c) CEM cell lines infected with SV40 776-1E, 776-2E or 776-2E-SM in optimised time course measured at 0, 2, 4, 6, 8 days post infection (d.p.i.). The values shown are the ratio of SV40 DNA mean copy number per cell, assuming two copies of RNAse P per cell, and are the average of four measurements for each target gene

Table 3.2: Quantification of SV40 776-1E T-ag DNA copies normalised to RNAse P cell number

	SV40 776-1E				RNAse P					
D.p.i.	**CT**	**CT**	**Mean CT**	**SV40 mean quantity**	**CT**	**CT**	**Mean CT**	**RNAse P mean quantity**	**RNAse P mean quantity/cell**	**SV40/RNAse P (T-ag copies/cell)**
0	22	22	22	8.9E+05	28	28	28	7.2E+03	3.6E+03	246
2	19	19	19	7.9E+06	24	24	24	1.9E+05	9.7E+04	82
4	22	22	22	8.8E+05	27	26	27	2.1E+04	1.1E+04	82
6	22	22	22	9.7E+05	25	25	25	8.2E+04	4.1E+04	24
8	22	21	21	1.1E+06	25	25	25	1.1E+05	5.6E+04	20
10	23	23	23	4.9E+05	24	24	24	1.8E+05	9.0E+04	5
13	23	23	23	3.6E+05	24	24	24	1.7E+05	8.5E+04	4

Table shows results for SV40 775-1E-infected DG75 B cell line culture. SV40 and RNAse P mean quantity values are derived from the standard curve mean C_T value. The RNAse P mean quantity is divided by two to calculate the RNAse P copy number per cell as there is one copy per human genome and human cells are diploid. The SV40 mean quantity was then divided by RNAse P mean quantity per cell to give the number of T-ag copies per cell. D.p.i.; days post infection, C_T; threshold cycle, T-ag; T-antigen

Table 3.3: Quantification of SV40 776-2E T-ag DNA copies normalised to RNAse P cell number

	SV40 776-2E				RNAse P					
D.p.i.	**CT**	**CT**	**Mean CT**	**SV40 mean quantity**	**CT**	**CT**	**Mean CT**	**RNAse P mean quantity**	**RNAse P mean quantity per cell**	**SV40/RNAse P (T-ag copies/cell)**
0	18	19	19	8.9E+06	26	25	25	5.0E+04	2.5E+04	357
2	17	17	17	2.1E+07	23	23	23	3.4E+05	1.7E+05	127
4	20	20	20	3.8E+06	26	25	26	5.0E+04	2.5E+04	154
6	20	20	20	2.7E+06	25	25	25	8.7E+04	4.4E+04	63
8	20	20	20	2.3E+06	24	25	24	1.2E+05	6.2E+04	36
10	22	21	21	1.3E+06	25	25	25	9.0E+04	4.5E+04	29
13	22	21	21	1.2E+06	24	24	24	1.6E+05	8.1E+04	14

Table shows results for SV40 775-2E-infected DG75 B cell line culture. SV40 and RNAse P mean quantity values are derived from the standard curve mean C_T value. The RNAse P mean quantity is divided by two to calculate the RNAse P copy number per cell as there is one copy per human genome and human cells are diploid. The SV40 mean quantity was then divided by RNAse P mean quantity per cell to give the number of T-ag copies per cell. D.p.i.; days post infection, C_T; threshold cycle, T-ag; T-antigen

Table 3.4: Quantification of SV40 776-2E-SM T-ag DNA copies normalised to RNAse P cell number

	SV40 776-2E-SM				RNAse P					
D.p.i.	**CT**	**CT**	**Mean CT**	**SV40 mean quantity**	**CT**	**CT**	**Mean CT**	**RNAse P mean quantity**	**RNAse P mean quantity/cell**	**SV40/RNAse P (T-ag copies/cell)**
0	22	21	21	1.4E+06	28	27	27	1.3E+04	6.3E+03	217
2	19	19	19	7.7E+06	23	23	23	2.2E+05	1.1E+05	70
4	21	21	21	1.2E+06	26	27	26	2.7E+04	1.3E+04	91
6	22	22	22	8.4E+05	28	27	27	1.2E+04	6.1E+03	138
8	22	22	22	6.7E+05	28	28	28	1.5E+04	7.3E+03	91
10	23	22	22	6.7E+05	28	26	27	2.3E+04	1.1E+04	59
13	21	21	21	1.9E+06	27	27	27	1.5E+04	7.7E+03	253

Table shows results for SV40 775-2E-SM-infected DG75 B cell line culture. SV40 and RNAse P mean quantity values are derived from the standard curve mean C_T value. The RNAse P mean quantity is divided by two to calculate the RNAse P copy number per cell as there is one copy per human genome and human cells are diploid. The SV40 mean quantity was then divided by RNAse P mean quantity per cell to give the number of T-ag copies per cell. D.p.i.; days post infection, C_T; threshold cycle, T-ag; T-antigen

4.0 Discussion

More than forty years after the discovery of Simian virus 40 (SV40), a major controversy exists regarding its association with human cancer, almost dividing research groups into 'believers' and 'non-believers'. Some investigators question the presence of SV40 in humans, thereby obviating the need to study the role of SV40 in human disease. Nevertheless, evidence has accumulated over the past few decades implicating SV40 as a cause of cancer in the human host. Several reports have described the association of SV40 with malignant mesothelioma and studies have characterised SV40-mediated *in vitro* transformation of human mesothelial cells. In more recent years, data has accumulated showing the association of SV40 with human lymphomas. While SV40-lymphoma research to date has frequently focused on the presence or absence of the virus in human lymphomas, the mechanism by which SV40 may infect or transform lymphocytes has not yet been studied.

This current study was designed to investigate SV40 infection in human lymphocytes and therefore potentially reveal insights into the pathogenesis of SV40 infection in humans. SV40 has been detected in human peripheral blood mononuclear cells, tonsils, and NHL (Butel, 2009; Martini *et al*, 2007). In addition, SV40 has been shown to induce lymphomas of B cell and histiocytic origin in the Syrian golden hamster model (McNees *et al*, 2009). These findings document the lymphotropic capacity of SV40.

To begin the studies of SV40 infections in human lymphocytes, human cell lines were chosen because they are readily available and easy to grow in tissue culture, are quickly expanded to large quantities, and provide a tissue setting for optimising and reproducing *in vitro* experiments. However, the use of cell lines does not allow for opportunities to

study viral transformation as they are already immortalised. Experiments in primary human lymphocytes may offer more mechanistic insights, but have limitations of fewer cell numbers and possible donor variability. Future follow up studies should include experiments in primary human cells once methods and interpretations are standardised.

The results presented herein were collected from an infection time course experiment in which three different lymphocyte cell lines, the B cell lines, BJAB and DG75, and a T cell line, CEM, were infected with three viral strains of SV40. Two variants of the SV40 776 strain, 776-1E and 776-2E, containing one and two enhancer elements, respectively, were compared to reveal if the regulatory region of SV40 may influence viral interaction with lymphocytes. A previous study comparing -1E and -2E variants revealed a strong contribution of the regulatory region to viral oncogenicity in the hamster model, with the -1E virus causing more tumours (Sroller *et al*, 2008). A miRNA mutant virus, SV40 776-2E-SM, was also included to evaluate a possible role of SV40 miRNA in lymphocyte infections. The study described here is the first investigation of these viral strains in human lymphoid cells.

During a two-week time course following SV40-infection, lymphocyte cultures were analysed for proliferation and viability, changes in lymphocyte surface markers, intracellular expression of T-ag and replication of SV40 genomes. Both SV40 wild-type viruses, 776-1E and –2E, induced proliferation in the DG75 B cell line, with a four-fold increase in cell numbers when compared with an uninfected mock sample at each time point. Increased proliferation reflects alteration in cell cycle control and this effect of the virus may play a role in cancer development. The lymphoproliferation was not uniform in both B cell lines, which were derived from different human cancerous cells and are

genetically distinct. It is therefore possible that the DG75 cell line may be more sensitive to the SV40-cell cycle effects than the BJAB cell line. While both B cell lines are EBV negative, it is also possible that DG75 expresses other co-factors conducive to increased proliferation, that are absent in the BJAB cell line. This observation may support the hypothesis that additional factors may be required to act in synergy with SV40 infection for the induction of a cancerous process in lymphocytes. In other cancer types, the role of an SV40 co-factor is strongly indicated. It has been suggested that SV40 is a co-carcinogen with asbestos in the development of malignant mesothelioma as demonstrated *in vitro* with human mesothelial cells (Bocchetta *et al*, 2000). The aetiology of the many different types of lymphoma is multi-factorial in nature, and viruses have been shown to be involved in some cases. Given the strong oncogenicity of SV40, if it is present in human lymphocytes then it could conceivably function as a co-factor in lymphomagenesis. The suggestion of a co-carcinogenic role for SV40 is further strengthened given that this theory has been proven for other transforming viruses. EBV has long been associated with Burkitt's lymphoma but presence of the virus is only one factor involved in disease development, along with the *c-myc* translocation and exposure to the malaria parasite (Thorley-Lawson and Allday, 2008). Another example is the risk of developing HBV-induced liver cancer is greatly increased by other co-factors such as the hepatotoxin aflatoxin (Javier and Butel, 2008).

While increased cell proliferation was observed in DG75 cells infected with the wild-type 776-1E and -2E SV40 virus strains, this increase in cell growth was not seen in B cell lines infected with the miRNA mutant, 776-2E-SM. Cells infected with this virus lacking SV40 miRNA appeared to have arrested growth in both BJAB and DG75 cell lines. This lack of cell growth was not due to cell death, as decrease in cell viability was not

observed. It is therefore possible that a function of the SV40 miRNA is to promote cell division, thereby faciltating virus replication. One reported function of SV40 miRNA is to decrease expression of the early region genes, including the large and small T antigens (Sullivan *et al*, 2005). The decrease in cell division may be a consequence of increased T-ag expression caused by the absence of the SV40 miRNA. Perhaps too much T antigen is toxic for the B-lymphocytes. Interestingly, the cell growth stagnation noted in the -2E-SM infected B cell lines was not observed in the T cell line CEM, where normal cell division occurred relative to the uninfected cells.

The cell growth and viability data were obtained using a single approach based on the exclusion of trypan blue dye. This is a subjective technique, with limited sensitivity. To confirm the growth and viability data, future work should include more sensitive assays, such as the MTT assay and AnnexinV and PI staining followed by flow cytometry that would allow for a greater number of cells to be counted and possibly assess a cell function. Another approach to further characterise the influence of SV40 miRNA absent in the -2E-SM virus is using a TUNEL assay (terminal dUTP nick-end labelling) to detect whether apoptosis is occurring in -infected B cells.

CD69 is an early leukocyte activation marker, expressed in chronic inflammation (Sancho *et al*, 2005). The co-stimulatory molecules CD80 and CD86 provide "signal 2" required to generate an antigen-specific immune response, with "signal 1" being the antigenic peptide presented by MHC molecules to T cell receptors. A decrease in expression of these co-stimulatory molecules would result in compromised activation of naïve T cells, thereby blocking a critical stage in the immune system in recognising and clearing an infectious agent. To evaluate what effects, if any, SV40 infection in human lymphocytes

has on the lymphocyte cell surface markers CD69, CD80, and CD86, staining on live cells for flow cytometry were performed during the infection time course.

While few changes were noted in B cells infected with the -1E and -2E viruses, a clear pattern of CD69 upregulation and CD80 downregulation was evident in -2E-SM-infected B cells. As with proliferation studies, these effects were not consistently seen in both B cell lines, with the most notable cell surface marker changes being observed in the BJAB cell line. Once again, this difference in B cell response could be due to genetic differences between the two B cell lines. The mutant virus, with its increased expression of T-ag, suggests that T-ag is playing a role in the observed expression changes in surface markers CD69 and CD80, and may hint at a potential function of T-ag to participate in immune evasion. Future work should include infecting cells using a dose response curve to reveal the effect of T-ag expression at various levels.

Modulation of lymphocyte cell surface molecules required in initiating antigen-specific immune responses is a common mechanism used by viruses to evade the human immune system, thereby facilitating viral replication and persistence. Changes in cell surface marker expression may also contribute to tumourigenesis by allowing a tumour cell to remain unrecognisable to the host immune response. Examples of viral proteins modulating host immune responses in this manner include the Nef protein of HIV, which has been shown to induce a downregulation of MHC and the co-stimulatory molecules CD80 and CD86 on monocytes, macrophages and dendritic cells (Chaudhry *et al*, 2005). CD86 has also been shown to be downregulated by the MIR2 protein in KSHV, a virus that mainly infects B-lymphocytes (Coscoy, 2007). Like other viral agents, cell surface marker –up or –down regulation in SV40 infection of lymphocytes could result from the

direct action of a viral protein, or it could be an indirect effect of virus presence in the cell. Cell surface marker changes could represent one of the pathways targeted by SV40 in its attempt to make it unrecognisable to a CTL response, thus, enabling its survival. It has previously been shown that lack of miRNA makes the SV40 virus more sensitive to CTL killing with more cytokine production observed, representing further evidence of immune evasion strategies at work in the wild type (Sullivan *et al*, 2005). An interesting follow up study would involve the determination of the cytokine-profile of the SV40-infected cells to see if cytokine expression corresponds to the modulation of the surface markers observed. Further investigation into the mechanisms by which SV40 modulates host cell signalling proteins may reveal novel immune evasion and viral oncogenesis strategies.

The SV40 T-ag is required for viral replication and cellular transformation, and is only expressed after entry into a host cell (zur Hausen, 2008). Measuring T-ag expression in infected lymphocytes is thus a critical component in testing the hypothesis that SV40 plays a role in human lymphomagenesis. Cells analysed from the same cultures for the surface staining experiments were also permeabilised and stained for intracellular T-ag. Low-level T-ag expression was consistently detected in the B cell lines BJAB and DG75 infected with all three viruses. The percentage B cells infected with SV40 776-1E and –2E expressing T-ag remained between 1-5%, with the peak expression on day 10 post infection. A higher percentage of 776-2E-SM-infected B cells expressed T-ag, with up to 17% positivity observed. In the fully permissive positive control monkey kidney TC7 cell line, the highest percentage expression of T-ag was seen in –2E-SM infected cells, followed by –2E then –1E. The increased percentage T-ag expression observed in all cell lines infected with the miRNA mutant confirms previous findings where western blot

analysis showed that production of the T antigens in –2E-SM-infected permissive cells was enhanced relative to the wild-type (Sullivan *et al*, 2005). The observation that the percentage of T-ag positive cells is higher in –2E-infected cells than –1E is also in agreement with studies where faster replication of –2E viruses has been demonstrated *in vitro* (Lednicky *et al*, 1995*a*). The *in vitro* expression of T-ag in SV40-infected B-lymphocytes is a key finding in this study of SV40-lymphomagenesis. It indicates the expression of viral early genes. The fact that a small percentage of cells were positive may indicate that a subset of the clonal populations are infected or that T-ag is expressed at levels near the limit of detection. Although only 10-15% of B cells were positive for T-ag expression later in infection, the changes in CD86 and CD69 expression in cells from the same cultures at these same time points seemed to be occur on all cells. This might suggest that virus infection is indirectly changing cell phenotypes, perhaps by a cytokine-mediated effect.

Another key feature in analysing the ability of SV40 to infect human lymphocytes is the replication of viral DNA. SV40 viral load was measured during the infection time course from 0-13 days by RQ-PCR. Results showed that viral copy numbers appear to gradually decrease in the CEM T cell line. Detection of SV40 DNA from all three viral strains after 13 days at a level of at least 1-10 genomes/cell indicated possible low-level maintenance and/or replication of the viral genome in the B cell lines BJAB and DG75. Although the level of SV40 DNA maintained at the end of the time course was low, similar low levels of virus have been reported in a previous B lymphocyte cell line study (Dolcetti *et al*, 2003) and in numerous studies detecting SV40 in human tumours. It is possible this low level persistent infection may be all that is required to initiate a tumourigenic process over time, away from immune system surveillance. In persistent EBV infection, the EBV

virus is present in very few B cells, approximately one in a million but this can be sufficient to lead to EBV-associated diseases such as Burkitt lymphoma, post-transplantation lymphoproliferative disorder, nasopharyngeal carcinoma and gastric carcinoma (Kutok and Wang, 2006). Although infection and persistence of B cell lines with SV40 has previously been described (Dolcetti *et al*, 2003), this current study is unique in that SV40 viral load was monitored over a period of time. In addition, the results of RQ-PCR obtained in this study are further strengthened by the efforts made to optimise the infection time course experiment to standardise factors such as removal of sample volume and difference in viral inoculum. This study also incorporated an accurate quantification strategy where viral target was quantified relative to the human RNAse P gene. Furthermore, the RNAse P quantification served as an effective internal control for performance of PCR from extraction through to amplification. The design of this experiment also included suitable controls in the form of an uninfected mock cell culture for each cell line.

The finding of SV40 DNA maintenance in B-lymphocytes, while suggestive of SV40 infection, does not prove viral replication. Confirmation of SV40 replication, if occurring, in virally infected lymphocytes would require further studies using reverse-transcriptase PCR to measure SV40 mRNA in a similar time course experiment. Increasing levels of SV40 mRNA would correlate to active viral transcription.

An additional fundamental limitation of this study was the fact that, although method optimisation was performed, the presented results represent a single infection time course. Preliminary experiments, including an initial infection time course, while showing some similar trends in results, were not included as they differed in set up and therefore could

not be compared to the optimised time course. As a result, although all experiments were controlled adequately throughout, reproducibility to confirm results could not be demonstrated. This failure to repeat experiments also meant that statistical analysis could not be performed. Future work would include repeating the presented optimised time course a number of times to confirm results and trends, and analysing the results statistically to evaluate the significance of findings. Upon completion of additional experiments, the observation of low-level SV40 replication in addition to T-ag expression in B-lymphocytes would provide convincing evidence that SV40 infects this cell type and the potent oncogenicity of the virus may account for the development of certain types of lymphoma in humans.

Evidence of SV40 has been found in an array of human tumours, which correspond to the types of tumour induced in laboratory animal models. The detection of maintained SV40 DNA sequences and T-ag protein *in vitro* and in other studies investigating human tumours forms the basis of the association of SV40 with human cancer. Furthermore, the recovery of infectious SV40 from a brain tumour adds weight to the argument (Lednicky *et al*, 1995*b*). DNA sequence analysis of SV40 virus detected in human tumours reveal that these viruses are similar to those found in natural primate infections, being mostly of the simple regulatory region type (-1E virus), differing from the –2E laboratory-adapted virus strains. The mounting body of evidence supporting the oncogenic role of SV40 in human tumours is building.

The identification of SV40, a monkey virus, in human tumours is still met with some scepticism (Butel, 2000). Despite all the data in support of a role for SV40 in human cancer, some researchers remain unconvinced. Uncertainty has arisen from the lack of

standardisation and reproducibility in SV40 detection methods among various research laboratories. In past studies involving nucleic-acid amplification-based approaches, technical issues such as choice of DNA extraction method, PCR primers and the number of PCR cycles were problematic in SV40 detection in tumour samples. This is in part due to fixation methods of archival samples. DNA in formalin-fixed tissues can be damaged and difficult to recover. The detection of SV40 DNA in tumour tissue may require 40-60 cycles of PCR, necessitating sensitive and specific detection techniques to obtain a true positive result. While some SV40 negative reports can be attributed to geographical and population factors, other negative reports likely result from technical limitations in the laboratory. One particular research team, which have consistently challenged the presence of SV40 in human tumours and have reported negative findings (Strickler *et al*, 2001), have since acknowledged sensitivity problems that raise questions about these negative reports (MacLachlan, 2002). Additional studies have reported SV40 negative results using low sensitivity PCR (reviewed in Carbone *et al*, 2003). Nowadays, RQ-PCR assays like the one used in this study, represent the most sensitive method for detection of low numbers of SV40 virus in human samples.

The potential for the occurrence of laboratory contamination of human samples with SV40 sequences adds to the controversial association of SV40 with human cancers. The widespread use of SV40 sequences in cloning vectors has been cited as a source of contamination by some researchers, and may account for the detection of SV40 sequences in some tumours. However, it should be pointed out that in recent years rigorous precautions have been taken in most studies to guard against SV40 laboratory contamination (Martini *et al*, 2007). The concern about SV40 contamination has also been reduced by the development of RQ-PCR systems where amplification and detection

of PCR products occur in a 'closed' automated platform, without the need for post-PCR manipulation. In addition, assays to detect viral protein expression in human tissue eliminate the possibility of false positive PCR results. More recent studies use two detection methods for evidence of SV40: a PCR-based method and immunohistochemical staining for T-ag. The agreement of two independent detection methods thus almost guarantees against laboratory contamination being responsible for the presence of SV40 (Vilchez *et al*, 2005).

Beyond the debate of SV40 being associated with human tumours, there is also speculation that SV40 may act only as a 'passenger' virus, rather than exerting an oncogenic influence in the human host. In this case, the tumour tissue provides a favourable environment for SV40 viral residence or replication (Butel and Lednicky, 2000). However, if SV40 acted as a bystander, it would be expected that tumour appearance would precede virus infection, with early-stage tumours being virus negative and SV40 only being detected in more advanced tumours. In this respect, it is significant that SV40 sequences have been found in both pre-cancerous and tumour cells in mesothelioma, indicating viral presence in the earliest recognisable tumour stage (Shivapurkar *et al*, 1999).

Another point in the argument of association versus causation is the observation that SV40 DNA or T-ag is not found in every cell of an SV40-positive tumour. This is in contrast to other viral-cancer associations, such as HPV and cervical cancer, and EBV and lymphoproliferative-disorders where viral genomes are widespread in the tumour (Garcea and Imperiale, 2003). The absence of SV40 in all associated cancer cells may result from the proposed theory that SV40 may operate using a 'hit and run' mechanism.

While it is known that many oncogenic viruses play an essential role in both the early initiation and subsequent progression of cancer, it is possible that tumour cells lacking SV40 T-ag have already experienced a 'hit and run' infection and have thereby lost the viral genome. Subsequent tumour progression and accumulation or mutations in the cell may allow functional T-ag to become dispensable once it has fulfilled its role in initiating the cancerous process. This mechanism has been proposed in relation to SV40-associated lymphoma development based on the finding of higher SV40 prevalence in reactive lymphadenopthies than in overt lymphoma, supporting a role for the virus in the early phases of lymphomagenesis (Martini *et al*, 1998).

Another possible explanation for the absence of SV40 in some cells of a tumour is that viral sequences and viral gene expression may only be maintained in a small fraction of cancer cells, which secrete factors that promote abnormal proliferation of surrounding uninfected cells (Javier and Butel, 2008). It has been shown in human mesothelial cells that SV40 activates an autocrine/paracrine loop, involving hepatocyte growth factor (HGF) and vascular endothelial growth factor (VEGF) and their cellular receptors. These growth factors, HGF and VEGF, are released from SV40-positive human cells and they bind to their receptors in neighbouring and distant SV40 positive and negative cells, driving them into proliferation and tumourigenesis (Martini *et al*, 2007). This mechanism of SV40-induced tumourigenesis in human cells may explain why SV40 T-ag is able to direct SV40-negative cells toward malignant transformation, thereby explaining the absence of SV40 T-ag in some cancer cells.

In light of such controversy, the role of SV40 in human infection and cancer such as lymphomas may only be established by the provision of more compelling evidence.

Firstly, the mechanism of the virus in host cell manipulation and immune evasion needs to be established. A key feature of transforming viruses is that they are able to infect, but not kill, their host cell. To ensure survival of both the virus and host cell, viral agents must evolve clever methods of reprogramming host cellular signalling pathways so that both can co-exist. In their manipulation of host cellular processes, a common theme is for viruses to encode proteins that interfere with important biological processes such as control of cell cycle, differentiation, cell death, genomic integrity, and host mechanisms for recognition of infectious agents. As regulatory mediators, these proteins contribute to the oncogenic capacity of the virus.

In addition to the well-characterised oncogenic T-ag protein, SV40 encodes a microRNA. Although the study of viral microRNAs is still in its infancy, their role in immune evasion and oncogenesis is firmly established (Swaminathan, 2008). Over 120 different viral miRNAs have been identified, in particular in the herpesvirus family (Sullivan, 2008). Two oncogenic herpesviruses, EBV and KSHV, which infect and persist in B-lymphocytes in a manner similar to that proposed for SV40, have been shown to encode abundant amounts of evolutionary conserved non-coding RNA, suggesting an essential role in the biology of this, and possibly other, virus families (Swaminathan, 2008). Viral miRNAs have been shown to modulate cellular gene expression, viral persistence, viral replication, and survival of infected cells. Additional investigations on the influence of SV40 miRNA in host cells during infection may uncover similar mechanisms as those seen in other oncogenic viruses, providing clues to SV40 pathogenesis.

In future lymphoma studies, lessons could be learned from the association of SV40 with mesothelioma, which has been studied extensively *in vitro*. It has been widely accepted

that a strong link exists between SV40 and the development of malignant mesothelioma, due in large part to the demonstration of a unique susceptibility of this cell type to SV40 and the observation of *in vitro* transformation (Bocchetta *et al,* 2000). This SV40-mediated transformation of mesothelial cells has shown to be enhanced by the presence of asbestos, with SV40 and asbestos acting as co-carcinogens *in vitro* (Bocchetta *et al*, 2000). Indeed, the fundamental concept of tumour virology is that viruses generally act as initiating or promoting factors of the carcinogenic process, rather than being complete carcinogens. This is consistent with the principle that cancer development occurs not by a single event but the accumulation of co-operating events (Javier and Butel, 2008). Further *in vitro* studies with lymphocytes could lead to similar insights in evaluating lymphocyte susceptibility and mechanism of transformation by SV40.

In lymphomas, chromosomal translocations are the most frequently recognised oncogenic events (Martini *et al*, 1998). A possibility to be considered is that SV40 may co-operate with such alterations through T-ag ability to bind and inactivate the tumour suppressors p53 and pRb. In the EBV association with Burkitt's lymphoma, a consistent feature of this lymphoma type is the *c-myc* chromosomal translocation, whereby the proto-oncogene *c-myc* is placed under the control of the immunoglobulin loci. The outcome of this translocation is that *c-myc* becomes constitutively activated in mature B cells and the *c-myc* protein can accumulate (Thorley-Lawson and Allday, 2008). The *c-myc* gene product is a DNA-binding nuclear phosphoprotein involved in the control of cell growth and proliferation (Vilchez and Butel, 2003*a*). The net effect of *c-myc* activation is cell growth, uncontrolled proliferation and decreased genomic stability (Thorley-Lawson and Allday, 2008). In normal cells, the potent proliferative activity of *c-myc* is controlled by, among others, the action of the tumour suppressor protein p53, often referred to as the

'guardian of the genome'. In the event of DNA damage or uncontrolled proliferation, p53 acts by halting the cell cycle for DNA repair or by directing the damaged cell for apoptosis. For lymphoma outgrowth, at least one of the apoptotic pathways must be suppressed (Thorley-Lawson and Allday, 2008). Inactivation of any one of several *c-myc* effectors, including p53, can allow cell proliferation and initiate lymphomagenesis. It is speculated that EBV may be involved in Burkitt's lymphoma development through the expression of anti-apoptotic proteins, contributing to increased tumourigenicity (Thorley-Lawson and Allday, 2008). As translocations involving *c-myc* are common in lymphomas, similar co-carcinogenic mechanisms could be at play in SV40-mediated lymphomagenesis. Data have indicated that, similar to EBV and Burkitt's lymphoma, *c-myc* over-expression may facilitate the replication of SV40 in human lymphoma cell lines, with the demonstration that co-transfection of BJAB cells with a *c-myc* construct increases SV40 replication ten-fold (Classon *et al*, 1987; Classon *et al*, 1990). The combined effect of *c-myc*-induced proliferation with the removal of the p53 tumour suppressor checkpoint following SV40 T-ag binding may thus result in uncontrolled cell growth and subsequent lymphoma development.

It is notable that the tumour suppressor proteins p53 and pRb are commonly lost or mutated in human tumours. The major mechanism of SV40 cell transformation in binding of T-ag to tumour suppressors is compatible with a role for SV40 in lymphomagenesis because the funtional inactivation of genes that monitor genome integrity is a trait of lymphomas (Vilchez and Butel, 2003*a*). In particular, it has been shown that patients with diffuse large B cell lymphoma as well as follicular lymphomas, the two types of NHL in which SV40 is most frequently found, often have detectable p53 alterations. SV40 is not alone in targeting p53 and pRb. Several DNA viruses encode

unique oncoproteins that target pRb and p53, emphasising the central power these two proteins exert over cell cycle control. SV40 T-ag is the only viral oncoprotein with the ability to interact with both p53 and pRb family members, underlining its potency and power as a multifunctional transforming protein. Complex-formation of p53 and pRb with T-ag has been observed in SV40-positive brain tumours and mesotheliomas. Similarly, the co-incident detection of SV40 T-ag and p53 alterations in lymphoma would be informative (Malkin, 2002). Evidence of these interactions, both in SV40 immune evasion and alteration of tumour suppressors in lymphoma, could be significant in unlocking the complex causation of this group of diseases and pursuing possible novel treatment options, with the prospect of T-ag expression by malignant cells being exploited for immunotherapy (Carbone *et al*, 1997).

The current body of evidence is inadequate to accept or reject a causal relation between SV40 and cancer. In 2002 the Institute of Medicine outlined that whilst the body of evidence that SV40 exposure could lead to cancer in humans under natural conditions is of *moderate* strength, the evidence that SV40 is indeed a transforming virus is *strong* (Stratton *et al*, 2002). The finding of such a potent transforming virus in human tumours is highly unlikely to be present merely by chance, without some act or part to play in the cancer process. This study supports and adds to the theory that SV40 is involved in cancer development, in particular in human lymphomas. The results of this study demonstrated expression of of the viral oncoprotein T-ag and maintenance and possible replication of SV40 DNA in B cells. In addition, cell proliferation and activation was noted in B cells infected with wild-type viruses. The kinetics of these events were also coincident with the downregulation of the co-stimulation molecule CD80 following infection with a mutant strain. Collectively, these results indicate that human B cell may

be a susceptible to a semi-permissive or latent type of infection cycle by SV40. The T cell line CEM did not show any evidence of SV40 infection in that results were similar for mock and infected samples in each assay. The B-lymphocyte cell lines BJAB and DG75 and the T-lymphocyte cell line, CEM, express similar levels of the SV40 receptor MHC class I, indicating differences between these cell types are at a post-binding and entry step. Future work using additional T cell lines or primary human T cells might reveal a tropism for SV40 to specific lymphocyte subsets.

These data support the possibility that SV40 can establish low-level persistent infection in some types of human lymphocytes, and therefore contribute to human disease, both in the development of B cell lymphomas and in transport of the virus to other organs in the body. In the near future, studies employing an approach with similar experimental design and sensitive detection methods in investigation of SV40 interaction with primary human lymphocytes may provide valuable insights into SV40 lymphomagenesis in humans.

5.0 Bibliography

Ahuja D, Sáenz-Robles MT, Pipas JM. SV40 large T antigen targets multiple cellular pathways to elicit cellular transformation. *Oncogene* 2005; **24:** 7729-45

Allander T, Andreasson K, Gupta S *et al.* Identification of a third human polyomavirus. *J Virol* 2007; **81:** 4130-6

Amara K, Trimeche M, Ziadi S *et al.* Presence of simian virus 40 DNA sequences in diffuse large B-cell lymphomas in Tunisia correlates with aberrant promoter hypermethylation of multiple tumor suppressor genes. *Int J Cancer* 2007; **121:** 2693-702

Anderson HA, Chen Y, Norkin LC. Bound simian virus 40 translocates to caveolin-enriched membrane domains, and its entry is inhibited by drugs that selectively disrupt caveolae. *Mol Biol Cell* 1996; **7:** 1825-34

Applied Biosystems - Real-Time Vs. Traditional PCR
Available online: www.appliedbiosystems.com/support/tutorials/pdf/rtpcr_vs_tradpcr.pdf

Arrington AS, Moore MS, Butel JS. SV40-positive brain tumor in scientist with risk of laboratory exposure to the virus. *Oncogene* 2004; **23:** 2231-5

Atwood WJ. Cellular Receptors for the Polyomaviruses. *In* Human Polyomaviruses: Molecular and Clinical Perspective. Khalili K, Stoner GL. Wiley-Liss, New York. 2001: p. 179-196

BD Biosciences - Introduction to Flow Cytometry: A Learning Guide. Manual Part Number: 11-11032-01 April 2000. BD Biosciences, San Jose, CA
Available online: http://www.bcm.edu/flowcytometry/?pmid=5748

Ben-Bassat H, Goldblum N, Mitrani S *et al.* Establishment in continuous culture of a new type of lymphocyte from a "Burkitt like" malignant lymphoma (line D.G.-75). *Int J Cancer* 1977; **19:** 27-33

Berger JR. Progressive multifocal leukoencephalopathy in acquired immunodeficiency syndrome: explaining the high incidence and disproportionate frequency of the illness relative to other immunosuppressive conditions. *J Neurovirol* 2003; **9:** 38-41

Bergsagel DJ, Finegold MJ, Butel JS, Kupsky WJ, Garcea RL. DNA sequences similar to those of simian virus 40 in ependymomas and choroid plexus tumors of childhood. *N Engl J Med* 1992; **326:** 988-93

Bocchetta M, Di Resta I, Powers A *et al.* Human mesothelial cells are unusually susceptible to simian virus 40-mediated transformation and asbestos cocarcinogenicity. *Proc Natl Acad Sci U S A* 2000; **97:** 10214-9

Bocharov G, Ludewig B, Bertoletti A et al. Underwhelming the immune response: effect of slow virus growth on CD8+-T-lymphocyte responses. *J Virol* 2004; **78:** 2247-54

Breau WC, Atwood WJ, Norkin LC. Class I major histocompatibility proteins are an essential component of the simian virus 40 receptor. *J Virol* 1992; **66:** 2037-45

Brugge JS, Butel JS. Role of simian virus 40 gene A function in maintenance of transformation. *J Virol* 1975; **15:** 619-35.

Butel JS, Jafar S, Wong C *et al.* Evidence of SV40 Infections in Hospitalized Children. *Hum Pathol* 1999; **30:** 1496-1502

Butel JS, Lednicky JA. Cell and molecular biology of simian virus 40: implications for human infections and disease. *J Natl Cancer Inst* 1999; **91:** 119-34

Butel JS, Lednicky JA. Response to more about: cell and molecular biology of simian virus 40: implications for human infections and disease. *J Natl Cancer Inst* 2000; **92:** 496-7

Butel JS. Viral carcinogenesis: revelation of molecular mechanisms and etiology of human disease. *Carcinogenesis* 2000; **21:** 405-26

Butel, J.S. SV40, human infections, and cancer: emerging concepts and causality considerations. *In*: Khalili, K. and Jeang, K.T. (ed.), Viral Oncology: Basic Science and Clinical Applications, Wiley-Blackwell, 2009.

Capello D, Cerri M, Muti G *et al.* Molecular histogenesis of posttransplantation lymphoproliferative disorders. *Blood* 2003; **102:** 3775-85

Carbone M, Pass HI, Miele L, Bocchetta M. New developments about the association of SV40 with human mesothelioma. *Oncogene* 2003; **22:** 5173-80

Carbone M, Pass HI, Rizzo P *et al.* Simian virus 40-like DNA sequences in human pleural mesothelioma. *Oncogene* 1994; **9:** 1781-90

Carbone M, Rizzo P, Pass HI. Simian virus 40, poliovaccines and human tumors: a review of recent developments. *Oncogene* 1997; **15:** 1877-88

Carbone M, Rizzo P, Procopio A *et al.* SV40-like sequences in human bone tumors. *Oncogene* 1996; **13:** 527-35

Chaudhry A, Das SR, Hussain A *et al.* The Nef protein of HIV-1 induces loss of cell surface costimulatory molecules CD80 and CD86 in APCs. *J Immunol* 2005; **175:** 4566-74

Chen PM, Yen CC, Yang MH *et al.* High prevalence of SV40 infection in patients with nodal non-Hodgkin's lymphoma but not acute leukemia independent of contaminated polio vaccines in Taiwan. *Cancer Invest* 2006; **24:** 223-8

Cicala C, Pompetti F, Carbone M. SV40 induces mesotheliomas in hamsters. *Am J Pathol* 1993; **142:** 1524-33

Cicala C, Pompetti F, Nguyen P, Dixon K, Levine AS, Carbone M. SV40 small t deletion mutants preferentially transform mononuclear phagocytes and B lymphocytes *in vivo*. *Virology* 1992; **190:** 475-9

Classon M, Henriksson M, Klein G, Sümegi J. The effect of myc proteins on SV40 replication in human lymphoid cells. *Oncogene* 1990; **5:** 1371-6

Classon M, Henriksson M, Sümegi J, Klein G, Hammarskjöld ML. Elevated c-myc expression facilitates the replication of SV40 DNA in human lymphoma cells. *Nature* 1987; **330:** 272-4

Clustal w software. Available online at: http://www.ebi.ac.uk

Coe JE, Green I. B-cell origin of hamster lymphoid tumors induced by simian virus 40. *J Natl Cancer Inst* 1975; **54:** 269-70

Coscoy L. Immune evasion by Kaposi's sarcoma-associated herpesvirus. *Nat Rev Immunol* 2007; **7:** 391-401

Cullen BR. Viruses and microRNAs. *Nat Genet* 2006; **38:** S25-30

Cutrone R, Lednicky J, Dunn G *et al.* Some oral poliovirus vaccines were contaminated with infectious SV40 after 1961. *Cancer Res* 2005; **65:** 10273-9

Daibata M, Nemoto Y, Takemoto S, Miyoshi I, Taguchi H. Epstein-Barr virus in concomitant gastric carcinoma and adult T-cell leukemia/lymphoma. *Am J Med* 2003; **114:** 509-10

Dalianis T, Ramqvist T, Andreasson K, Kean JM, Garcea RL. KI, WU and Merkel cell polyomaviruses: a new era for human polyomavirus research. *Semin Cancer Biol* 2009; **19:** 270-5

Daniels R, Sadowicz D, Hebert DN. A very late viral protein triggers the lytic release of SV40. *PLoS Pathog* 2007; **3:** e98

David H, Mendoza S, Konishi T, Miller CW. Simian virus 40 is present in human lymphomas and normal blood. *Cancer Lett* 2001; **162:** 57-64

Diamandopoulos GT. Induction of lymphocytic leukemia, lymphosarcoma, reticulum cell sarcoma, and osteogenic sarcoma in the Syrian golden hamster by oncogenic DNA simian virus 40. *J Natl Cancer Inst* 1973; **50:** 1347-65

Diamandopoulos GT. Leukemia, lymphoma, and osteosarcoma induced in the Syrian golden hamster by simian virus 40. *Science* 1972; **176:** 173-5

Dolcetti R, Martini F, Quaia M *et al.* Simian virus 40 sequences in human lymphoblastoid B-cell lines. *J Virol* 2003; **77:** 1595-7

Eddy BE, Borman GS, Berkeley WH, Young RD. Tumors induced in hamsters by injection of rhesus monkey kidney cell extracts. *Proc Soc Exp Biol Med* 1961; **107:** 191-7

Engels EA. Infectious agents as causes of non-Hodgkin lymphoma. *Cancer Epidemiol Biomarkers Prev* 2007; **16:** 401-4

Feng H, Shuda M, Chang Y, Moore PS. Clonal integration of a polyomavirus in human Merkel cell carcinoma. *Science* 2008; **319:** 1096-100

Filipowicz W, Bhattacharyya SN, Sonenberg N. Mechanisms of post-transcriptional regulation by microRNAs: are the answers in sight? *Nat Rev Genet* 2008; **9:** 102-14

FlowJo basic tutorial.
Available online at: http://offsite.treestar.com/downloads/BasicTutorial0709web.pdf

Foley GE, Lazarus H, Farber S, Uzman BG, Boone BA, McCarthy RE. Continuous culture of human lymphoblasts from peripheral blood of a child with acute leukemia. *Cancer* 1965; **18:** 522-9

Garcea RL, Imperiale MJ. Simian virus 40 infection of humans. *J Virol* 2003; **77:** 5039-45

Gardner SD, Field AM, Coleman DV, Hulme B. New human papovavirus (B.K.) isolated from urine after renal transplantation. *Lancet* 1971; **1:** 1253-7

Gaynor AM, Nissen MD, Whiley DM *et al.* Identification of a novel polyomavirus from patients with acute respiratory tract infections. *PLoS Pathog* 2007; **3:** e64

Goudsmit J, Wertheim-van Dillen P, van Strien A, van der Noordaa J. The role of BK virus in acute respiratory tract disease and the presence of BKV DNA in tonsils. *J Med Virol* 1982; **10:** 91-9

Gross L. A filterable agent, recovered from Ak leukemic extracts, causing salivary gland carcinomas in C3H mice. *Proc Soc Exp Biol Med* 1953; **83:** 414-21

Grulich AE, Vajdic CM. The epidemiology of non-Hodgkin lymphoma. *Pathology* 2005; **37:** 409-19

Hirsch HH, Knowles W, Dickenmann M *et al.* Prospective study of polyomavirus type BK replication and nephropathy in renal-transplant recipients. *N Engl J Med* 2002; **347:** 488-96

Hirvonen A, Mattson K, Karjalainen A *et al.* Simian virus 40 (SV40)-like DNA sequences not detectable in finnish mesothelioma patients not exposed to SV40-contaminated polio vaccines. *Mol Carcinog* 1999; **26:** 93-9

Imperiale MJ. The human polyoma viruses: an overview. *In* Human Polyomaviruses: Molecular and Clinical Perspective. Khalili K, Stoner GL. Wiley-Liss, New York. 2001: 53-77

Javier RT, Butel JS. The history of tumor virology. *Cancer Res* 2008; **68:** 7693-706

Jensen F, Koprowski H, Pagano JS, Ponten J, Ravdin RG. Autologous and homologous implantation of human cells transformed in vitro by SV40. *J Natl Cancer Inst* 1964; **32:** 917-932

Jiang M, Abend JR, Johnson SF, Imperiale MJ. The role of polyomaviruses in human disease. *Virology* 2009; **384:** 266-73

Kindt TJ, Goldsby RA, Osborne BA. Experimental Systems. *In* Kuby Immunology. W.H. Freeman and Company, New York. 2007: p 546-574

Kirschstein RL, Gerber P. Ependymomas produced after intracerebral inoculation of SV40 into new-born hamsters. *Nature* 1962; **195:** 299-300

Knowles WA, Pipkin P, Andrews N *et al.* Population-based study of antibody to the human polyomaviruses BKV and JCV and the simian polyomavirus SV40. *J Med Virol* 2003; **71:** 115-23

Kroczynska B, Cutrone R, Bocchetta M *et al.* Crocidolite asbestos and SV40 are cocarcinogens in human mesothelial cells and in causing mesothelioma in hamsters. *Proc Natl Acad Sci U S A* 2006; **103:** 14128-33

Krumbholz A, Bininda-Emonds OR, Wutzler P, Zell R. Phylogenetics, evolution, and medical importance of polyomaviruses. *Infect Genet Evol* 2009; **9:** 784-99

Kutok JL, Wang F. Spectrum of Epstein-Barr virus-associated diseases. *Annu RevPathol* 2006; **1:** 375-404

Kwong YL. Predicting the outcome in non-Hodgkin lymphoma with molecular markers. *Br J Haematol* 2007; **137:** 273-87

LeBien TW, Tedder TF. B lymphocytes: how they develop and function. *Blood* 2008; **112:** 1570-80.

Lednicky JA, Arrington AS, Stewart AR *et al.* Natural isolates of simian virus 40 from immunocompromised monkeys display extensive genetic heterogeneity: new implications for polyomavirus disease. *J Virol* 1998; **72:** 3980-90

Lednicky JA, Butel JS. Simian virus 40 regulatory region structural diversity and the association of viral archetypal regulatory regions with human brain tumors. *Semin Cancer Biol* 2001; **11:** 39-47

Lednicky JA, Butel JS. Tissue culture adaptation of natural isolates of simian virus 40: changes occur in viral regulatory region but not in carboxy-terminal domain of large T-antigen. *J Gen Virol* 1997; **78:** 1697-705

Lednicky JA, Garcea RL, Bergsagel DJ, Butel JS. Natural simian virus 40 strains are present in human choroid plexus and ependymoma tumors. *Virology* 1995*b*; **212:** 710-7

Lednicky JA, Stewart AR, Jenkins JJ 3rd, Finegold MJ, Butel JS. SV40 DNA in human osteosarcomas shows sequence variation among T-antigen genes. *Int J Cancer* 1997; **72:** 791-800

Lednicky JA, Wong C, Butel JS. Artificial modification of the viral regulatory region improves tissue culture growth of SV40 strain 776. *Virus Res* 1995*a*; **35:** 143-53

MacKenzie J, Wilson KS, Perry J, Gallagher A, Jarrett RF. Association between simian virus 40 DNA and lymphoma in the United kingdom. *J Natl Cancer Inst* 2003; **95:** 1001-3

MacLachlan DS. SV40 in human tumors: new documents shed light on the apparent controversy. *Anticancer Res* 2002; **22:** 3495-9

Malkin D. Simian virus 40 and non-Hodgkin lymphoma. Lancet 2002; 359: 812-3.

Martini F, Corallini A, Balatti V, Sabbioni S, Pancaldi C, Tognon M. Simian virus 40 in humans. *Infect Agent Cancer* 2007; **2:** 13

Martini F, Dolcetti R, Gloghini A *et al.* Simian-virus-40 footprints in human lymphoproliferative disorders of HIV- and HIV+ patients. *Int J Cancer* 1998*b*; **78:** 669-74

Martini F, Iaccheri L, Lazzarin L *et al.* SV40 early region and large T antigen in human brain tumors, peripheral blood cells, and sperm fluids from healthy individuals. *Cancer Res* 1996; **56:** 4820-5

Martini F, Lazzarin L, Iaccheri L *et al.* Different simian virus 40 genomic regions and sequences homologous with SV40 large T antigen in DNA of human brain and bone tumors and of leukocytes from blood donors. *Cancer* 2002; **94:** 1037-48

Martini F, Lazzarin L, Iaccheri L, Corallini A, Gerosa M, Trabanelli C, Calza N, Barbanti-Brodano G, Tognon M. Simian virus 40 footprints in normal human tissues, brain and bone tumours of different histotypes. *Dev Biol Stand* 1998*a*; **94:** 55-66

Marzio R, Mauël J, Betz-Corradin S. CD69 and regulation of the immune function. *Immunopharmacol Immunotoxicol* 1999; **21:** 565-82

McNees AL, Vilchez RA, Heard TC *et al.* SV40 lymphomagenesis in Syrian golden hamsters. *Virology* 2009; **384:** 114-24

McNees AL, White ZS, Zanwar P, Vilchez RA, Butel JS. Specific and quantitative detection of human polyomaviruses BKV, JCV, and SV40 by real time PCR. *J Clin Virol* 2005; **34**: 52-62

Melnick JL, Stinebaugh S. Excretion of vacuolating SV-40 virus (papova virus group) after ingestion as a contaminant of oral poliovaccine. *Proc Soc Exp Biol Med* 1962; **109:** 965-8

Mendoza SM, Konishi T, Miller CW. Integration of SV40 in human osteosarcoma DNA. *Oncogene* 1998; **17:** 2457-62

Meneses A, Lopez-Terrada D, Zanwar P *et al.* Lymphoproliferative disorders in Costa Rica and simian virus 40. *Haematologica* 2005; **90:** 1635-42

Menezes J, Leibold W, Klein G, Clements G. Establishment and characterization of an Epstein-Barr virus (EBV)-negative lymphoblastoid cell line (BJA-B) from an exceptional, EBV-genome-negative African Burkitt's lymphoma. *Biomedicine* 1975; **22:** 276-84

Minor P, Pipkin PA, Cutler K, Dunn G. Natural infection and transmission of SV40. *Virology* 2003; **314:** 403-9

Monaco MC, Atwood WJ, Gravell M, Tornatore CS, Major EO. JC virus infection of hematopoietic progenitor cells, primary B lymphocytes, and tonsillar stromal cells: implications for viral latency. *J Virol* 1996; **70:** 7004-12

Morris JA, Johnson KM, Aulisio CG, Chanock RM, Knight V. Clinical and serologic responses in volunteers given vacuolating virus (SV-40) by respiratory route. *Proc Soc Exp Biol Med* 1961; **108:** 56-9

Nakatsuka S, Liu A, Dong Z *et al.* Simian virus 40 sequences in malignant lymphomas in Japan. *Cancer Res* 2003; **63:** 7606-8

Newman JS, Baskin GB, Frisque RJ. Identification of SV40 in brain, kidney and urine of healthy and SIV-infected rhesus monkeys. *J Neurovirol* 1998; **4:** 394-406

Norkin LC. Simian virus 40 infection via MHC class I molecules and caveolae. *Immunol Rev* 1999; **168:** 13-22

Padgett BL, Walker DL, ZuRhein GM, Eckroade RJ, Dessel BH. Cultivation of papova-like virus from human brain with progressive multifocal leucoencephalopathy. *Lancet* 1971; **1:** 1257-60

Patel NC, Halvorson SJ, Sroller V *et al.* Viral regulatory region effects on vertical transmission of polyomavirus SV40 in hamsters. *Virology* 2009; **386:** 94-101

Patel NC, Vilchez RA, Killen DE *et al.* Detection of polyomavirus SV40 in tonsils from immunocompetent children. *J Clin Virol* 2008; **43:** 66-72

Pathol 2006; **1:** 375-404.

Poulin DL, DeCaprio JA. Is there a role for SV40 in human cancer? *J Clin Oncol* 2006; **24:** 4356-65

Randhawa PS, Demetris AJ. Nephropathy due to polyomavirus type BK. *N Engl J Med* 2000; **342:** 1361-3

Rizzo P, Bocchetta M, Powers A *et al.* SV40 and the pathogenesis of mesothelioma. *Semin Cancer Biol* 2001; **11:** 63-71.

Robb JA, Huebner K. Effect of cell chromosome number on simian virus 40 replication. *Exp Cell Res* 1973; **81:** 120-6

Sáenz-Robles MT, Sullivan CS, Pipas JM. Transforming functions of Simian Virus 40. *Oncogene* 2001; **20:** 7899-907

Sancho D, Gómez M, Sánchez-Madrid F. CD69 is an immunoregulatory molecule induced following activation. *Trends Immunol*2005; **26:** 136-40

Sarnow P, Jopling CL, Norman KL, Schütz S, Wehner KA. MicroRNAs: expression, avoidance and subversion by vertebrate viruses. *Nat Rev Microbiol* 2006; **4:** 651-9

Schein HM, Enders, JF. Transformation induced by simian virus 40 in human renal cell cultures. I. Morphology and growth characteristics. *Proc Natl Acad Sci USA* 1962; **48:** 1164-72

Schüler F, Dölken SC, Hirt C *et al.* No evidence for simian virus 40 DNA sequences in malignant non-Hodgkin lymphomas. *Int J Cancer* 2006; **118:** 498-504

Shah KV. SV40 and human cancer: a review of recent data. *Int J Cancer* 2007; **120:** 215-23

Shaikh S, Skoczylas C, Longnecker R, Rundell K. Inability of simian virus 40 to establish productive infection of lymphoblastic cell lines. *J Virol* 2004; **78:** 4917-20

Shivapurkar N, Harada K, Reddy J *et al.* Presence of simian virus 40 DNA sequences in human lymphomas. *Lancet* 2002; **359:** 851-2

Shivapurkar N, Takahashi T, Reddy J *et al.* Presence of simian virus 40 DNA sequences in human lymphoid and hematopoietic malignancies and their relationship to aberrant promoter methylation of multiple genes. *Cancer Res* 2004; **64:** 3757-60

Shivapurkar N, Wiethege T, Wistuba II *et al.* Presence of simian virus 40 sequences in malignant mesotheliomas and mesothelial cell proliferations. *J Cell Biochem* 1999; **76:** 181-8

Sroller V, Vilchez RA, Stewart AR, Wong C, Butel JS. Influence of the viral regulatory region on tumor induction by simian virus 40 in hamsters. *J Virol* 2008; **82:** 871-9

Staudt LM, Wilson WH. Focus on lymphomas. *Cancer Cell* 2002; **2:** 363-6

Stewart AR, Lednicky JA, Butel JS. Sequence analyses of human tumor-associated SV40 DNAs and SV40 viral isolates from monkeys and humans. *J Neurovirol* 1998; **4:** 182-93

Stewart SE, Eddy BE, Borgese N. Neoplasms in mice inoculated with a tumor agent carried in tissue culture. *J Natl Cancer Inst* 1958; **20:** 1223-43

Stratton K, Almario DA, McCormick MC. Immunization safety review: SV40 contamination of polio vaccine and cancer. The National Academies Press, Washington, D.C., 2002. Downloaded from: http://www.nap.edu/catalog/10534.html

Strickler HD; International SV40 Working Group. A multicenter evaluation of assays for detection of SV40 DNA and results in masked mesothelioma specimens. *Cancer Epidemiol Biomarkers Prev* 2001; **10:** 523-32

Sui LF, Williamson J, Lowenthal RM, Parker AJ. Absence of simian virus 40 (SV40) DNA in lymphoma samples from Tasmania, Australia. *Pathology* 2005; **37:** 157-9

Sullivan CS, Grundhoff AT, Tevethia S, Pipas JM, Ganem D. SV40-encoded microRNAs regulate viral gene expression and reduce susceptibility to cytotoxic T cells. *Nature* 2005; **435:** 682-6

Sullivan CS. New roles for large and small viral RNAs in evading host defences. *Nat Rev Genet* 2008; **9:** 503-7

Swaminathan S. Noncoding RNAs produced by oncogenic human herpesviruses. *J Cell Physiol* 2008; **216:** 321-6

Sweet BH and Hilleman MR. The vacuolating virus, S.V. 40. *Proc Soc Exp Biol Med* 1960; **105:** 420-7.

Thorley-Lawson DA, Allday MJ. The curious case of the tumour virus: 50 years of Burkitt's lymphoma. *Nat Rev Microbiol* 2008; **6:** 913-24

Tortorella D, Gewurz BE, Furman MH, Schust DJ, Ploegh HL. Viral subversion of the immune system. *Annu Rev Immunol* 2000; **18:** 861-926

Vilchez RA, Brayton CF, Wong C *et al.* Differential ability of two simian virus 40 strains to induce malignancies in weanling hamsters. *Virology* 2004; **330:** 168-77

Zekri AR, Mohamed W, Bahnassy A *et al.* Detection of simian virus 40 DNA sequences in Egyptian patients with different hematological malignancies. *Leuk Lymphoma* 2007; **48:** 1828-34

Zhen HN, Zhang X, Bu XY *et al.* Expression of the simian virus 40 large tumor antigen (Tag) and formation of Tag-p53 and Tag-pRb complexes in human brain tumors. *Cancer* 1999; **86:** 2124-32

Ziegler SF, Ramsdell F, Alderson MR. The activation antigen CD69. *Stem Cells* 1994; **12:** 456-65

Zou W, Chen L. Inhibitory B7-family molecules in the tumour microenvironment. *Nat Rev Immunol* 2008; **8:** 467-77

zur Hausen H. Novel human polyomaviruses--re-emergence of a well known virus family as possible human carcinogens. *Int J Cancer* 2008; **123:** 247-50

Appendix I: CD69 expression on SV40-infected BJAB cell line

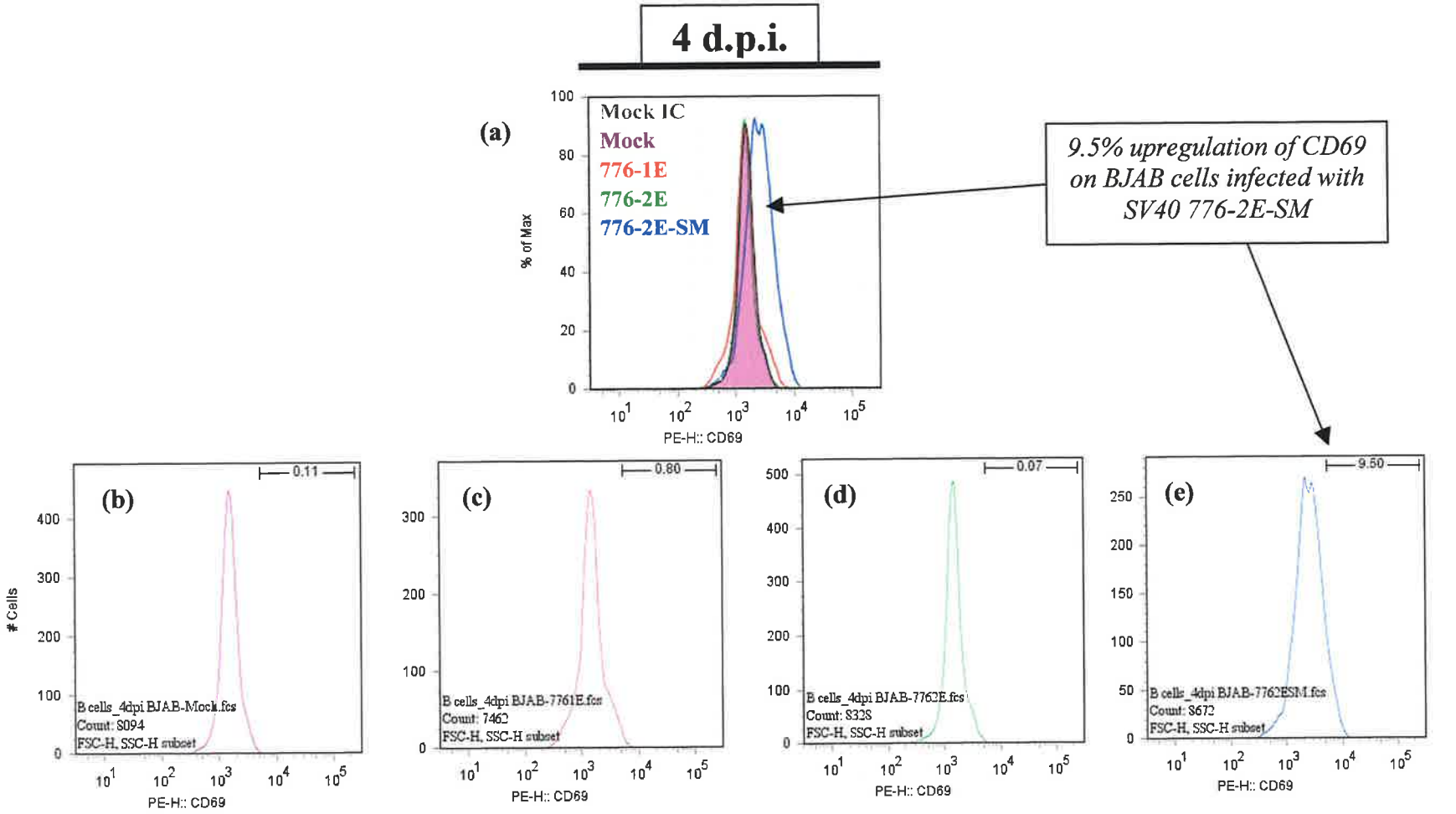

AI.1: **CD69 expression on SV40-infected BJAB cell line at 4 d.p.i.** Flow cytometric analysis of CD69 expression on BJAB cells at 4 days post infection (d.p.i.) showing (a) overlayed histograms of (b) uninfected mock and cells infected with (c) SV40 776-1E, (d) SV40 776-2E and (e) SV40 776-2E-SM.

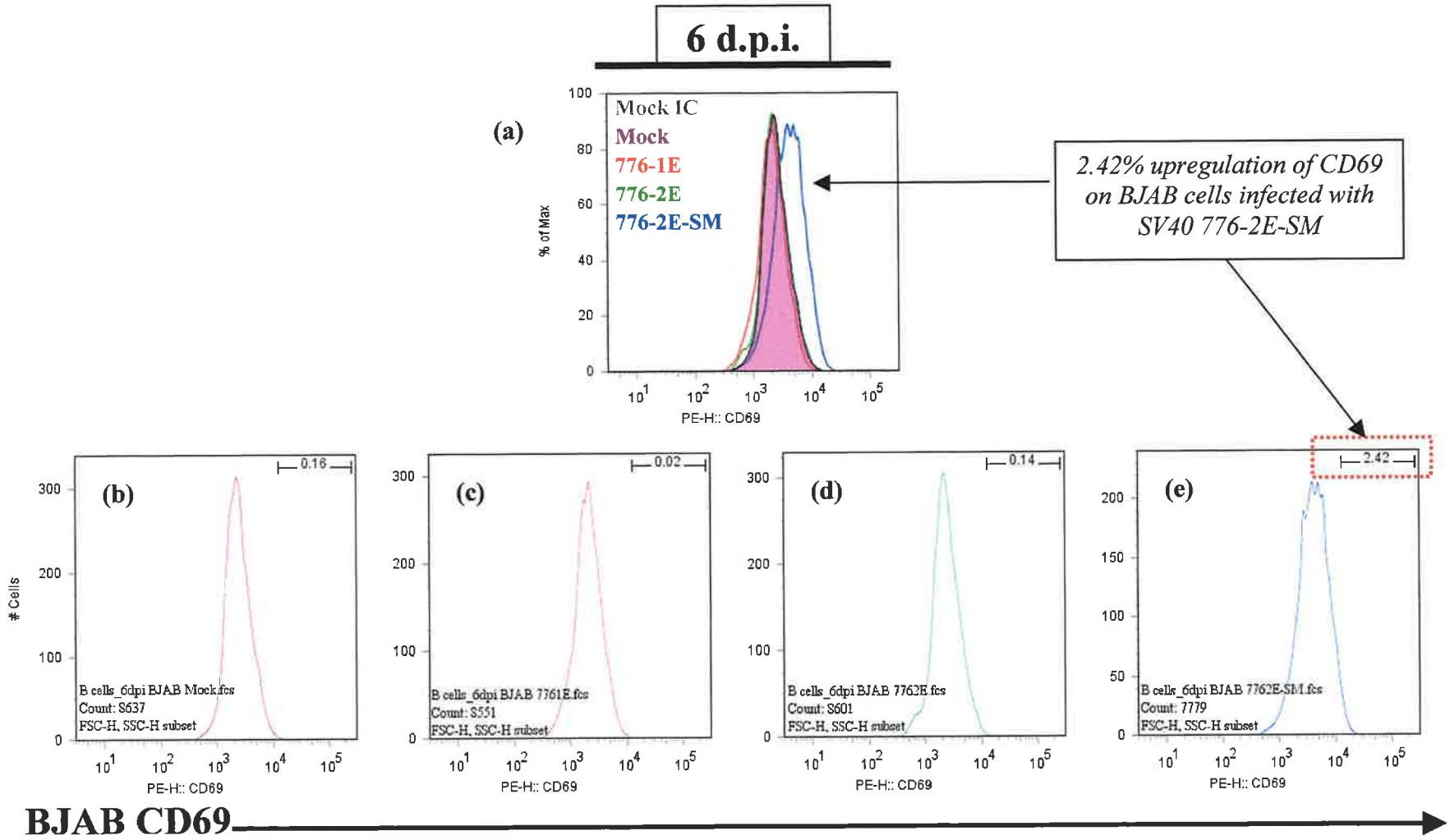

AI.2: CD69 expression on SV40-infected BJAB cell line at 6 d.p.i. Flow cytometric analysis of CD69 expression on BJAB cell line at 6 days post infection (d.p.i.) showing (a) overlayed histograms of (b) uninfected mock and cells infected with (c) SV40 776-1E, (d) SV40 776-2E and (e) SV40 776-2E-SM.

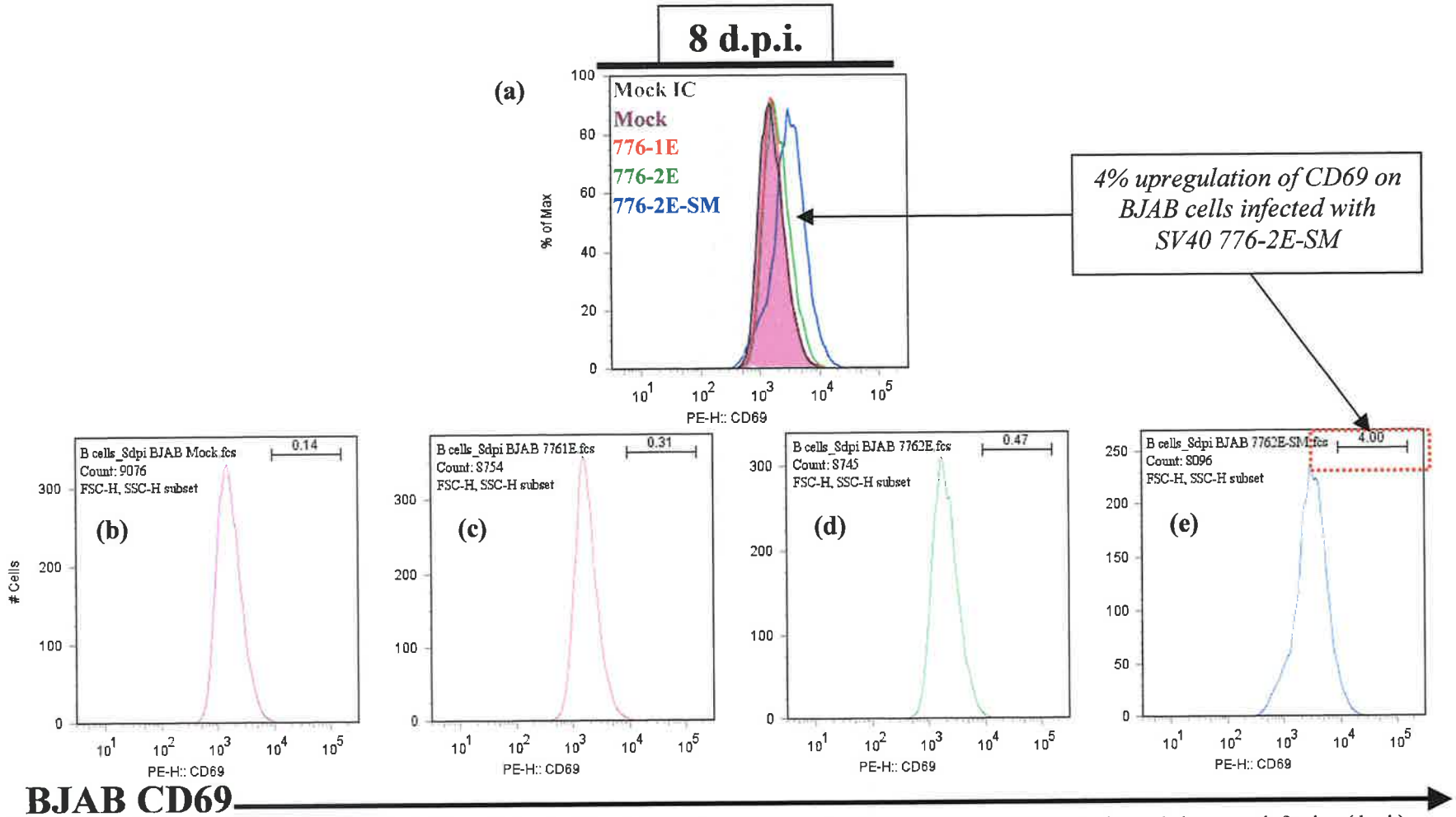

AI.3: CD69 expression on SV40-infected BJAB cell line at 8 d.p.i. Flow cytometric analysis of CD69 expression on BJAB cell line at 8 days post infection (d.p.i.) showing (a) overlayed histograms of (b) uninfected mock and cells infected with (c) SV40 776-1E, (d) SV40 776-2E and (e) SV40 776-2E-SM.

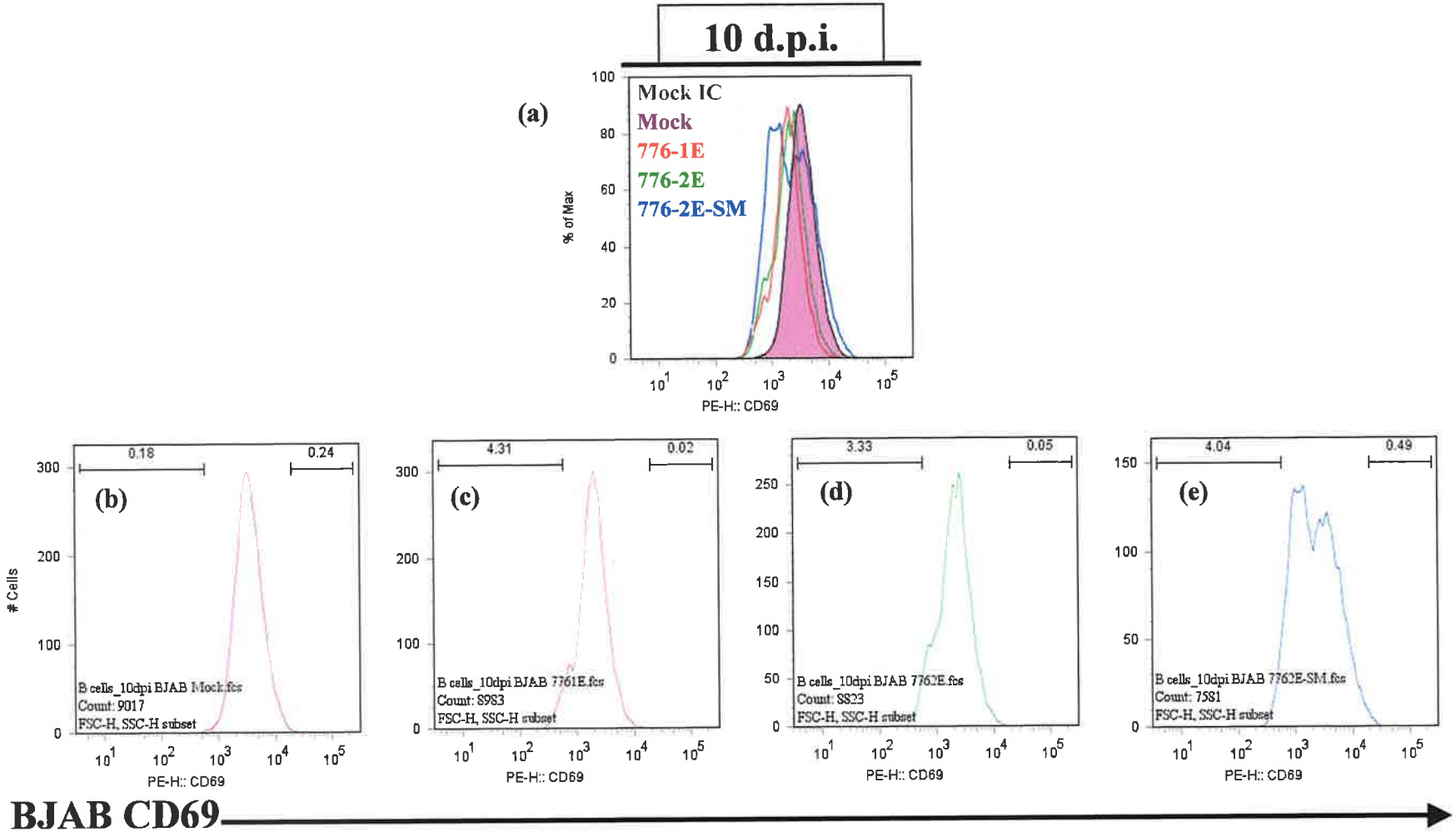

AI.4: CD69 expression on SV40-infected BJAB cell line at 10 d.p.i. Flow cytometric analysis of CD69 expression on BJAB cell line at 10 days post infection (d.p.i.) showing (a) overlayed histograms of (b) uninfected mock and cells infected with (c) SV40 776-1E, (d) SV40 776-2E and (e) SV40 776-2E-SM.

7.0 Publications

A poster presentation of the findings of this project was presented at the Genetic Instability and Cancer Symposium, Dan L. Duncan Cancer Center at Baylor College of Medicine, Houston, Texas, in April 2009.